GLYCOSAMINOGLYCANS AND PROTEOGLYCANS IN THE DEVELOPING RAT BRAIN

by
Mary Elizabeth Herndon

B. S. Biology
University of Houston, 1984

Submitted to the Department of Biology in partial fulfillment of the requirements for the degree of

Doctor of Philosophy
in Biology

at the
Massachusetts Institute of Technology
February, 1996

Signature of Author

Mary E. Herndon, Department of Biology

Certified by

Arthur D. Lander, Associate Professor, Depts. of Biology and Brain and Cognitive Sciences, Thesis supervisor

Accepted by

Frank Solomon, Chairman of the Graduate Committee
Department of Biology

GLYCOSAMINOGLYCANS AND PROTEOGLYCANS IN THE DEVELOPING RAT BRAIN

by
Mary Elizabeth Herndon

B. S. Biology
University of Houston, 1984

Submitted to the Department of Biology on February 9th, 1996 in partial fulfillment of the requirements for the degree of Doctor of Philosophy in Biology

ABSTRACT

Cellular interactions in neural development are influenced by various extracellular proteins, many of which bind glycosaminoglycans (GAGs) or proteoglycans (PGs). The work presented here is an attempt to establish a foundation for understanding how PGs and GAGs in the brain may, through their binding of other developmentally important molecules, affect the pericellular events that control neural cell behaviors during development. The diversity and temporal expression of brain proteoglycans was evaluated in the first part of this undertaking: Analysis of subcellular fractions of rat brain revealed that at least twenty-five putative proteoglycan core proteins are present in developing brain. Levels of many of these cores varied considerably during development. Two of the membrane-associated heparan sulfate (HeS) PGs that are covalently linked to glycosylphosphatidyl-inositol lipid, and that have core M_r's of 59 and 50 kD, have been cloned and subsequently identified, respectively, as glypican and as cerebroglycan, a nervous-system specific glypican-related PG ([Litwack, E., C. Stipp, A. Kumbasar, and A. Lander. 1994. *J. Neurosci.* 14: 3713-3724]; [Stipp, C., E. Litwack, and A. Lander. 1994. *J. Cell Biol.* 124:149-160]). The data indicate that brain PGs are abundant, structurally diverse, and developmentally regulated. To better understand the functions of the GAG component of PGs, the binding of purified GAGs to various heparin-binding proteins that are expressed in the brain was examined using affinity co-electrophoresis (ACE); in some cases, a new technique, reverse ACE, was also used. Equilibrium dissociation constants are reported for binding between heparan and chondroitin sulfate (HeS and ChS)

preparations purified from membrane-associated and soluble fraction brain PGs, as well as several commercial GAG preparations, and the following proteins: laminin-1, fibronectin, thrombospondin-1, NCAM, L1, protease nexin-1 [PN-1], urokinase plasminogen activator [uPA], thrombin, and FGF-2. This set of proteins exhibited both selectivity and specificity in GAG binding, and the ranges of affinities for HeS and ChS binding were broad, varying over 170- and 130-fold, respectively. Measurements of immunopurified cerebroglycan and syndecan-3 binding to thrombospondin-1 reveal that intact PGs bind significantly better than free HeS does. To assess possible functional roles for brain GAGs, GAG-mediated changes in the inhibitory activity of PN-1 toward both thrombin and uPA were tested in short-term kinetic assays. Measurements of apparent second order rate constants in the two assays show that both brain HeS and brain ChS behave similarly, and that brain GAGs accelerate PN-1 inhibition of thrombin, but decrease PN-1 inhibition of uPA. Thus, brain GAGs appear to shift the specificity of PN-1 away from one substrate, uPA, and toward a second substrate, thrombin. The diversity of PGs and the range of GAG affinities for a large group of developmentally relevant proteins, together with direct evidence that brain GAGs can affect protein function, suggest that brain GAGs and PGs may be widely involved neural development.

Thesis Supervisor: Arthur D. Lander

Title: Associate Professor,

Departments of Biology and Brain and Cognitive Sciences

DEDICATION

To my grandfather, Raymond F. Herndon, Jr.,
who always wants to know what I'm doing

ACKNOWLEDGMENTS

My deepest gratitude, of course, goes to Arthur Lander, an advisor who takes the role seriously, to the benefit of all of his students. His guidance, patience, wit, and kindness, not to mention his great cooking, all made graduate school a better place for me. The intellectual discussions I have enjoyed with Arthur provided me not only with information, but a better understanding of what it means to be a scientist.

My standing thesis committee members, Bob Rosenberg and Richard Hynes are thanked for their encouragement and insight at my infrequent committee meetings.

My appreciation goes also to Frank Solomon for the support, both emotional and administrative, he has provided me during some difficult times in my graduate career.

I would like to express my appreciation for many of the fellow women in my entering class at MIT (you know who you are). The wonderful humor and support that our group shared truly made my life at M.I.T. bearable. Also, Charlotte Schwartz is thanked for her boundless encouragement and for helping me to see things more clearly.

Finally, I would like to express my heartfelt gratitude for Chris Stipp, my friend and partner. Chris helped substantially with the preparation of this thesis (and most of the time did the preparation of dinner, as well). During my years in graduate school, he has acted as a sounding board for my ideas, an invaluable source of chemistry information, and sometimes a shoulder to cry on. My graduate career could not have happened without his support.

Table of Contents

List of Figures and Tables

INTRODUCTION

During development, a complex series of carefully regulated events generates the elaborate structure that is the brain. Brain maturation involves different cellular behaviors including cell proliferation and migration, axon growth and guidance, and synaptogenesis. A large number of the pericellular molecules that have been found to affect these events have also been found to bind glycosaminoglycans (table1). Increasingly, glycosaminoglycans and the proteins that bear them, proteoglycans, have also been implicated in cellular behaviors, often through their binding to other cell-surface and extracellular proteins.

Proteoglycans

Proteoglycans are ubiquitous molecules both in the extracellular matrix and on the surfaces of cells. A proteoglycan (PG) is composed a polypeptide core that is covalently linked to one or more glycosaminoglycan chains (GAGs), which are linear, sulfated carbohydrate molecules (figure 1). As they are discovered, PG core proteins are often classified into families based on relatedness of structure and polypeptide sequence (see Table 2), yet few functions have been assigned to core proteins per se. At the most basic level, the core protein of the PG is required for targeting the PG to the cell surface, intracellular vesicles, or the extracellular matrix. However, in some cases, other functional activities for the PGs, such as ligand binding, have been assigned to the core protein as well. For example, both the proteoglycans decorin and betaglycan, a TGF-β receptor, bind to TGF-β via their core proteins (Cheifetz and Massague, 1989; Yamaguchi et al., 1990); and the proteoglycans phosphacan and neurocan each bind to tenascin as well as interfere with NCAM and NgCAM function, even if their GAG chains are removed (Grumet et al., 1993; Friedlander et al., 1994; Grumet et al., 1994). In each of these cases, the core protein accounts for most or all of the measurable binding.

Traditionally, proteoglycans have been classified based on the type of glycosaminoglycan chains they bear. This has been fortuitous, because, frequently, related cores carry the same GAG type, and the type of GAG appears to have much to do with the function of the PG. For example, perturbation of specific GAG types or GAG attachment to

PGs may alter a cellular response such as cellular adhesion or proliferation [e.g., cellular attachment to fibronectin (LeBaron et al., 1988) or thrombospondin-1 (Murphy-Ullrich et al., 1988; Adams and Lawler, 1994); fibroblast growth factor induction of cellular growth and differentiation (Rapraeger et al., 1991)].

Glycosaminoglycans

All glycosaminoglycans are unbranched, sulfated, polysaccharide co-polymers, composed of alternating amino sugar and uronic acid units. The two most common types of GAG chains attached to PG core proteins are heparan sulfate (HeS) and chondroitin sulfate (ChS), illustrated in figure 1. HeS is composed of alternating glucosamine and glucuronate or iduronate residues, while ChS features alternating galactosamine and glucuronate residues. Both GAGs are sulfated at various positions, a property responsible for the highly acidic and hydrophilic nature of GAGs. HeS is closely related to the GAG heparin, which is more highly sulfated and contains largely iduronate rather than glucuronate. Another GAG with iduronate as the major uronic acid component is dermatan sulfate (DS), which is basically an epimerized version of ChS (in fact, the DS/ChS distinction may be arbitrary, as DS regions have been found in ChS chains). NMR studies reveal that three different stable conformations have been found for sulfated iduronate residues in GAG chains, providing an extra degree of rotational freedom over glucuronate-containing residues in the GAG chain (Casu et al., 1988). The flexibility conferred by iduronate residues may facilitate GAG, and thus PG, binding to the molecules they interact with. Two remaining GAGs, keratan sulfate (KS), which is rare in the nervous system, and hyaluronate (HyA), an unsulfated GAG that is not attached to PG cores, will not be discussed here.

Figure 2 shows a postulated model for the biosynthesis of HeS, based on and patterned after a model for the synthesis of heparin (Lindahl et al., 1986). Lindahl and colleagues have found the modification steps in heparin synthesis to be sequential, where each modification is required to form the correct substrate for the next modification. Gallagher and colleagues have described a feature of HeS, that it contains alternating domains of high and low sulfation,

that is a consequence of this stepwise modification [reviewed in (Gallagher et al., 1992)]. Because the epimerization step is pre-requisite to all sulfation steps, only iduronate-containing regions will have high levels of sulfation. In HeS from human skin fibroblasts, the highly sulfated domains averaged five disaccharides in length, while the N-acetlylated regions were roughly 18 disaccharides long (figure 1). The domain structure of HeS sets it apart from heparin, which is highly modified along the full length of the chain.

Cellular control of glycosaminoglycan structure

Patterns of sulfation can confer sequence specificity to GAG structures. For example, heparin and some heparan sulfates contain a particular pentasaccharide sequence that is strongly bound by the serine protease inhibitor antithrombin III (figure 3). Heparin or HeS molecules that do not contain this sequence bind to antithrombin with an affinity that is 1000-fold lower than molecules that bear the pentasaccharide [reviewed in (Bjork and Lindahl, 1982)] Intriguingly, recent work involving overexpression of the heparan sulfate proteoglycan (HSPG) syndecan-4/ryudocan in L cells implies the existence of a regulatory factor that both recognizes the core protein and is required for construction of the pentasaccharide sequence (Shworak et al., 1994b): When the core protein (even a core with no GAG attachment sites) was overexpressed, GAG sulfation levels (including the rare 3-O sulfation found in the pentasaccharide) were unaffected; however, the net level of pentasaccharide sequence produced did not plateau as might be expected, but rather *declined*, suggesting that the pentasaccharide may be constructed by multi-component complex which includes a non-biosynthetic regulatory factor that the core may titrate out. Conceivably, the regulation of the GAG structure of PGs, including GAG type as well as particular GAG modifications, could involve such regulatory intermediates that couple particular PG cores with molecules (or cellular locations) that are required for such GAG modifications.

The heparin sequences required for binding of fibroblast growth factors 1 and 2 [FGF-1 (acidic FGF) and FGF-2 (basic FGF)] have also been elucidated [figure 3; (Habuchi et al., 1992; Turnbull et al., 1992;

Mach et al., 1993)]. Several studies of FGF function support the idea that formation of these specific GAG sequences is under cellular control, and that particular PG cores may receive specific GAG modifications. Aviezer et al. (1994b) found that the cell-surface HSPGs syndecan-1, glypican, and syndecan-2/fibroglycan, immunopurified from human fetal lung fibroblasts, not only failed to promote FGF-2 binding to its high affinity receptor, but also reversibly inhibited, in a dose-dependent manner, the stimulation by heparin of FGF-2 receptor binding. On the other hand, the basement membrane HSPG perlecan, produced in the same cells as the cell-surface PGs, promotes FGF-2 binding to its receptor, an activity that is abolished by removal of perlecan's HeS chains with heparinase (Aviezer et al., 1994b). At least one of the cell-surface PGs isolated from a different source, syndecan-1 from mouse mammary epithelial cells, has been shown to bind to FGF-2 via its HeS chains (Bernfield and Hooper, 1991). Thus, the inhibitory effect of the cell-surface PGs on FGF receptor binding is unlikely to be caused by core protein interference. These results suggest that cell-surface HSPGs and a secreted HSPG from the same cell type have opposite effects on FGF-2 binding to the cell surface. The recognition of particular PG cores as candidates for attachment of specific GAG modifications within a single cell type implies the existence of regulatory factors that discriminate among core proteins. No basis for such identification has been suggested by the primary sequences of cores; presumably, core secondary structure forms a recognition signal of some sort.

The developmental stage of a cell or tissue may also determine specific GAG modifications. Nurcombe et al., (1993) found that an HSPG secreted by murine neuroepithelial cells exhibited developmentally controlled binding to FGFs: PG purified from embryonic day E9 cells preferentially bound FGF-2, while PG isolated from E11 cells bound FGF-1 about twice as well as FGF-2. Additionally, David et al., (1992) have demonstrated that antibodies to specific HeS epitopes reveal distinct, non-overlapping patterns throughout hamster embryonic development.

Functions of glycosaminoglycan binding

How does GAG binding affect protein function? Although in most cases, the direct effects of GAG binding are not known, a few cases where GAG effects have been found suggest that a conformational change in the protein often results from GAG binding. Such a conformational change may, in turn, affect the protein's ability to interact with and affect the activity of other ligands, and eventually, the behavior of cells.

Several heparin-binding proteins have demonstrated GAG-mediated conformational changes, or changes in activity that suggest conformational change. When Osterlund et al. (1985) isolated alveolar HeS fractions on the basis of sulfation, then bound these fractions to the extracellular matrix glycoprotein fibronectin, the protein underwent a conformational change, the magnitude of which roughly corresponded to the degree of sulfation in the HeS fractions. Activation of the FGF signalling pathway is likely to involve a conformational change in FGF caused by heparin binding: Ornitz et al. (1995) found that even small, nonsulfated di- and tri-saccharides found within heparin could activate the FGF-2 signalling pathway and cause dimerization of the growth factor. Although high concentrations of the oligosaccharides were required, they are still too small to bridge two FGF molecules together, suggesting that these oligosaccharides are inducing a conformational change in FGF-2 that facilitates dimerization, and thus activation of the high affinity receptor. This result does not rule out that heparin bridging between FGF molecules ("template effect") may also be occurring during FGF dimerization and activation by larger heparin and HeS molecules.

Another possible effect of GAG binding is ternary complex formation or the template effect [also called the "coreceptor hypothesis" (Bernfield et al., 1992)], which describes GAG binding that facilitates protein-protein interactions between two GAG-binding molecules. In fact, for another secreted molecule, antithrombin III, activation is likely to involve both template and allosteric effects. Heparin-mediated activation of antithrombin's inhibition of one of its protease substrates, thrombin, undoubtedly involves formation of a ternary complex between the three molecules [(Hoylaerts et al., 1984;

Peterson et al., 1987; Olson et al., 1991; Pratt et al., 1992; Streusand et al., 1995); reviewed in (Bjork and Lindahl, 1982)]. However, the antithrombin-binding pentasaccharide sequence found in heparin and HeS (figure 3), not only elicits a conformational change in antithrombin, but also activates antithrombin inhibition of thrombin to some extent (Streusand et al., 1995). Furthermore, the pentasaccharide sequence accelerates antithrombin inhibition of other proteases (e.g., factor Xa; plasmin) that do not bind heparin and thus cannot form a ternary complex with antithrombin and heparin (Jordan et al., 1980; Streusand et al., 1995). These studies suggest that one effect of GAG binding by antithrombin is to induce a conformational change that increases the activity of the protein. On the other hand, template effects are considerable: Second-order rate constants for maximal heparin-mediated acceleration of antithrombin inhibition of thrombin have been reported to be as high as $4x10^7$ $M^{-1}s^{-1}$ (Streusand et al., 1995), close to the diffusion controlled limit of 10^8 - 10^9 $M^{-1}s^{-1}$ (Fersht, 1985), and ~2700-fold higher than antithrombin acceleration due to pentasaccharide-binding alone (Streusand et al., 1995).

The examples of antithrombin and FGF-2 binding to heparin suggest that a feature of GAGs that may control binding is the presence of specific, strong ligand-binding sequences. However, a recent study by Olson and colleagues (Streusand et al., 1995) suggests that high- and low-affinity heparin binding differ more with respect to the *magnitude* of the effect of heparin binding than to the *kind* of effect. Using fractions of heparin with low and high affinity for antithrombin (LAH and HAH, respectively), these authors measured both conformational effects and activation of anti-protease activity in antithrombin. Their result showed that LAH and HAH bound at the same site on and induced a similar conformational change in antithrombin, but the *magnitude* of the change was decreased 5-6 fold when LAH was bound than when HAH was bound. The magnitude of the conformational change mirrored the effect on antithrombin activity: At heparin concentrations 100-fold higher than was needed with HAH, maximal acceleration of antithrombin's rate of inhibition of factor Xa by LAH was reduced 4-fold compared to acceleration due to HAH. (The effect of LAH on the thrombin inhibition rate was reduced

much more, but this result is due to changes in ternary complex order of binding -- see discussion in chapter III). This study suggests, therefore, that while specific, strong-binding sequences in GAGs may greatly affect a GAG-binding protein's activity, weaker-binding GAGs, under conditions of high concentration, may effect similar and significant responses. In the brain, GAG concentrations are high (probably in the mg/ml range -- see chapter III); It may be, therefore, that GAG effects that appear weak in vitro have more significance in vivo.

Studies using deletion mutations, substitution mutations, and function-blocking antibodies have revealed that for many proteins, the polypeptide sequences responsible for GAG binding fall into consensus patterns, first proposed by Cardin and Weintraub (1989), of BBXB or BBBXXB, where B refers to a basic amino acid. Molecules that have consensus sequences or similar clusters of basic amino acids in their heparin binding domains include antithrombin III, FGF-1 and -2, fibronectin's two heparin binding domains, four binding sites on laminin-1, and the amino-terminal heparin binding site in thrombospondin-1 (Jackson et al., 1991). In antithrombin, basic amino acid residues within distinct disulfide loops of the molecule come together to form the heparin binding domain (Jackson et al., 1991). In a few cases, heparin binding sequences that have few or no basic amino acids have been proposed. For example, in thrombospondin-1, a putative heparin binding sequence, located in the type 1 repeat region of the molecule, has the sequence, Trp-Ser-Xaa-Trp (WSXW) (Guo et al., 1992). Peptides containing this sequence bind weakly to heparin conjugated to BSA, compete with thrombospondin-1 and laminin-1 binding to immobilized heparin-BSA, and inhibit heparin-dependent binding of FGF-2 to corneal endothelial cells (Guo et al., 1992; Vogel et al., 1993). Another non-consensus heparin binding domain may lie closer to the calcium-binding carboxy termain region of thrombospondin: A 140 kD thrombospondin-derived monomer that has the type 1 repeats deleted but includes thrombospondin's calcium-binding domain, binds heparin agarose well, eluting at 0.3M salt, but only binds in the presence of calcium (Lawler et al., 1992). This suggests that tertiary structure resulting

from calcium binding controls the heparin binding conformation of this region.

Finally, a feature of GAG-binding that has remained largely unexplored with respect to many of the large, extracellular matrix glycoproteins is that of multimeric binding of GAGs. Intact laminin-1 and fibronectin molecules have at least four heparin-binding sites, while the trimeric thrombospondin-1 molecule may have as many as nine. Multisite binding by individual PGs or GAGs is quite possible: Cerebroglycan, a nervous system specific HSPG, has an estimated diameter of 130 Å [from Stokes radius determination†, (Stipp, 1996)], and HeS chains, which range from 30 to 100 disaccharides in length (Gallagher et al., 1992), have estimated extended lengths of 250 to 840 Å. For comparison, a thrombospondin-1 molecule appears 540 Å long from end to end in electron microscopy (Lawler et al., 1985); heparin binding domains along the monomer are expected to be closer, while those on adjacent arms may directly adjoin each other. GAGs and PGs, in view of their extended molecular shape, have the potential to participate in multimeric binding both between adjacent molecules and between relatively distant sites on large extracellular matrix molecules.

Potential ligands for brain proteoglycans and glycosaminoglycans

The work presented in this thesis involves the use of a large group of heparin-binding (or potential heparin-binding) molecules found in the brain. Molecules from three categories were chosen: extracellular matrix molecules, cell-surface adhesion molecules, and cell-secreted molecules. Each of these proteins is known, not only for its ability to bind heparin and its expression in the developing brain, but also for its effects on the in vitro behaviors of neural cells.

Extracellular matrix glycoproteins are represented by fibronectin, laminin-1, and thrombospondin-1. Fibronectin has expression patterns that suggest roles in axon growth in the developing cortex (Stewart and Pearlman, 1987; Sheppard et al., 1991) and in neural crest cell migration, while in vitro, fibronectin supports both cell

---

† Cerebroglycan's core protein is only ~ 57 kD, yet the Stokes radius for the intact PG is similar to that of β-galactosidase, a 540 kD protein.

attachment and neurite outgrowth of sensory and sympathetic neurons [reviewed in (Rogers et al., 1989; Hynes and Lander, 1992)]. Laminin-1 is also implicated in axon outgrowth and guidance in the nervous system. For example, laminin is expressed in the avian optic tract at times when retinal ganglion cells are extending axons; further, laminin substrata promote neurite extension by retinal ganglion cells in vitro only when the cells have been isolated from developmental stages that correspond with laminin expression (Cohen et al., 1986; Cohen et al., 1987). Thrombospondin-1 expression is widespread in neural development (O'Shea and Dixit, 1988), and may be associated with cell migration. For example, antibodies to thrombospondin-1 block the migration of granule cells from the external granule layer to the molecular layer during cerebellar development (O'Shea et al., 1990).

Two molecules, NCAM and the related molecule L1, represented cell-surface adhesion proteins in this study. Both proteins can participate in homophilic cell-cell adhesion, and numerous studies have implicated HeS and/or HSPGs in NCAM-mediated cell-cell adhesion, as well as cellular adhesion to NCAM substrates (Cole et al., 1985; Cole et al., 1986; Cole and Glaser, 1986b; Cole and Burg, 1989; Reyes et al., 1990; Kallapur and Akeson, 1992). NCAM is found throughout the developing nervous system, where its expression is present on all neurons examined and with a relatively uniform distribution in the brain [reviewed in (Linnemann and Bock, 1989)]. In vivo effects of anti-NCAM antibodies include perturbation of optic fibre projection to the optic tectum in Xenopus, and inhibition of cerebellar granule cell migration [reviewed in (Linnemann and Bock, 1989; Goridis and Brunet, 1992)].

In embryonic and early postnatal NCAM preparations, a significant fraction of the molecules are N-substituted with a significant amount of long chains of α2,8-polysialic acid (Finne et al., 1983). In the cerebellum, PSA-NCAM forms a subset of NCAM expression, and is detectable only in postmitotic and migrating granule neurons, while expresssion by other cerebellar cells (including Bergmann glia, Purkinje cells, stellate and basket cells) ceases at the end of cerebellar histogenesis (Hekmat et al., 1990).

Rutishauser and others postulate that one function of PSA may be to serve as a negative regulator of cell-cell interactions: the length and anionic nature of PSA provide charge repulsion and hydration effects that physically restrict cell-cell membrane contacts [cf (Yang et al., 1994)]. Two recent studies give credence to this hypothesis: First, membrane vesicles containing PSA-NCAM are less adhesive in low ionic strength buffers than in higher salt conditions (where the PSA is expected to be more collapsed) (Yang et al., 1994); and second, enzymatic removal of PSA slows the rate of retinal cell process outgrowth on chick tectal membranes, an effect that is partially reversed by anti-L1 antibodies, suggesting that PSA inhibits L1 binding between cells (Zhang et al., 1992). In accord with this putative role for PSA, PSA-NCAM is most prominently expressed during histogenesis of the central nervous system, a time when a plenitude of cell migrations and axon extensions are occurring [cf (Sunshine et al., 1987; Becker et al., 1993)].

L1, also called NgCAM in chick, is a cell-adhesion molecule that is structurally related to NCAM, but has a more restricted distribution in the nervous system, and its expression is closely correlated with neuronal migration, axonogenesis, and maturation [reviewed in (Linnemann and Bock, 1989)]. L1-mediated cell-cell adhesion appears to occur by homophilic binding between neurons and by heterophilic binding to an unidentified molecule in neural-glial cell interactions [reviewed in (Linnemann and Bock, 1989)]. In developing cerebellar explant cultures from both mouse and chick, L1 is strongly expressed on postmitotic and migrating granule neurons, and anti-L1 Fab fragments and antibodies inhibit granule cell migration (Lindner et al., 1983; Grumet, 1992). Anti-L1 antibodies also inhibit the ensheathment of neurons by Schwann cells in vitro (Seilheimer et al., 1989). It is not known if L1 binds heparin, and effects, if any, of heparin or other GAGs on L1 function have not been reported.

Four molecules in this thesis represent cell-secreted proteins of the nervous system. Each of these molecules, fibroblast growth factor-2 (FGF-2, also called basic FGF), protease nexin-1 (PN-1), thrombin, and urokinase plasminogen activator (uPA), is abundant during and after development of the nervous system, and each is a

heparin-binding protein. Thus the likelihood of GAG and/or PG regulation of the behaviors of these molecules is significant.

FGF-2 along with the related growth factor FGF-1 (acidic FGF), is widely expressed both throughout development of the nervous sytem and in adult tissues (Gonzalez et al., 1990; Fu et al., 1991; Wilcox and Unnerstall, 1991; Gomez-Pinilla et al., 1992). In vitro, FGF-2 stimulates the proliferation and survival of neural cells (Walicke et al., 1986; Unsicker et al., 1987; Walicke, 1988; Murphy et al., 1990; Hughes et al., 1993), and its effects are mediated by heparin and HeS binding, including binding to the cell surface HSPG syndecan-1 and the extracellular matrix PG perlecan [see above; also (Kiefer et al., 1990)].

The remaining three cell-secreted molecules used in this study form a functionally related set of molecules that each play roles in neural behaviors; each is also known to bind heparin. Two serine proteases found in brain, urokinase plasminogen activator (uPA) and thrombin, are inhibited by another brain molecule, the serine protease inhibitor (or "serpin"), protease nexin-1 (PN-1). Inhibition of thrombin and uPA by PN-1 occurs when PN-1 binds its target protease at the site of the protease's reactive serine, forming a long-lived complex (for more details on serpin-protease reactions, see chapter III). PN-1 (also known as glial-derived nexin), is expressed by both neural and glial cell lines, and is very abundant in both the central and peripheral nervous systems throughout development (Wagner et al., 1991; Mansuy et al., 1993). In the mature mouse, constitutive expression of PN-1 is high in the olfactory bulb, while brain glial cell expression is elevated in response to injury (Reinhard et al., 1988; Reinhard et al., 1994). In vitro, PN-1 stimulates neurite outgrowth in neuroblastoma cells [(Monard et al., 1983); reviewed in (Cunningham et al., 1992)]; inhibits cerebellar cell migration in culture (Lindner et al., 1986); and reverses thrombin-mediated inhibition of astrocyte stellation (Cunningham et al., 1992).

The serine proteases thrombin and uPA are also neurally expressed molecules that have known effects on neural cell behaviors. Prothrombin mRNA and thrombin receptor mRNA expression patterns suggest that widespread and abundant expression of thrombin occurs throughout brain development (Dihanich et al., 1991;

Weinstein et al., 1995), while uPA mRNA is strongly expressed throughout and after development, in both the peripheral and central nervous systems (Sumi et al., 1992; Dent et al., 1993).

Thrombin inhibits astrocyte stellation in cultured astroglia and induces neurite retraction in cultured neuroblastoma cells (Cavanaugh et al., 1990; Cunningham, 1992). Each of these thrombin activities is completely reversible by the addition of PN-1. The effects of uPA exhibit dependence on neural cell type: Inhibition of uPA slows the migration of cultured cerebellar granule neurons (Moonen et al., 1992), while inhibition of uPA protease activity increases neurite outgrowth and growth cone lamellipodial activity in cultured sympathetic neurons (Pittmann et al., 1989). Interestingly, while PN-1 will inhibit uPA in the culture medium from neuroblastoma cells, cell-bound PN-1 appears unable to inhibit uPA (Wagner et al., 1991).

PN-1 is related to antithrombin, and like antithrombin, its inhibitory activity toward thrombin is increased in the presence of heparin (see discussion of GAG binding above and chapter III). It seemed likely, therefore that brain GAGs may also influence the inhibition of thrombin and uPA by PN-1. This issue is addressed by work presented in Chapter III of this thesis.

Chapter II addresses the binding of each of these extracellular, secreted, and cell-surface proteins to glycosaminoglcans purifed from brain proteoglycans at two developmental stages. And Chapter I begins the thesis with some earlier work that demonstrated the abundance and diversity of proteoglycans expressed in the developing rat brain. Overall, the work is an attempt to establish a foundation for understanding how PGs and GAGs in the brain may affect the pericellular events that control cell behaviors during development.

Acknowledgements

I am grateful to Chris Stipp for providing Table 2, and for his assistance in creating the remaining figures and table for this chapter, which were shared productions.

REFERENCES

Adams, J.C. and J. Lawler. 1994. Cell-type specific adhesive interactions of skeletal myoblasts with thrombospondin-1. Molec. Biol. Cell 5:423-437.

Aviezer, D., D. Hecht, M. Safran, M. Eisinger, G. David, and A. Yayon. 1994b. Perlecan, basal lamina proteoglycan, promotes basic fibroblast growth factor-receptor binding, mitogenesis, and angiogenesis. Cell 79:1005-1013.

Baciu, P.C., C. Acaster, and P.F. Goetinck. 1994. Molecular cloning and genomic organization of chicken syndecan-4. J. Biol. Chem. 269:669-703.

Bahr, B.A., K. Noremberg, G.A. Rogers, B.W. Hicks, and S.M. Parsons. 1992. Linkage of the acetylcholine transporter-vesamicol receptor to proteoglycan in synaptic vesicles. Biochem. 31:5778-5784.

Bajjalieh, S.M., K. Peterson, R. Shinghal, and R.H. Scheller. 1992. SV2, a brain synaptic vesicle protein homologous to bacterial transporters. Science 257:1271-1273.

Becker, T., C.G. Becker, U. Niemann, C. Naujoks-Manteuffel, R. Gerardy-Schahn, and G. Roth. 1993. Amphibian-specific regulation of polysialic acid and the neural cell adhesion molecule in development and regeneration of the retinotectal system of the salamander Pleurodeles waltl. J. Comp. Neurol. 336:532-544.

Bernfield, M. and K.C. Hooper. 1991. Possible regulation of FGF activity by syndecan, an integral membrane heparan sulfate proteoglycan. Ann. NY Acad. Sci. 638:182-194.

Bernfield, M., R. Kokenyesi, M. Kato, M.T. Hinkes, J. Spring, R.L. Gallo, and E.J. Lose. 1992. Biology of the syndecans: a family of

transmembrane heparan sulfate proteoglycans. Annu. Rev. Cell Biol. 8:365-393.

Bjork, I. and U. Lindahl. 1982. Mechanism of the anticoagulant action of heparin. Molec. Cell. Biochem. 48:161-182.

Cardin, A.D. and H.J.R. Weintraub. 1989. Molecular modeling of protein-glycosaminoglycan interactions. Arteriosclerosis 9:21-32.

Carey, D., D. Evans, R. Stahl, V. Asundi, K. Conner, P. Garbes, and G. Cizmeci-Smith. 1992. Molecular cloning and characterization of N-syndecan, a novel transmembrane heparan sulfate proteoglycan. J. Cell Biol. 117:191-201.

Carey, D.J., R.C. Stahl, V.K. Asundi, and B. Tucker. 1993. Processing and subcellular distribution of the Schwann cell lipid-anchored heparan sulfate proteoglycan and identification as glypican. Exp. Cell Res. 208:10-18.

Casu, B., M. Petitou, M. Provasoli, and P. Sinay. 1988. Conformational flexibility: a new concept for explaining binding and biological properties of iduronic acid-containing glycosaminoglycans. TIBS 13:221-225.

Cavanaugh, K.P., D. Gurwitz, D.D. Cunningham, and R.A. Bradshaw. 1990. Reciprocal modulation of astrocyte stellation by thrombin and protease nexin-1. J. Neurochem. 54:1735-1743.

Cheifetz, S. and J. Massague. 1989. The TGF-β receptor proteoglycan: cell surface expression and ligand binding in the absence of glycosaminoglycan chains. J. Biol. Chem. 264:12025-12028.

Cohen, J., J.F. Burne, C. McKinlay, and J. Winter. 1987. The role of laminin and the laminin/fibronectin receptor complex in the outgrowth of retinal ganglion cell axons. Dev. Biol. 122:407-418.

Cohen, J., J.F. Burne, J. Winter, and P. Bartlett. 1986. Retinal ganglion cells lose response to laminin with maturation. Nature 322:465-467.

Cole, G.J. and M. Burg. 1989. Characterization of a heparan sulfate proteolglycan that copurifies with the neural cell adhesion molecule. Exp. Cell Res. 182:44-60.

Cole, G.J. and L. Glaser. 1986b. A heparin-binding domain from N-CAM is involved in neural cell-substratum adhesion. J. Cell Biol. 102:403-412.

Cole, G.J., A. Loewy, and L. Glaser. 1986. Neuronal cell-cell adhesion depends on interactions of N-CAM with heparin-like molecules. Nature 320:445-447.

Cole, G.J., D. Schubert, and L. Glaser. 1985. Cell-substratum adhesion in chick neural retinal depends upon protein-heparan sulfate interactions. J.B.C. 100:1192-1199.

Cunningham, D.D. 1992. Regulation of neuronal cells and astrocytes by protease nexin-1 and thrombin. Ann. N. Y. Acad. Sci. 674:228-236.

Cunningham, D.D., S.L. Wagner, and D.H. Farrell. 1992. Regulation of protease nexin-1 activity by heparin and heparan sulfate. *In* Heparin and Related Polysaccharides, Lane, D. A., I. Bjork, and U. Lindahl, editors. (New York: Plenum), pp. 297-306.

David, G., X.M. Bai, B.V.D. Schueren, J.J. Cassiman, and H.V.D. Berghe. 1992. Developmental changes in heparan sulfate expression: In situ detection with mAbs. J. Cell Biol. 119:961-975.

David, G., X.M. Bai, B.Y.d. Schueren, P. Marynen, J. Cassiman, and H.V.d. Berghe. 1993. Spatial and temporal changes in the expression of fibroglycan (syndecan-2) during mouse embryonic development. Development 119:841-854.

Dent, M.A.R., Y. Sumi, R.J. Morris, and P.J. Seeley. 1993. Urokinase-type plasminogen activator expression by neurons and oligodendrocytes during process outgrowth in developing rat brain. Eur. J. Neurosci. 5:633-647.

Dihanich, M., M. Kaser, E. Reinhard, D. Cunningham, and D. Monard. 1991. Prothrombin mRNA is expressed by cells of the nervous system. Neuron 6:575-581.

Dou, C. and J.M. Levine. 1994. Inhibition of neurite growth by the NG2 chondrotin sulfate proteoglycan. J. Neurosci. 14:7616-7628.

Faissner, A., A. Clement, A. Lochter, A. Streit, C. Mandl, and M. Schachner. 1994. Isolation of a neural chondroitin sulfate proteoglycan with neurite outgrowth promoting properties. J. Cell Biol. 126:783-799.

Feany, M.B., S. Lee, R.H. Edwards, and K.M. Buckley. 1992. The synaptic vesicle protein SV2 is a novel type of transmembrane transporter. Cell 70:861-867.

Fersht, A. (1985). Enzyme Structure and Mechanism, 2nd Edition (New York: W. H. Freeman and Company).

Filmus, J., J.G. Church, and R.N. Buick. 1988. Isolation of a cDNA corresponding to a developmentally regulated transcript in rat intestine. Mol. Cell Biol. 8:4243-4249.

Filmus, J., W. Shi, Z.M. Wong, and M.J. Wong. 1995. Identification of a new membrane-bound heparan sulfate proteoglycan. Biochem. J. 311:561-565.

Finne, J., U. Finne, H. Deagostini-Bazin, and C. Goridis. 1983. Occurence of α2-8 linked polysialosyl units in a neural cell adhesion molecule. Biochem. Biophys. Res. Comm. 112:482-490.

Friedlander, D.R., P. Milev, L. Karthikeyan, R.K. Margolis, R.U. Margolis, and M. Grumet. 1994. The neuronal chondroitin sulfate proteoglycan neurocan binds to the neural cell adhesion molecules Ng-CAM/L1/NILE and N-CAM, and inhibits neuronal adhesion and neurite outgrowth. J. Cell Biol. 125:669-680.

Fryer, H.J.L., G.M. Kelly, L. Molinaro, and S. Hockfield. 1992. The high molecular weight Cat-301 chondroitin sulfate proteoglycan from brain is related to the large aggregation proteoglycan from cartilage, aggrecan. J. Biol. Chem. 267:9874-9883.

Fu, Y.-M., P. Spirito, Z.-X. Yu, S. Biro, J. Sasse, J. Lei, V.J. Ferrans, S.E. Epstein, and W. Casscells. 1991. Acidic fibroblast growth factor in the developing rat embryo. J. Cell Biol. 114:1261-1273.

Gallagher, J.T., J.E. Turnbull, and M. Lyon. 1992. Patterns of sulphation in heparan sulfate: polymorphism based on a common structural theme. Int. J. Biochem. 24:553-560.

Gomez-Pinilla, F., J.W.-K. Lee, and C.W. Cotman. 1992. Basic FGF in adult rat brain: Cellular distribution and response to entorhinal lesion and fimbria-fornix transection. J. Neurosci. 12:345-355.

Gonzalez, A., M. Buscaglia, M. Ong, and A. Baird. 1990. Distribution of basic fibroblast growth factor in the 18-day rat fetus: localization in the basement membrane of diverse tissues. J. Cell Biol. 110:753-765.

Goridis, C. and J.F. Brunet. 1992. NCAM: structural diversity, function, and regulation of expression. Semin. Cell Biol. 3:189-197.

Gould, S.E., W.B. Upholt, and R.A. Kosher. 1992. Syndecan 3: A member of the syndecan family of membrane-intercalated proteoglycans that is expressed in high amounts at the onset of chicken limb cartilage differentiation. Proc. Natl. Acad. Sci. USA 89:3271-3275.

Gould, S.E., W.B. Upholt, and R.A. Kosher. 1995. Characterization of chicken syndecan-3 as a heparan sulfate proteoglycan and its expression during embryogenesis. Dev. Biol. 168:438-451.

Grumet, M. 1992. Structure, expression, and function of Ng-CAM, a member of the immunoglobulin superfamily involved in neuron-neuron and neuron-glia adhesion. J. Neurosci. Res. 31:1-13.

Grumet, M., A. Flaccus, and R.U. Margolis. 1993. Functional characterization of chondroitin sulfate proteoglycans of brain: Interactions with neurons and neural cell adhesion molecules. J. Cell Biol. 120:815-824.

Grumet, M., P. Milev, T. Sakurai, L. Karthikeyan, M. Bourdon, R.K. Margolis, and R.U. Margolis. 1994. Interactions with tenascin and differential effects on cell adhesion of neurocan and phosphacan, two major chondroitin sulfate proteoglycans of nervous tissue. J. Biol. Chem. 262:12142-12146.

Guo, N., H.C. Krutzsch, E. Negre, V.S. Zabrenetzky, and D.D. Roberts. 1992. Heparin-binding peptides from the type I repeats of thrombospondin. J. Biol. Chem. 267:19349-19355.

Habuchi, H., S. Suzuki, T. Saito, T. Tamura, T. Harada, K. Yoshida, and K. Kimata. 1992. Structure of a heparan sulphate oligosaccharide that binds to basic fibroblast growth factor. Biochem. J. 285:805-813.

Halfter, W. 1993. a heparan sulfate proteoglycan in developing avian axonal tracts. J. Neurosci. 13:2863-2873.

Halfter, W. and B. Schurer. 1994. A new heparan sulfate proteoglycan in the extracellular matrix of the developing chick embryo. Exp. Cell Res. 214:285-296.

Hanemann, C.O., G. Kuhn, A. Lie, C. Gillen, F. Bosse, P. Spreyer, and H.W. Muller. 1993. Expression of decorin mRNA in the nervous system of rat. J. Histochem. Cytochem. 41:1383-1391.

Hekmat, A., D. Bitter-Suermann, and M. Schachner. 1990. Immunocytological localization of the highly polysialylated form of the neural cell adhesion molecule during development of the murine cerebellar cortex. J. Comp. Neurol. 291:457-467.

Hockfield, S., R.G. Kalb, S. Zaremba, and H.J.L. Fryer. 1990. Expression of neural proteoglycans correlates with the acquisition of mature neruonal properties in the mammalian brain. Cold Spring Harbor Symp. Quant. Biol. 55:505-514.

Hoylaerts, M., W.G. Owen, and D. Collen. 1984. Involvement of heparin chain length in the heparin-catalyzed inhibition of thrombin by antithrombin III. J. Biol. Chem. 259:5670-5677.

Hughes, R.A., M. Sendtner, M. Goldfarb, D. Lindholm, and H. Thoenen. 1993. Evidence that fibroblast growth factor 5 is a major muscle-derived survival factor for cultured spinal motoneurons. Neuron 10:369-377.

Hynes, R.O. and A.D. Lander. 1992. Contact and adhesive specificities in the associations, migrations, and targeting of cells and axons. Cell 68:303-322.

Iozzo, R.V., I.R. Cohen, S. Grassel, and A.D. Murdoch. 1994. The biology of perlecan: The multifaceted heparan sulphate proteoglycan of basement membranes and pericellular matrices. Biochem. J. 302:625-639.

Iwata, M. and S.S. Carlson. 1993. A brain extracellular matrix proteoglycan forms aggregates with hyaluronan. J. Biol. Chem. 268:15061-15069.

Jackson, R.L., S.J. Busch, and A.D. Cardin. 1991. Glycosaminoglycans: molecular properties, protein interactions, and role in physiological processes. Physiol. Rev. 71:481-539.

Jordan, R.E., G.M. Oosta, W.T. Gardner, and R.D. Rosenberg. 1980. The kinetics of hemostatic enzyme-antithrombin interactions in the presence of low molecular weight heparin. J. Biol. Chem. 255:10081-10090.

Joseph, S.J., M.D. Ford, and V. Nurcombe. 1995. A novel heparan sulfate proteoglycan involved in the regulation of FGFs in mouse embryonic brain is a putative perlecan homologue. Soc. Neurosci. Abstracts 21:1041.

Kallapur, S.G. and R.A. Akeson. 1992. The neural cell adhesion molecule (NCAM) heparin binding domain binds to cell surface heparan sulfate proteoglycans. J. Neurosci. Res. 33:538-548.

Karthikeyan, L., M. Flad, M. Engel, B. Meyer-Puttlitz, R.U. Margolis, and R.K. Margolis. 1994. Immunocytochemical and in situ hybridization studies of the heparan sulfate proteoglycan, glypican, in nervous tissue. J. Cell Sci. 107:3213-3222.

Kiefer, M.C., J.C. Stephans, K. Crawford, K. Okino, and P.J. Barr. 1990. Ligand-affinity cloning and structure of a cell surface heparan sulfate proteoglycan that binds basic fibroblast growth factor. Proc. Natl. Acad. Sci. USA 87:6985-6989.

Kim, C.W., O.A. Goldberger, R.L. Gallo, and M. Bernfield. 1994. Members of the syndecan family of heparan sulfate proteoglycans are expressed in distinct cell-, tissue-, and development-specific patterns. Mol. Biol. Cell 5:797-805.

Kojima, T., N.W. Shworak, and R.D. Rosenberg. 1992. Molecular cloning an expression of two distinct cDNA-encoding heparan sulfate

proteoglycan core proteins from a rat endothelial cell line. J. Biol. Chem. 267:4870-4877.

Krueger, N.X. and H. Saito. 1992. A human transmembrane protein-tyrosine phosphatase PTPζ, is expressed in brain and has an N-terminal receptor domain homologous to carbonic anhydrases. Proc. Natl. Acad. Sci. USA 89:7417-7421.

Krusius, T. and E. Ruoslahti. 1986. Primary structure of an extracellular matrix proteoglycan core protein deduced form cloned cDNA. Proc. Natl. Acad. Sci. USA 83:7683-7687.

Lawler, J., L.H. Derick, J.E. Connolly, J.-H. Chen, and F.C. Chao. 1985. The structure of human platelet thrombospondin. J. Biol. Chem. 260:3762-3772.

Lawler, J., P. Ferro, and M. Duquette. 1992. Expression and mutagenesis of thrombospondin. Biochemistry 31:1175-1180.

LeBaron, R.G., J.D. Esko, A. Woods, S. Johansson, and M. Höök. 1988. Adhesion of glycosaminoglycan-deficient Chinese hamster ovary cell mutants to fibronectin substrata. J. Cell Biol. 106:945-952.

Levine, J.M. 1994. Increased expression of the NG2 chondrotin-sulfate proteoglycan after brain injury. J. Neurosci. 14:4716-4730.

Levine, J.M. and W.B. Stallcup. 1987. Plasticity of developing cerebellar cells in vitro studied with antibodies against the NG2 antigen. J. Neurosci. 7:2721-2731.

Lin, W. 1990. Immunogold localization of basal laminar heparan sulfate proteoglycan in rat brain and retinal capillaries. Brain Res. Bull. 24:533-536.

Lindahl, U., D.S. Feingold, and L. Roden. 1986. Biosynthesis of heparin. Trends Biochem. Sci. 11:221-225.

Lindner, J., J. Guenther, H. Nick, G. Zinser, H. Antonicek, M. Schachner, and D. Mondar. 1986. Modulation of granule cell migration by a glia-derived protein. Proc. Natl. Acad. Sci. (USA) 83:4568-4571.

Lindner, J., F.G. Rathjen, and M. Schachner. 1983. L1 mono- and polyclonal antibodies modify cell migration in early postnatal mouse cerebellum. Nature 305:427-430.

Linnemann, D. and E. Bock. 1989. Cell adhesion molecules in neural development. Dev. Neurosci. 11:149-173.

Litwack, E.D. 1995. Expression and function of proteoglycans in the nervous system. PhD Thesis, Massachusetts Institute of Technology, Cambridge, MA.

Litwack, E.D., C.S. Stipp, A. Kumbasar, and A.D. Lander. 1994. Neuronal expression of glypican, a cell-surface glycosylphosphatidylinositol-anchored heparan sulfate proteoglycan, in the adult rat nervous system. J. Neurosci. 14:3713-3724.

Ma, E., R. Morgan, and E.W. Godfrey. 1994. Distribution of agrin mRNA in the chick embryo nervous system. J. Neurosci. 14:2943-2952.

Mach, H., D.B. Volkin, C.J. Burke, C.R. Middaugh, R.J. Linhardt, J.R. Fromm, D. Loganathan, and L. Mattson. 1993. Nature of the interaction of heparin with acidic fibroblast growth factor. Biochem. 32:5480-5489.

Mansuy, I.M., H.V.D. Putten, P. Schmid, M. Meins, F.M. Botteri, and D. Mondar. 1993. Variable and multiple expression of protease nexin-1 during mouse organogenesis and nervous system development. Development 119:1119-1134.

Maurel, P., U. Rauch, M. Flad, R.K. Margolis, and R.U. Margolis. 1994. Phosphacan, a chondroitin sulfate proteoglycan of brain that interacts with neurons and neural cell adhesion molecules, is an extracellular variant of a receptor-type protein tyrosine phosphatase. Proc. Natl. Acad. Sci. USA 91:2512-2516.

McMahon, U.J. 1990. The agrin hypothesis. Cold Spring Harbor Symp. Quant. Biol. 50:407-418.

Milev, P., D.R. Friedlander, T. Sakurai, L. Karthikeyan, M. Flad, R.K. Margolis, M. Grumet, and R.U. Margolis. 1994. Interactions of the chondroitin sulfate proteoglycan phosphocan, the extracellular domain of a receptor-type protein tyrosine phosphatase, with neurons, glia, and neural cell adhesion molecules. J. Cell. Biol. 127:1703-1715.

Miller, B., A.M. Sheppard, and A.L. Pearlman. 1992. Expression of two chondroitin sulfate proteoglycan core proteins in the subplate pathway of early cortical afferents. Soc. Neurosci. Abstr. 18:778.

Monard, D., E. Niday, A. Limat, and F. Solomon. 1983. Inhibition of protease activity can lead to neurite extension in neuroblastoma cells. Prog. Brain Res. 58:359.

Moonen, G., M.-P. Grau-Wagemans, and I. Selak. 1992. Plasminogen activator-plasmin system and neuronal migration. Nature 298:753-755.

Murphy, M., J. Drago, and P.F. Bartlett. 1990. Fibroblast growth factor stimulates the proliferation and differentiation of neural precursor cells in vitro. J. Neurosci. Res. 25:463-475.

Murphy-Ullrich, J.E., L.G. Westrick, J.D. Esko, and D.R. Mosher. 1988. Altered metabolism of thrombospondin by Chinese hamster ovary cells defective in glycosaminoglycan synthesis. J. Biol. Chem. 263:6400-6406.

Nakato, H., T.A. Futch, and S.B. Selleck. 1995. The division abnormally delated *(dally)* gene: A putative integral membrane proteoglycan required for cell division patterning during post-embryonic development of the nervous system in Drosophila. Development 121:3687.

Nurcombe, V., M.D. Ford, J.A. Wildschut, and P.F. Bartlett. 1993. Developmental regulation of neural response to FGF-1 and FGF-2 by heparan sulfate proteoglycan. Science 260:103-106.

O'Connor, L.T., J.C. Lauterborn, C.M. Gall, and M.A. Smith. 1994. Localization and alternative splicing of agrin mRNA in adult rat brain Transcripts encoding isoforms that aggregate acetylcholine receptors are not restricted to cholinergic regions. J. Neurosci. 14:1141-1152.

O'Shea, K.S. and V.M. Dixit. 1988. Unique distribution of the extracellular matrix component thrombospondin in the developing mouse embryo. J. Cell Biol. 107:2737-2748.

O'Shea, K.S., J.S.T. Rheinheimer, and V.M. Dixit. 1990. Deposition and role of thrombospondin in the histogenesis of the cerebellar cortex. J. Cell Biol. 110:1275-1284.

Olson, S.T., H.R. Halvorson, and I. Bjork. 1991. Quantitative characterization of the thrombin-heparin interaction. J.C.B. 266:6342-6352.

Oohira, A., F. Matsui, E. Watanabe, Y. Kushima, and N. Maeda. 1994. Developmentally regulated expression of a brain specific species of chondroitin sulfate proteoglycan, neurocan, identified with a monoclonal antibody 1G2 in the rat cerebrum. Neurosci. 60:145-157.

Ornitz, D.M., A.B. Herr, M. Nilsson, J. Westman, C.M. Svahn, and G. Waksman. 1995. FGF binding and FGF receptor activation by synthetic heparan-derived di- and trisaccharides. Science 268:432-436.

Osterlund, E., I. Eronen, K. Osterlund, and M. Vuento. 1985. Secondary structure of human plasma fibronectin: Conformational change induced by calf alveolar heparan sulfates. Biochemistry 24:2661-2667.

Perides, G., F. Rahemtulla, W.S. Lane, R.A. Asher, and A. Bignami. 1992. Isolation of a large, aggregating proteoglycan from human brain. J. Biol. Chem. 267:23883-23887.

Peterson, C.B., M.T. Morgon, and M.N. Blackburn. 1987. Identification of a lysyl residue in antithrombin which is essential for heparin binding. J. Biol. Chem. 262:8061-8065.

Pittmann, R.N., J.K. Ivins, and H.M. Buettner. 1989. Neuronal plasminogen activators: Cell surface binding sites and involvement in neurite outgrowth. J. Neurosci. 9:4269-4286.

Pratt, C.W., H.C. Whinna, and F.C. Church. 1992. A comparison of three heparin-binding serine proteinase inhibitors. J. Biol. Chem. 267:8795-8801.

Rapraeger, A., A. Krufka, and B.B. Olwin. 1991. Requirement of heparan sulfate for bFGF-mediated fibroblast growth and myoblast differentiation. Science 252:1705-1708.

Rauch, U., P. Gao, A. Janetzko, A. Flaccus, L. Hilgenberg, H. Tekotte, R.K. Margolis, and R.U. Margolis. 1991. Isolation and characterization of developmentally regulated chondroitin sulfate and chondrotin/keratan sulfate proteoglycans of brain identified with monoclonal antibodies. J. Biol Chem. 266:14785-14801.

Rauch, U., L. Karthikeyan, P. Maurel, R.U. Margolis, and R.K. Margolis. 1992. Cloning and primary structure of neurocan, a developmentally regulated, aggregating chondroitin sulfate proteoglycan. J. Biol. Chem. 267:19536-19547.

Reinhard, E., R. Meier, W. Halfter, G. Rovelli, and D. Monard. 1988. Detection of glia-derived nexin in the olfactory system of the rat. Neuron 1:387-394.

Reinhard, E., H.S. Suidan, A. Pavlik, and D. Monard. 1994. Glia-derived nexin/protease nexin-1 is expressed by a subset of neurons in the rat brain. J. Neurosci. Res. 37:256-270.

Reyes, A.A., R. Akeson, L. Brezina, and G.J. Cole. 1990. Structural requirements for neural cell adhesion molecule-heparin interaction. Cell Regulation 1:567-576.

Rogers, S.L., P.C. Letourneau, and I.V. Pech. 1989. The role of fibronectin in neural development. Dev. Neurosci. 11:248-265.

Saunders, S., M. Jalkanen, S. O'Farrell, and M. Bernfield. 1989. Molecular cloning of syndecan, an integral membrane proteoglycan. J. Biol. Chem. 108:1547-1556.

Scholzen, T., M. Solursh, S. Suzuki, R. Reiter, J.L. Morgan, A.M. Buchberg, L.D. Siracusa, and R.V. Iozzo. 1994. The murine decorin. J. Biol. Chem. 269:28270-28281.

Scranton, T.W., M. Iwata, and S.S. Carlson. 1993. The SV2 protein of synaptic vesicles is a keratan sulfate proteoglycan. J. Neurochem. 61:29-44.

Seilheimer, B., E. Persohn, and M. Schachner. 1989. Antibodies to the L1 adhesion molecule inhibit Schwann cell ensheathment of neurons in vitro. J. Cell Biol. 109:3095-3103.

Sheppard, M.M., S.K. Hamilton, and A.L. Pearlman. 1991. Changes in the distribution of extracellular matrix components accompany early morphogenetic events of mammalian cortical development. J. Neurosci. 11:3928-3942.

Shitara, K., H. Yamada, K. Watanabe, M. Shimonaka, and Y. Yamaguchi. 1994. Brain-specific receptor-type protein tyrosine phosphatase RPTPβ-is a chondroitin sulfate proteoglycan in vivo. J. Biol. Chem. 269:20189-20193.

Shworak, N.W., M. Shirakawa, S. Colliec-Jouault, J. Liu, R.C. Mulligan, L.K. Birinyi, and R.D. Rosenberg. 1994b. Pathway-specific regulation of the synthesis of anticoagulantly active heparan sulfate. J. Biol. Chem. 269:24941-24952.

Snow, A.D., H. Mar, D. Nochlin, H. Kresse, and T.N. Wight. 1992. Peripheral distribution of dermatan sulfate proteoglycans (decorin) in amyloid-containing plaques and their presence in neurofibrillary tangles of Alzheimer's disease. J. Hisotchem. Cytochem. 40:105-113.

Spring, J., S. Paine-Saunders, R.O. Hynes, and M. Bernfield. 1994. Drosophila syndecan: Conservation of a cell-surface heparan sulfate proteoglycan. Proc. Natl. Acad. Sci. USA 91:3334-3338.

Stallcup, W.B., L. Beasley, and J. Levine. 1983. Cell surface molecules that characterize different stages in the development of cerebellar interneurons. Cold Spring Harbor Symp. Quant. Biol. 48:761-774.

Steindler, D.A., D. Settles, H.P. Erickson, E.D. Laywell, A. Yoshiki, A. Faissner, and M. Kusakabe. 1995. Tenascin knockout mice: barrels, boundary molceules, and glial scars. J. Neurosci. 15:1971-1983.

Stewart, G.R. and A.L. Pearlman. 1987. Fibronectin-like immunoreactivity in the developing cerebral cortex. J. Neurosci. 7:3325-3333.

Stipp, C.S. 1996. Identification, Molecular Cloning, and Characterization of Cerebroglycan, A Cell Surface Heparan Sulfate Proteoglycan of the Developing Rat Brain. PhD Thesis, Massachusetts Institute of Technology, Cambridge, MA.

Stipp, C.S., E.D. Litwack, and A.D. Lander. 1994. Cerebroglycan: an integral membrane heparan sulfate proteoglycan that is unique to the developing nervous system and expressed specifically during neuronal differentiation. J. Cell Biol. 124:149-160.

Streusand, V.J., I. Bjork, P.G.W. Gettins, M. Petitou, and S.T. Olson. 1995. Mechanism of acceleration of antithrombin-proteinase reactions by low affinity heparin. J. Biol. Chem. 270:9043-9051.

Sumi, Y., M.A.R. Dent, D.E. Owen, P.J. Seeley, and a.R.J. Morris. 1992. The expression of tissue and urokinase-type plasminogen activators in neural development suggests different modes of proteolytic involvement in neuronal growth. Development 116:625-637.

Sunshine, J., K. Balak, U. Rutishauser, and M. Jacobson. 1987. Changes in neural cell adhesion molecule (NCAM) structure during vertbrate neural development. Proc. Natl. Acad. Sci. (USA) 84:5986-5990.

Tsen, G., W. Halfter, S. Kroger, and G.J. Cole. 1995. Agrin is a heparan sulfate proteoglycan. J. Biol. Chem. 270:3392-3399.

Turnbull, J.E., D.G. Fernig, Y. Ke, M.C. Wilkinson, and J.T. Gallagher. 1992. Identification of the basic fibroblast growth factor binding sequence in fibroblast heparan sulfate. J. Biol. Chem. 267:10337-10341.

Unsicker, K., H. Reichert-Preibsch, R. Schmidt, B. Pettmann, G. Labourdette, and M. Sensenbrenner. 1987. Astroglial and fibroblast growth factors have neurotrophic functions for cultured periperal and central nervous system neurons. Proc. Natl. Acad. Sci. USA 84:5459-5463.

Vogel, T., N. Guo, H.C. Krutzsch, D.A. Blake, J. Hartman, S. Mendolovitz, A. Panet, and D.D. Roberts. 1993. Modulation of

endothelial cell proliferation, adhesion, and motility by recombinant heparin-binding domain and synthetic peptides from the type I repeats of thrombospondin. J. Cell. Biochem. 53:74-84.

Wagner, S.L., A.L. Lau, A. Nguyen, J. Mimuro, D.J. Loskutoff, P.J. Isackson, and D.D. Cunningham. 1991. Inhibitors of urokinase and thrombin in cultured neural cells. J. Neurochem. 56:234-242.

Walicke, P. 1988. Basic and acidic fibroblast growth factors have trophic effects on neurons from multiple CNS regions. J. Neurosci. 8:2618-2627.

Walicke, P., W.M. Cowan, N. Ueno, A. Baird, and R. Guillemin. 1986. Fibroblast growth factor promotes survival of dissociated hippocampal neurons and enhances neurite extension. Proc. Natl. Acad. Sci. USA 83:3012-3016.

Watanabe, K., H. Yamada, and Y. Yamaguchi. 1995. K-glypican: a novel gpi-anchored heparan sulfate proteoglycan that is highly expressed in developing brain and kidney. J. Cell Biol. 130:1207-1218.

Weinstein, J.R., S.J. Gold, D.D. Cunningham, and C.M. Gall. 1995. Cellular localization of thrombin receptor mRNA in rat brain: Expression by mesencephalic dopaminergic neurons and codistribution with prothrombin mRNA. J. Neurosci. 15:2906-2919.

Wilcox, J.B. and J.R. Unnerstall. 1991. Expression of acidic fibroblast growth factor mRNA in the developing and adult brain. Neuron 6:397-409.

Yamada, H., K. Watanabe, M. Shimonaka, and Y. Yamaguchi. 1994. Molecular cloning of brevican, a novel brain proteoglycan of the aggrecan/versican family. J. Biol. Chem. 269:10119-10126.

Yamaguchi, Y., D.M. Mann, and E. Ruoslahti. 1990. Negative regulation of transforming growth factor-β by the proteoglycan decorin. Nature 346:281-284.

Yang, P., D. Major, and U. Rutishauser. 1994. Role of charge and hydration in effects of polysialic acid on molecular interactions on and between cell membranes. J. Biol. Chem. 269:23039-23044.

Zhang, H., R.H. Miller, and U. Rutishauser. 1992. Polysialic acid is required for optimal growth of axons on a neuronal substrate. J. Neurosci. 12:3107-3114.

Table 1. Proteins to which Glycosaminoglycans Bind

Extracellular Matrix Molecules

Laminin	Fibronectin	Thrombospondins
tenascin	many Collagens	Vitronectin

Cell Adhesion Molecules

NCAM	L1/NgCAM	PECAM-1
Myelin-associated glycoprotein		

Cytokines

FGFs 1 thru 7	PDGF	VEGF
HB-EGF	TGF-β	IL3
Neural Schwann Cell Mitogen	chemokines (e.g., Il-8, MIP-1β)	

Proteases and Anti-proteases

Antithrombin III	Protease Nexin-1	Heparin Cofactor II
Amyloid β-protein precursor	Urokinase plasminogen activator	Tissue plasminogen activator
Thrombin		

Figure 1. Proteoglycan and Glycosaminoglycan Structure

To illustrate several features of proteoglycan and glycosaminoglycan structure, the structures of the two major families of cell surface HSPGs are compared. **(A)** A representative structure of the syndecan family of HSPGs. The syndecan family is characterized by a conserved intracellular domain that contains potential tyrosine phosphorylation sites and that is also thought to interact with cytoskeletal components. The syndecan family members syndecan-1 and ryudocan (syndecan-4) have been shown to be substituted with both heparan sulfate and chondroitin sulfate chains. **(B)** A representative structure of the glypican family of HSPGs. The glypicans are characterized by a lipid anchorage to the outer leaflet of the plasma membrane, and a conserved pattern of cysteine residues that is likely to result in a highly folded tertiary structure, stabilized by disulfide bonds. The heparan sulfate chains on both PGs contain regions of highly modified structure separated by spans of sparsely modified disaccharides. **(C)** Representative structures of sparsely modified heparan sulfate, highly modified heparan sulfate, and chondroitin/dermatan sulfate are shown, as well as the basic structure of the glycosyl-phosphatidylinositol lipid anchor of the glypican family PGs. GlcNAc = N-acetylglucosamine; GlcUA = glucuronic acid; $GlcNSO^{3-}$ = N-sulfoglucosamine; IdoUA = iduronic acid; GalNAc = N-acetyl-galactosamine; 4S, 2S, etc. indicate sites of O-sulfation.

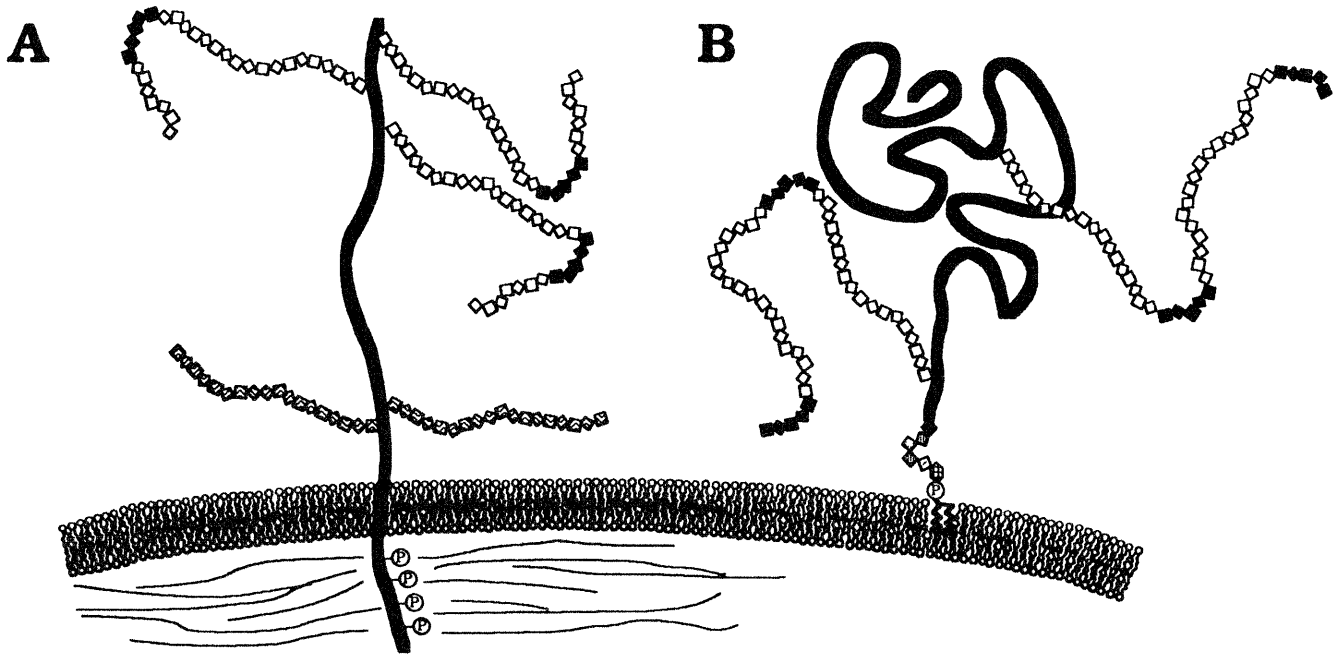

C

Heparan sulfate, N-acetlyated domains ( ):

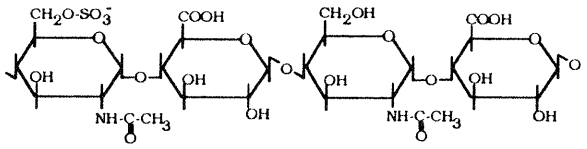

Heparan sulfate, highly sulfated domains ( ):

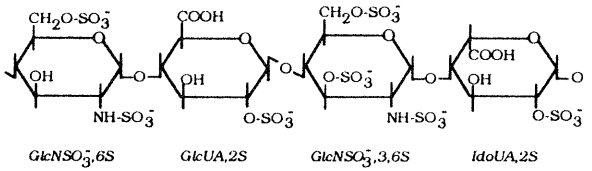

Chondroitin sulfate/ Dermatan sulfate ( ):

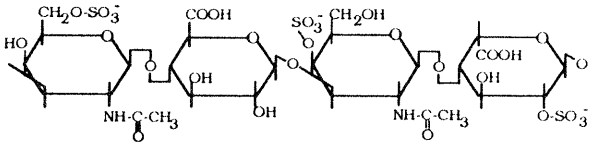

Potential tyrosine phosphorylation site: -Ⓟ

Glycosylphosphatidylinositol anchor:

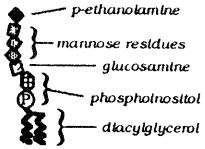

Table 2. Proteoglycan Families in the Nervous System

Molecule	GAG Type	Expression and localization[a]	Notes	Refs
Syndecan family PGs				
syndecan-1	HS/CS	(t.m.) early neural plate	(core M_r 33 kD[b]); conserved cytoplasmic domain that interacts with cytoskeleton common to all family members	38,39
syndecan-2	HS	(t.m.) mRNA detected in brain; possibly from meninges	(core M_r 23 kD[b]);	38,40
syndecan-3	HS	(t.m.) widespread in neonatal brain; floorplate of chick neural tube; neurons in culture	(core M_r 43 kD[b])	38,41 42, 45,46
ryudocan	HS/CS	(t.m.) CNS and PNS	(core M_r 22 kD[b]); also called syndecan-4	43,44
Drosophila syndecan	HS	(t.m.) CNS and PNS	(core M_r 39 kD[b])	47
Glypican family PGs				
glypican	HS	(GPI) ventricular zones of early CNS; widespread in CNS later; abundant but restricted in adult; esp. assoc. w/projection neurons; axon tracts	(core M_r 64 kD); lipid (GPI) anchored to plasma membrane; pattern of 14 cys residues conserved in all family members	15, 48-50
OCI-5	HS	(GPI) mRNA detected in rat brain	(core M_r 69 kD)	51-53
k-glypican	HS	(GPI) abundant in developing rat brain, esp. in ventricular zones; less abundant in adult	(core M_r 57.5 kD)	53
cerebro-glycan	HS	(GPI) immature post-mitotic neurons; assoc. w/ axon tracts of developing nervous system	(core M_r 57 kD); restricted to nervous system; (see chapter 3, this thesis)	54
dally	-	(prob. GPI) Dros. nervous system incl. morphogentic furrow and lamina furrow	(core M_r 63 kD); orig. identified in genetic screen for cell cycle progression mutants	55

(Table continued on next page)

Table 2. Proteoglycan Families in the Nervous System (continued)

Molecule	GAG Type	Expression and localization[a]	Notes	Refs
Aggregating CSPGs				
aggrecan	CS/KS	(sec.) found in chick brain	(core M_r 180-370 kD)	1
versican	CS	(sec.) glia of CNS and PNS	(core M_r 290-400 kD)	2
neurocan	CS	(sec.) neurons in cerebellum; cortical subplate; and barrel field boundaries in cortex	(core M_r 220-245 kD)	3,4
Cat-301	CS	(sec.) spinal motoneurons, neurons in visual circuits	(core M_r 580kD); expression highly restricted to subsets of neurons	5,6
brevican	CS	(sec.) brain; glial cells in culture	(core M_r 145kD)	7
pgT1	CS	(sec.) white matter and gray matter throughout nervous system	(core M_r 300 kD)	8
DSD-1	CS/DS	(sec.) barrel field boundaries of somatosensory cortex; glial cells in vitro	(core M_r 350-400 kD)	9,10
Other PGs				
decorin	CS/DS	(sec.) pons; floorplate of spinal cord; amyloid plaques; Schwann cells; neurons	(core M_r 38 kD); binds to netrin, probably via core protein; other decorin-type molecules outside nervous system	11-15
NG2	CS	(t.m.) glial progenitor cells; deep regions of molecular layer of cerebellum	(core M_r 300 kD); neurite repulsive activity in vitro	16-19
phosphacan	CS	(sec./t.m.) glia, including Bergmann glia of cerebellum; spinal cord roof plate; cortical subplate	(core M_r 300-400 kD); alternatively spliced form or RPTPβ, a brain-specif. receptor protein tyrosine phosphatase	7, 20-24
SV2	KS	(ves.) membranes of synaptic vesicles throughout brain	(core M_r 100-250 kD); homology to neurotrans-mitter transporters	25-28
perlecan	HS	(sec.) basement membrane of capillaries within brain; basal lamina of neural tube; endoneurium of peripheral nerves	(core M_r 400-700 kD); a small HSPG of core Mr~ 45kDa and homology to perlecan has been found in emb. mouse neuroepithelium	29-32
agrin	HS	(sec.) neurons and Schwann cells of PNS; ventricular zones of CNS; spinal cord motoneurons; throughout adult brain	(core M_r 250 kD); non-glycanated forms exist; orig. purified on the basis of AChR clustering activity; prob. involved in synaptogenesis	33-37

(Table continued on next page)

Table 2. Proteoglycan Families in the Nervous System (continued)

[a] Expression and localization abbreviations are (t.m.), transmembrane molecule; (GPI), glycosyl-phosphatidylinositol- linked protein core; (sec.), secreted proteoglycan; (ves.), molecule that has been localized to the lumen of synaptic vesicles.

[b] Syndecan family core protein values shown here are those predicted from protein sequences (not the much larger values obtained from SDS-PAGE analysis of cores).

The data in this table was assembled from information found in (Litwack, 1995, Chapter 1).

TABLE REFERENCES:

(1) (Krueger and Saito, 1992)
(2) (Perides et al., 1992)
(3) (Rauch et al., 1992)
(4) (Oohira et al., 1994)
(5) (Fryer et al., 1992)
(6) (Hockfield et al., 1990)
(7) (Yamada et al., 1994)
(8) (Iwata and Carlson, 1993)
(9) (Faissner et al., 1994)
(10) (Steindler et al., 1995)
(11) (Krusius and Ruoslahti, 1986)
(12) (Scholzen et al., 1994)
(13) (Snow et al., 1992)
(14) (Hanemann et al., 1993)
(15) (Litwack, 1995)
(16) (Stallcup et al., 1983)
(17) (Levine and Stallcup, 1987)
(18) (Dou and Levine, 1994)
(19) (Levine, 1994)
(20) (Rauch et al., 1991)
(21) (Maurel et al., 1994)
(22) (Shitara et al., 1994)
(23) (Milev et al., 1994)
(24) (Miller et al., 1992)
(25) (Scranton et al., 1993)
(26) (Feany et al., 1992)
(27) (Bajjalieh et al., 1992)
(28) (Bahr et al., 1992)
(29) (Iozzo et al., 1994)
(30) (Lin, 1990)
(31) (Halfter and Schurer, 1994)
(32) (Joseph et al., 1995)
(33) (Tsen et al., 1995)
(34) (McMahon, 1990)
(35) (Ma et al., 1994)
(36) (Halfter, 1993)
(37) (O'Connor et al., 1994)
(38) (Bernfield and Hooper, 1991)
(39) (Saunders et al., 1989)
(40) (David et al., 1993)
(41) (Carey et al., 1992)
(42) (Gould et al., 1992)
(43) (Kojima et al., 1992)
(44) (Baciu et al., 1994)
(45) (Kim et al., 1994)
(46) (Gould et al., 1995)
(47) (Spring et al., 1994)
(48) (Litwack et al., 1994)
(49) (Karthikeyan et al., 1994)
(50) (Carey et al., 1993)
(51) (Filmus et al., 1988)
(52) (Filmus et al., 1995)
(53) (Watanabe et al., 1995)
(54) (Stipp et al., 1994)
(55) (Nakato et al., 1995)

Figure 2. Biosynthesis of Heparan Sulfate.
The biosynthesis of heparan sulfate (HeS) is represented schematically in **(A)**. Abbreviations are: ER, endoplasmic reticulum; GlcNAc, N-acetylyglucosamine; GlcA, glucuronate; UDP, uridine diphosphate. The diagram traces the biosynthesis from preliminary steps thought to occur in the ER to the polymerization of the HeS chain which occurs in the Golgi. The nascent chain is partially but extensively modified while still in the Golgi, as depicted in **(B)**. The basic structure of GlcNAc-GlcA is modified in a series of stepwise modifications in which the product of one step forms the substrate for the next step. The modifications occur sporadically along the length of the HeS chain. Some regions (represented by the four left-most saccharides in B) are heavily modified, while others (represented by the two right-most saccharides) remain essentially unmodified. (See also Figure 1). The 3-O-sulfation shown in the final step of biosynthesis is a rare modification that is crucial for the formation of a high affinity binding site for antithrombin III on the HeS chain.

A

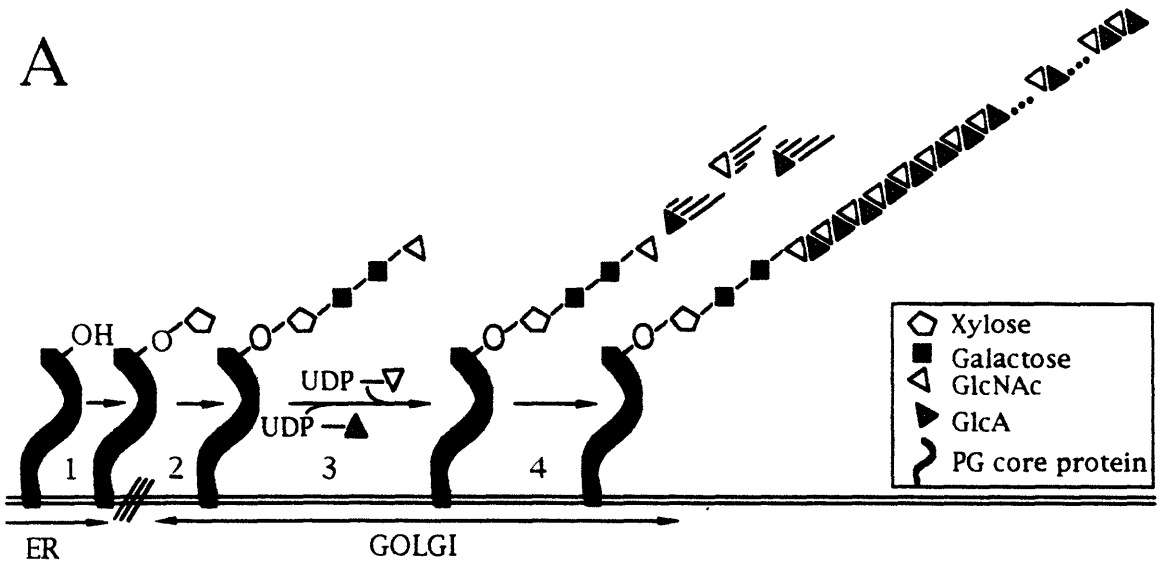

(1)	(2)	(3)	(4)
O-xylosyl-ation of the serine of the ser-gly dipeptide(s) in the PG core protein	Completion of the tetra-saccharide link upon which the HeS chain will be polymerised	Successive addition of GlcA and GlcNAc from UDP-linked precursors	HeS chain attains a degree of polymeri-zationof 30-200 disaccharide units and is partially but extensively modified as described below.

B

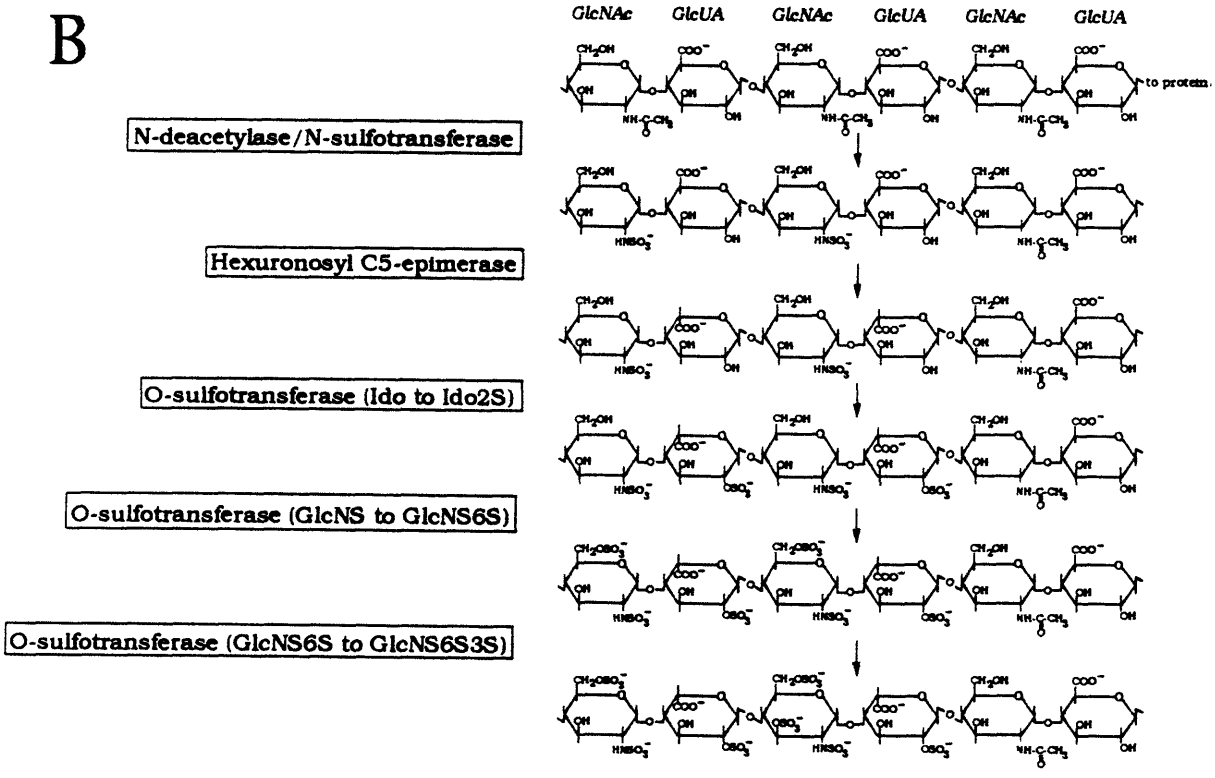

Figure 3. Protein binding sites within heparan sulfate chains.
(A) The structure of the antithrombin III binding site. Functional groups required for binding with high affinity to antithrombin III are indicated with asterisks. The dagger indicates the location of a rare 3-O-sulfate that is also required for binding to antithrombin III. The majority of 3-O-sulfates found on heparan sulfate chains are found within antithrombin III binding sites. (B) The structure of a disaccharide required for binding to FGF-2. (C) The structure of a disaccharide required for binding to FGF-1. The structures in B and C occur in the context of longer oligosaccharides with variable structures. Abbreviations: $GlcNSO^{3-}$, N-sulfoglucosamine; GlcUA, glucuronate; IdoUA, iduronate; 2S, 3S, 6S, indicate sites of O-sulfations; R, -H or $-SO^{3-}$ substituent.

A. Antithrombin III

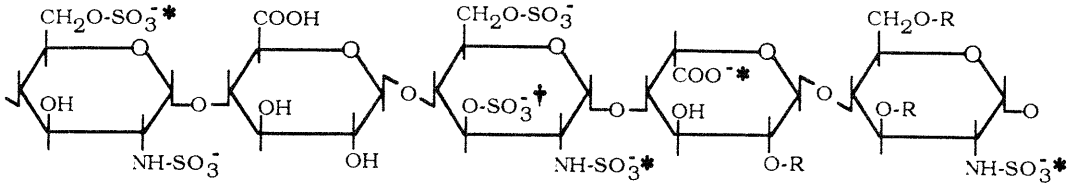

GlcNSO$_3^-$,6S *GlcUA* *GlcNSO$_3^-$,3,6S* *IdoUA±2S* *GlcNSO$_3^-$,±3S,±6S*

B. FGF-2

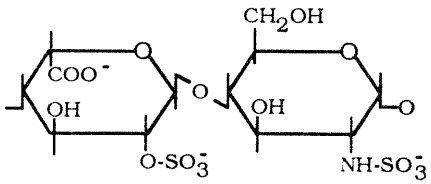

IdoUA,2S *GlcNSO$_3^-$*

C. FGF-1

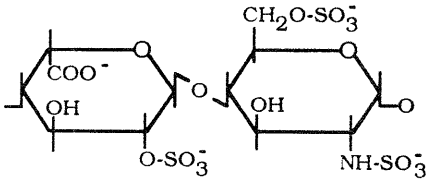

IdoUA,2S *GlcNSO$_3^-$,6S*

CHAPTER I

A Diverse Set of Developmentally Regulated Proteoglycans is Expressed in Rat Central Nervous System

INTRODUCTION†

The behaviors of developing neural cells--e.g., directed cell migration, axon outgrowth and navigation, synaptogenesis, and selective cell death--require the precise orchestration of cell-cell and cell-matrix interactions. Nervous system molecules that are believed to play a role in mediating such interactions include members of diverse categories, such as extracellular matrix glycoproteins, cell surface adhesion molecules, polypeptide growth factors and extracellular proteases and protease inhibitors (Lander, 1987; Sanes, 1989; Walicke, 1989). Interestingly, a large proportion of nervous system molecules belonging to these categories exhibit binding to glycosaminoglycans (GAGs) and/or proteoglycans (PGs). Examples include laminin, fibronectin, thrombospondin, tenascin, NCAM, myelin-associated glycoprotein (reviewed by Lander, 1989), retinal purpurin (Schubert et al., 1986), amyloid b-protein precursor (Schubert et al., 1989), acidic and basic fibroblast growth factor (Lobb et al., 1986), a novel glial mitogen (Ratner et al., 1988), and protease nexin-1 (Gloor et al., 1986).

The observation that so many developmentally important extracellular proteins bind GAGs and/or PGs is intriguing, because it suggests that PGs might influence the localization, availability, or biological activities of many of these proteins in vivo. Indeed, the likelihood that PGs are involved in a wide variety of important events in neural development has been suggested by studies of neurulation (Morris-Kay and Crutch, 1982), neural cell-substratum adhesion (Schubert and LaCorbiere, 1982; Akeson and Warren, 1984; Schubert et al., 1986; Schubert et al., 1987), NCAM-mediated cell adhesion (Cole et al., 1986), migration of neural crest cells (Perris and Johansson, 1987), laminin-stimulated neurite outgrowth (Muir et al., 1989), axonal guidance (Carbonetto et al., 1983; Snow et al., 1990a), responsiveness to trophic factors (Schubert et al., 1987; Neufeld et al., 1987; Damon et al., 1987; Walicke, 1988), acetylcholine receptor clustering (Kidokoro and Hirano, 1988; Gordon and Hall, 1989a; Gordon and Hall, 1989b), and glial growth control (Ratner et al.,

---

† This chapter was previously published in its entirety in Neuron, Vol. 4, 949-961, June 1990.

1985).

The possibility that PGs have diverse biological functions during development raises an interesting question: Do distinct PGs with unique and highly specific biological activities exist in the nervous system? On the one hand, the fact that protein-PG interactions appear to be mediated by GAGs, of which only a handful of types exist (heparan sulfate, chondroitin sulfate, dermatan sulfate and keratan sulfate), suggests that the specificity of protein-PG interactions may be quite limited (Ruoslahti, 1989). On the other hand, examples have emerged recently of PGs exhibiting considerable specificity. For example, syndecan, a cell surface PG that contains heparan sulfate, interacts with fibronectin, but not laminin (Saunders and Bernfield, 1988; Saunders et al., 1989), even though both fibronectin and laminin bind purified preparations of heparan sulfate. Other cell surface PGs apparently distinguish among serine protease inhibitors in a cell-type specific manner (Cunningham et al., 1986; Marcum et al., 1987). Of two heparan sulfate PGs that bind laminin, only one is associated with an ability to block laminin's neurite outgrowth-promoting activity (Muir et al., 1989). Specificity in protein-PG interactions may be achieved through recognition of particular GAG modifications (e.g. Lindahl et al., 1984), or may involve contributions of PG core proteins to binding or function.

If PGs play multiple highly specific roles in nervous system development, it would be logical to expect (a) that a diverse set of PGs would be expressed in the nervous system during development, and (b) that the expression of at least some nervous system PGs would be temporally and/or spatially regulated during development. Recent immunohistochemical observations support the latter expectation (Aquino et al., 1984; Levine and Card, 1987; Stallcup and Beasley, 1987; Hoffman et al., 1988; Zaremba et al., 1989), but adequate biochemical studies of the diversity and timing of PG expression are lacking. Instead, biochemical studies of nervous system PGs have tended to focus on characterization of one or a few major species (e.g. Kiang et al., 1981; Klinger et al., 1985; Ripellino and Margolis, 1989). A notable exception is the recent study of Oohira et al. (1988), which suggests that as many as five chondroitin sulfate PGs can be isolated

from a single subcellular fraction of 10 day old rat brain.

The following study represents an initial attempt to assess the diversity and timing of expression of nervous system PGs. The experimental approach is similar to that developed by Bretscher (1985) and Lories et al. (1987) for analyzing the complexity of PGs expressed on the surfaces of cultured cells. The results indicate that a wide variety of heparan sulfate and chondroitin sulfate PGs can be identified in the mammalian brain, that individual PGs associate with particular subcellular fractions, that some integral membrane PGs of the brain are covalently attached to lipid, and that levels of many brain PGs change significantly during development from late fetal stages to adulthood. Using this approach, it may be possible to identify PGs with biochemical properties and patterns of expression suggestive of involvement in particular developmental events. The specificity of interaction of such PGs with appropriate neural PG-binding proteins could then be evaluated.

Some of these findings have been reported previously in abstract form (Lander et al., 1988; Herndon and Lander,1989).

MATERIALS AND METHODS

Materials

Heparitinase was prepared from *Flavobacterium heparinum* by hydroxyapatite chromatography as described by Linker and Hovingh (1972). Chondroitinase ABC and chondroitinase AC were obtained from Sigma, neuraminidase from *Arthrobacter ureafaciens* was from Calbiochem, and phosphatidylinositol-specific phospholipase C (PI-PLC) from *Bacillus cereus* was from Boehringer Mannheim. Triton X-100 and Triton X-114 were obtained from Sigma, while 3-[(3-Cholamidopropyl) dimethylammonio]-1-propanesulfonic acid (CHAPS) was from Boehringer Mannheim. Protease inhibitors, obtained from Sigma, were phenylmethylsulfonyl fluoride (PMSF), N-ethylmaleiimide (NEM), Pepstatin A and EDTA. Unless otherwise stated in the text, the term "protease inhibitors" should be taken to mean the combination of 1mM EDTA, 1μg/ml pepstatin, 0.25 mg/ml NEM (added within 1 hour of use) and 0.4mM PMSF (added within 5 minutes of use).

Subcellular Fractionation

Whole brains from embryonic, neonatal and adult Sprague-Dawley rats were obtained as follows: Adult rats were asphyxiated with CO_2 and brains were rapidly removed to dishes of ice-cold saline (0.9% NaCl). Newborn (postnatal day 0; P0) rats were anesthesized by cooling on ice, and brains removed to ice-cold saline. Embryonic day 18 (E18) animals were dissected under ice-cold saline. Brains were stripped free of all visible meninges, washed in saline, resuspended in 9 volumes of ice-cold buffer A (0.3M sucrose, 4mM HEPES pH 7.5 containing protease inhibitors) and homogenized using a teflon-on-glass homogenizer (Thomas Scientific) with pestle rotation provided by a Wheaton overhead stirrer (model 903475, setting 4). Homogenization and all subsequent steps were carried out quickly and at 4^0C.

Homogenates were centrifuged at low speed (12,000g, 30 minutes), pellets were re-homogenized in buffer A and re-centrifuged, and the two supernatants were pooled. This material was then centrifuged at high speed (378,000g, 30 min.) The resulting

supernatant, the brain "soluble" fraction, was clarified by centrifugation at 378,000g, 60 min., followed by 0.2μ filtration. The membrane-containing pellet from the first high speed spin was then homogenized in buffer B (50mM Tris-HCl pH 8.0, 0.15M NaCl, 1.0% CHAPS, EDTA [1mM], Pepstatin A [1μg/ml]) and centrifuged at 378,000g for 1 hour. The resulting pellet was re-homogenized in buffer B and centrifuged at 423,500g for 40 min. The two buffer B supernatants, representing a detergent extract of a crude brain membrane fraction, were pooled and clarified by 0.2μ filtration. Protein concentrations were determined using Amido Black binding (Schaffner and Weissmann, 1973).

Proteoglycan purification and radioiodination

Proteoglycans (PGs) were purified by anion exchange chromatography on DEAE-Sephacel (Pharmacia) equilibrated in buffer C (50mM Tris-HCl pH 8.0, 0.15 M NaCl, 0.5% CHAPS). Samples in buffer B were loaded directly onto columns containing the gel, while samples in buffer A were first made 0.15M in NaCl and 0.5% in CHAPS. Column volumes of 0.5 ml packed gel per mg protein were used. Columns were eluted stepwise with buffer C, buffer D [50mM Tris-HCl pH 8.0, 0.25 M NaCl, 0.1% Triton X-100], buffer E [50mM Tris-HCl pH 8.0, 6M Urea, 0.25M NaCl, 0.1% Triton X-100], and buffer F [50mM Sodium Formate pH 3.5, 6M Urea, 0.2M NaCl, 0.1% Triton X-100]. Column pH was restored with 50mM Tris-HCl pH 8.0, 0.5% CHAPS before elution of PGs with buffer G [50mM Tris-HCl pH 8.0, 0.75M NaCl, 0.5% CHAPS].

Material eluted with buffer G was diluted five-fold with 50mM Tris-HCl pH 8.0, 0.5% CHAPS and batch-adsorbed to 100ml packed volume DEAE Spectra/Gel M (Spectrum Scientific), equilibrated in buffer C. The gel was washed extensively with 50mM Tris-HCl pH 8.0, 0.15 M NaCl and bound material radioiodinated using chloramine-T, as described by Lories *et. al.* (1987) with the modification that 5mCi ^{125}I were used per reaction and reaction time was reduced to 3 minutes. After extensive washing with buffer C, radioiodinated material was eluted with buffer G. After measurement of protein concentration and radioactive specific activity, crystalline grade bovine serum albumin

was added to 1 mg/ml and aliquots were frozen and stored at -80^{0}C.

Enzymatic analysis of proteoglycans

Neuraminidase digestions were carried out in 25mM Tris-acetate pH 5.0 containing 0.16 mg/ml hemoglobin (human, 4X recrystallized, Sigma) and protease inhibitors. The enzyme was used at 0.5 U/ml for 1 hr at 37^{0}C. Heparitinase, chondroitinase AC, and chondroitinase ABC digestions were carried out in 50mM Tris-phosphate pH 7.0 containing 0.16 mg/ml hemoglobin and protease inhibitors. Heparitinase was used at 0.4 μg/ml for 1 hr at 37^{0}C, conditions empirically determined to give complete digestion of heparan sulfate PGs without demonstrable chondroitinase activity. Chondroitinase AC and ABC were used at 0.05 U/ml for 1 hr at 37^{0}C. PI-PLC digestion was carried out in 50mM Tris-phosphate pH 7.5, 0.16% Triton X-114, 0.16 mg/ml hemoglobin, EDTA (1mM) and pepstatin A (1μg/ml); the enzyme was used at 0.05U/ml for 1 hr at 37^{0}C. For all enzyme reactions, volumes were adjusted so that NaCl contributed from the PG-containing sample reached a final concentration of <0.2M or, in the case of phospholipase C digestion, ≤ 0.01M.

Enzyme-treated samples were analyzed by SDS-PAGE (Laemmli, 1970) under reducing and nonreducing conditions. Controls included both untreated and sham-digested samples. Molecular weights were determined using prestained protein standards (BRL) and, in some experiments, samples of mouse laminin and human plasma fibronectin (detected by Coomassie blue staining). Gels were dried and autoradiographed against pre-flashed Kodak XAR film at -80^{0}C.

Gel filtration of neonatal membrane proteoglycans

To 100ml of PGs in buffer G, solid sucrose was added to 5% and the mixture was loaded onto a Sepharose CL-4B (Pharmacia) column (0.5cm X 18cm), equilibrated in 50mM Tris HCl pH 8.0, 0.5 NaCl, 0.5% CHAPS, 1mg/ml crystalline bovine serum albumin, and protease inhibitors. Flow rate was 0.4ml/hr. and ~85ml fractions were collected. V_0 and V_t were determined by elution of b-galactosidase aggregates and $^{35}SO_4$, respectively.

Triton X-114 partitioning

PGs and enzyme-digested PGs were subjected to Triton X-114 (Tx114) phase partitioning as described by Bordier (1981). Briefly, PG's were diluted into 100ml 50mM Tris-phosphate pH 7.0, 2% Tx114 (sufficient to decrease the concentration of CHAPS to < 0.005%), and were layered over a cushion of 6% sucrose, 0.06% Tx114 in 50mM Tris-phosphate pH 7.0. After incubation for 5 min. at 35^{0}C, the tube was centrifuged at 1000 g, 10 min., 25^{0}C. The upper phase was removed, Tx114 was added to 0.5%, and the mixture was layered again over the original sucrose cushion. After incubation and centrifugation as above, the pellet (~10ml) was retrieved and diluted to 100ml in 50mM Tris-phosphate pH 7.0 ("detergent-rich phase"). The top phase was also saved and re-treated with Tx114 at 2%, incubated, centrifuged, and the top phase saved ("aqueous phase").

RESULTS

Isolation of Proteoglycan-Enriched Fractions

Anion-exchange chromatography was used to isolate PGs from two subcellular fractions of rat brain--a "soluble fraction" and a detergent extract of crude membranes--that had previously been shown to contain PGs (Margolis et al., 1975a; Kiang et al., 1981; Klinger et al., 1985). After adsorption of crude material to the ion exchange matrix, a series of buffers was employed to wash away non-PG proteins (cf. Bretscher, 1985). Subsequent application of a high salt buffer (buffer G) eluted a putative PG-containing fraction representing $\leq$ 0.3% of initial protein. Data from the fractionation of newborn brain (postnatal day zero; P0) are presented in Table 1.1. A comparison of overall recovery of protein in the buffer G-eluted fractions of embryonic (embryonic day 18; E18), P0 and adult brain is shown in Table 1.2.

Given the small amounts of protein in buffer G eluates (compared with the amounts eluted by previous washes), it was important to show that the material eluted by buffer G does not simply consist of residual amounts of abundant molecules most of which had already been eluted by buffers C-F. To address this question, the buffer G eluate from P0 brain membranes was radioiodinated, and a small amount mixed with a fresh, unlabeled membrane extract. The mixture was then subjected to anion exchange chromatography. As shown in Table 1.3, although approximately 5% of the labeled material failed to re-bind the ion exchange matrix (see discussion), very little of what did bind was eluted by buffers C-F (about 4%). Thus, the bulk of the molecules described below appear to be molecules specifically eluted by high salt (buffer G) and resistant to elution by moderate salt, urea, or low pH (buffers C-F). Table 1.3 also suggests that molecules eluted by buffer G may be particularly susceptible to loss due to irreversible binding to the ion-exchange matrix, since material eluted by buffer G is not quantitatively recovered following re-chromatography (see discussion).

Identification of Proteoglycans

In recent years, SDS-PAGE has been widely used for the

characterization of PGs. Typically, the presence of GAG chains causes PGs to migrate as diffuse smears of anomalously high apparent M_r. Enzymatic removal of GAG chains, however, generates PG core proteins (or, alternatively, "core preparations" [Hassell et al., 1986]) that behave similarly to other proteins and glycoproteins when subjected to SDS-PAGE. Thus, electrophoretic bands that appear in response to digestion of a sample with a single GAG lyase can be taken as evidence of individual PGs bearing GAG chains of the class recognized by that enzyme.

This approach was used to characterize PG fractions (i.e. buffer G eluates) derived from brain. To improve sensitivity, and to avoid the possibility that protein bands contributed by GAG lyases themselves would be mistakenly identified as core proteins, PG fractions were radioiodinated as described by Lories et al. (1987) and core proteins were identified by autoradiography. GAG lyases that digest chondroitin sulfate (chondroitinase AC), chondroitin sulfate and dermatan sulfate (chrondroitinase ABC) and heparan sulfate (heparitinase) were used. In early experiments, silver staining was also used to identify core proteins. This procedure adequately identified the most abundant PG cores. It was difficult, however, to estimate levels of PGs because many core proteins, when stained as described by Wray et al. (1981), gave rise to "negative bands", i.e. unstained areas over a lightly stained background (data not shown). In all cases where core protein bands could be identified by silver staining, the same bands could also be found by autoradiographic analysis of radioiodinated material.

Figure 1.1 shows the results obtained when samples derived from the membrane fraction (Panel A) and soluble fraction (Panel B) of P0 brain were analyzed in this way. Each GAG lyase produces a characteristic pattern of new bands. Bands are also seen that do not change in response to digestion with GAG lyases (Figure 1.1, asterisks); presumably these represent proteins that are not PGs, or are refractory to the GAG lyases used. Neuraminidase digestions were also performed to determine whether the presence of sialic acid could account for the tendency of some putative PG core protein bands to appear less sharp than others.

To minimize the possibility that some of the bands identified as

core proteins actually result from proteolysis during diagnostic digestions with glycosaminoglycan lyases (cf. Kato et al., 1985), all enzymatic digestions were carried out in the presence of fresh protease inhibitors and carrier protein. Enzymes were tested at several concentrations, and used only at concentrations well below those that resulted in detectable degradation of non-PG proteins. Time-course studies (not shown) indicate that the bands identified as core proteins all "appear" at about the same time after exposure to enzyme, and remain stable in apparent M_r and abundance for >4 hrs at 37°C, the longest time tested (e.g. high M_r bands were not seen to "chase" into bands of lower M_r).

Analyses similar to those in Figure 1.1 were performed for material derived from E18 and adult brain (not shown). To facilitate unambiguous identification and comparison of putative core protein species at each developmental stage, apparent M_rs were also determined from 5%, 10% and 5-15% (exponential gradient) gels run both under reducing and non-reducing conditions. Figure 1.2 shows examples of 10% non-reducing gels that compare the effects of chondroitinase ABC and heparitinase digestion on neuraminidase-treated membrane-associated and soluble PG fractions from all three developmental stages (equal amounts of radioactivity were loaded in each lane). The same samples were also analyzed on 5% gels to better resolve high molecular weight PGs (not shown). Results from Figure 1.1, Figure 1.2, and analyses not shown are summarized by Tables 1.4 and 1.5. Putative core proteins of the membrane fraction are designated M1-M16 and those of the soluble fractions S1-S9 (in descending order of M_r). Arrows in Figures 1.1 and 1.2 mark the positions of most of the neuraminidase treated putative core proteins mentioned in Tables 1.4 and 1.5. Not all core proteins are visible on every gel: M16 is only seen after reduction, and therefore is not shown by these non-reducing gels. Bands representing M2 and M3 are too faint to be seen in Figure 1.2A , but are easily resolved by 5% gels of the same samples (data not shown). Also, in Figure 1.2A, bands representing M10 (a heparan sulfate PG) and M11 (a chondroitin sulfate PG) have been pointed out only in the lanes in which they overlap (the sample treated with both chondroitinase and

heparitinase); separate bands representing M10 and M11 are present in samples treated with either heparitinase or chondroitinase, respectively, but are difficult to see in Figure 1.2A; they are more easily appreciated in Figure 1.1A . In Figure 1.2B, chondroitin sulfate PGs S4 and S5 overlap, but are readily distinguished by 5% gels (data not shown).

Tables 1.4 and 1.5 also contain information about salt gradient elution profiles of the PGs that give rise to certain putative core protein species, as well as pictorial representations of the relative amounts of putative core proteins at each of the developmental ages studied.

Gel Filtration Analysis of Membrane-Associated Proteoglycans

Although the methods used for isolating PG fractions are apparently highly selective for PGs over other proteins, some non-PGs are clearly not eliminated (Figures 1.1 and 1.2, asterisks). Possibly these represent proteins that remain highly anionic even at low pH, perhaps as a result of sulfation or phosphorylation. Alternatively, these may be proteins that strongly associate with PGs, and thereby co-purify with them. The latter possibility seemed particularly worth investigating in the PG fraction derived from brain membranes, because starting material could easily have contained extracellular matrix material associated with membranes. There is little information available on the behavior of extracellular matrix during subcellular fractionation of brain homogenates. However, at least one form of organized extracellular matrix, the synaptic junctional complex, is known to be recoverable from a membrane preparation similar to the one described here (Wang and Mahler, 1976).

A small amount of radiolabeled PO membrane-associated PGs was therefore fractionated on Sepharose CL4B. To reduce non-specific aggregation, the column buffer contained 0.5M NaCl, 0.5% CHAPS, and carrier protein (1mg/ml crystalline bovine serum albumin). Fractions were analyzed by non-reducing SDS-PAGE before and after triple digestion with neuraminidase, chondroitinase ABC, and heparitinase.

The results, shown in Figure 1.3, indicate that some components of the PG fraction behave as expected for typical non-

aggregating macromolecules, i.e. they elute as relatively compact peaks in order of their apparent M_r s. Examples of such molecules include M1, M3, M12, M13 (Figure 1.3B), and non-PG proteins of 43 kd, 37 kd, and 28 kd (indicated on Figure 1.3A by diamonds). In contrast, several molecules exhibit behaviors suggestive of aggregating species, such as co-elution with molecules of much higher apparent M_r s, or a broad elution profile smeared across nearly the entire column profile. Examples of these include M7, M8, M9 (Figure 1.3B), and non-PG proteins of 135 kd, 115 kd, 98 kd, 46 kd, 41 kd, 35 kd, and 30 kd (indicated on Figure 1.3A by asterisks). Preliminary results of velocity sedimentation of P0 membrane-associated PGs also suggest aggregation of the same species. Specifically, M1, M12, and M13 sedimented as compact peaks (at 7S, 3S and 3S, respectively), while M7, M8, M9 and non-PG proteins of 46kd, 41kd and 35kd were found together throughout all sucrose gradient fractions from 7S to the tube bottom (>26S) (unpublished observations).

Identification of Putative Integral Membrane Proteoglycans

Studies of cultured cells have identified cell surface PGs that are integral membrane components, as well as PGs that are only peripherally associated with the plasma membrane. To identify brain PGs that are integral membrane components, labeled PG fractions from each developmental age (E18, P0 and adult) were subjected to hydrophobic partitioning using the detergent Triton X-114 (Tx114). This method identifies molecules that contain hydrophobic domains sufficient to permit their incorporation into detergent micelles (Bordier, 1981). The results of analysis of PG fractions derived from brain membranes, shown in Figure 1.4, indicate that heparan sulfate PGs identified by cores M12 and M13, as well as two adult-specific non-PG proteins of 100 kd and 120 kd, partition significantly into a Tx114-rich phase, and suggest that these molecules may normally be integral membrane components. Small amounts of two other PGs, identified by cores M7 and M8, can also be recognized in the detergent-rich phase. However, since these PGs are among those suspected of some form of aggregation (cf. discussion of Figure 1.3, above), their presence in the detergent phase should be interpreted

with caution: macromolecular aggregates sufficiently large to pellet at 1,000 g would almost certainly have been collected along with the (lower) detergent phase irrespective of actual detergent-binding (or lack thereof).

Tx114 partitioning was also carried out using labeled PG fractions derived from the soluble fraction of E18, P0 and adult brain. In these experiments, no molecules were found to partition into the detergent-rich phase (data not shown).

Identification of Phosphatidylinositol-linked Integral Membrane PGs

Recent studies suggest that some integral membrane PGs are anchored in the membrane by attachment to glycosyl-phosphatidylinositol (GPI) lipids (Ishihara et al., 1987; Carey and Evans, 1989; Yanagishita and McQuillan, 1989). GPI linkages are also characteristic of other developmentally regulated nervous system molecules such as NCAM-120 (He et al., 1986) and Thy-1 (Low and Kincade, 1985). To determine whether any of the integral membrane PGs identified in rat brain exhibit this type of linkage, labeled membrane-associated PG's were treated with neuraminidase, then chondroitinase ABC and heparitinase with or without the addition of phosphatidylinositol-specific phospholipase C (PI-PLC). Samples were then subjected to Tx114 phase partitioning and the aqueous and detergent-rich phases analyzed by SDS-PAGE.

The results, shown in Figure 1.5, indicate that the detergent phase partitioning of two PGs, M12 (a major heparan sulfate PG) and M13 (a heparan sulfate PG found only in E18 and P0 samples) is significantly reduced by pre-treatment with PI-PLC. In addition, a 100 kd non-PG protein found only in the adult sample (Figure 1.5, lower asterisk) is also shifted from the detergent to aqueous phase by PI-PLC treatment. Importantly, the detergent partitioning behavior of some molecules (e.g., a 120 kd non-PG in the adult sample [Figure 1.5, upper asterisk]) was not altered by PI-PLC, indicating that presence of the enzyme does not interfere with the partitioning process itself. Thus, the results imply that the detergent-binding properties of M12, M13 and the 100 kd protein depend on covalent linkage to a phosphatidylinositol lipid.

DISCUSSION

Isolation of Brain Proteoglycans

This report describes the isolation and identification of rat brain PGs, and the characterization of changes in PG core protein expression during brain development. The method used for isolation of a PG-enriched fraction relies on the ability of sulfated PGs to remain bound to DEAE-cellulose even under chaotropic (6M urea) and acidic (pH 3.5) conditions. The material obtained is sufficiently depleted of non-PG proteins that individual PGs can be identified by the bands that appear on SDS-gels following digestions with glycosaminoglycan (GAG) lyases. Such methods have been used by others (e.g. Bretscher, 1985; Woods et al., 1985; Coster et al., 1986) for isolating PGs of cultured cells and, when combined with radioiodination (Lories et al., 1987) appear to provide a general and highly sensitive approach for analyzing the PG composition of cells or tissues.

PGs were isolated from subcellular fractions of rat brain in the amounts indicated in Table 1.2. These figures probably underestimate the abundance of brain PGs for four reasons: First, protein was measured using Amido Black binding; this anionic dye might be expected to bind less well to PGs than to other proteins. Second, some PGs may fail to bind initially to DEAE-Sephacel because they associate with other proteins in the tissue extract (this phenomenon could explain why, when labeled PGs were added back to initial tissue extracts, 5% of labelled material failed to rebind DEAE-Sephacel [Table 1.3]). Third, some brain PGs may elute prematurely during fractionation (e.g., PGs with low GAG content, or PGs with unsulfated GAGs); such PGs would not have been detected in this study. Fourth, some PGs may be lost due to failure to elute from DEAE-Sephacel. Indeed, even PGs that have been eluted once from the ion-exchange matrix are not completely re-elutable from a second round of chromatography (note loss of 44% on Table 1.3). Apparently, such losses result from the fact that application of a "step" of high salt to DEAE-Sephacel results in a PG peak followed by a "tail" of material that continues to elute for many column volumes (and is usually too dilute for recovery to be practical). Enzymatic analysis has so far detected no differences in PG composition between such peak and tail fractions,

nor has treatment of columns with 1.2M or 2.0M NaCl eluted PGs any different in amount or composition than what is eluted by 0.75M NaCl (unpublished observations).

Despite these potential sources of loss or of underestimation of PG content, it is noteworthy that the amounts of PG-protein in Table 1.2 are nonetheless in the same range as the amounts of total sulfated GAG reported in similar subcellular fractions (cf. Margolis et al., 1975a; Werz et al., 1985a; Werz et al., 1985b).

Evidence of Proteoglycan Diversity

The results summarized in Tables 1.4 and 1.5 suggest that as many as 25 PG core proteins may be expressed in the mammalian brain at various times during development. To minimize the possibility that some of the molecular species identified result from proteolysis during homogenization or fractionation, all steps were carried out quickly, in the cold, and in the presence of protease inhibitors. Significant differences in molecular weights or relative abundances of core proteins among independent preparations were not seen, nor were changes in apparent PG composition detected following long-term storage of either tissue extracts or purified PGs. Steps were also taken to ensure that proteolysis did not occur during exposure of PGs to GAG lyases (see Results). Indeed, the unique patterns of fractionation exhibited by PGs subjected to gel filtration, Tx114 partitioning, and salt gradient elution from DEAE -cellulose (Tables 1.4 and 1.5, Figures 1.3-1.5), imply that multiple distinct PG species clearly exist *before* treatment of samples with GAG lyases.

Even barring proteolysis, however, it is possible that Tables 1.4 and 1.5 might still overestimate the diversity of PG species in the brain. Some species identified in the membrane fraction may be identical or related to species of similar apparent M_r that are found in the soluble fraction (e.g. M1 and S1; M12 and S9). Some putative core proteins that are similar in apparent M_r may actually represent forms of a single protein that have been modified (e.g. by glycosylation) differently (e.g. S4 and S5; M5 and M6; M13 and M14). Ultimately, questions of relatedness among PG species will need to be settled using techniques such as peptide mapping or with antibody probes

(e.g. Lories et al., 1989). Recently, Oohira et al. (1988) used tryptic peptide mapping to show that three chondroitin sulfate PGs of the 10 day rat brain are unrelated to each other. Significantly, the extraction properties and M_rs of those PGs suggest they are identical to species S2, S3 and S4, while the two less abundant species identified by Oohira et al. (1988) may correspond to S5 and S8.

There are also reasons to suspect that the brain contains PGs not included on Tables 1.4 and 1.5: Unambiguous identification of putative core proteins was difficult in some cases due to overlapping of electrophoretic bands, and low-abundance PGs may have been missed. Indeed, faint signals on some autoradiograms suggested the possible existence of additional PG cores of 850, 600 and 140 kd in brain soluble fractions and 850 and 540 kd in brain membrane fractions. In addition, any keratan sulfate PGs that are present in brain would not be included in Tables 1.4 and 1.5, since keratanase or endo-b-galactosidase digestions were not carried out. Biochemical evidence indicates that very little keratan sulfate is present in brain (Werz et al., 1985a; Werz et al., 1985b; Eronen et al., 1985). Recent immunohistochemical studies suggest, however, that the small amount of keratan sulfate that is present is restricted to a developmentally interesting structure, the roof-plate (Snow et al., 1990b). It will undoubtedly be important in future to extend the data reported here to include keratan sulfate PGs.

These considerations notwithstanding, the data presented suggest that distinct sets of PGs are found in the membrane-associated and soluble fractions of rat brain; that heparan sulfate PGs are more abundant in the membrane-associated fraction while chondroitin sulfate PGs are more abundant in the soluble fraction; that dermatan sulfate PGs, if they are present in brain, are relatively rare (none were detected); and that the expression of PGs changes considerably during nervous system development. These data are in good aggreement with available information on brain GAGs, namely that heparan sulfate is most abundant in membranes, while chondroitin sulfate is found mostly in the soluble fraction (Margolis et al., 1975a); that low levels of dermatan sulfate are found in brain (Werz et al., 1985a; Werz et al., 1985b; Burkart and Wiesmann, 1987), and that levels of GAGs change

considerably during brain development (Margolis et al., 1975b; Werz et al., 1985b; Burkart and Wiesmann, 1987).

The data in Figure 1.1 and Tables 1.4 and 1.5 also suggest that many PG cores are sialylated. In particular, the electrophoretic band representing M7, the most abundant species found associated with neonatal membranes, shifts and sharpens considerably with neuraminidase treatment, suggesting that sialic acid might contribute significantly to the net charge of M7. The data in Figures 1.1 and 1.2 and Tables 1.4 and 1.5 do not provide evidence of PGs that contain more than one type of GAG. It is possible, however, that some of the core proteins that were identified as having a single type of GAG may contain small amounts of a second GAG type (cf. Ripellino and Margolis, 1989). Also, if some core proteins exist predominantly as PGs containing either heparan sulfate or chondroitin sulfate, and at lower levels as hybrid heparan sulfate/chondroitin sulfate PGs, it is unlikely that the contributions of the hybrid species to gels such as those in Figures 1.1 and 1.2 would have been noticed.

Most of the putative core protein species in Tables 1.4 and 1.5 exhibit apparent M_rs that are relatively similar when reduced and non-reduced. Given the inaccuracies inherent in estimating M_r under non-reducing conditions, the data are consistent with the interpretation that most brain PG cores consist of single polypeptide chains. One possible exception is M16. On non-reducing gels, no putative core protein is detected with an apparent M_r similar to that of M16, suggesting that M16 may be disulfide-linked to another polypeptide. Given its small apparent size, M16 could have been derived from one of the higher M_r core proteins without significantly altering the mobility of the latter. However, comparison of the gel filtration behavior of M16 with those of larger heparan sulfate PG cores (by analysis of the samples in Figure 1.3 under reducing conditions) has so far failed to suggest a particular species with which M16 is associated (not shown). Thus, M16 may derive from a unique species whose presence prior to reduction is masked by other electrophoretic bands.

Biochemical Properties and Developmental Changes: Implications for Potential Functions of Brain Proteoglycans

One striking implication of Tables 1.4 and 1.5 is that the expression of several PG core proteins in the nervous system changes dramatically over the course of development. Previous studies had shown that GAG levels, GAG synthesis, and GAG turnover change considerably during brain development (Margolis et al., 1975b; Werz et al., 1985b; Burkart and Wiesmann, 1987). Although such changes could result from alterations in GAG biosynthesis and breakdown per se, the present study raises the alternative possibility that such changes primarily reflect shifts in the types and amounts of core proteins that are expressed by neural cells.

The developmental changes seen in Tables 1.4 and 1.5 may provide clues about the physiological roles of PGs. For example, PGs that only appear postnatally, such as M4, M5, M14 and M15 may be involved in late developmental events such as myelination, or stabilization of synapses while PGs such as M2, M3, M6 and M13, which are restricted to embryonic or neonatal brain, might play a role in processes such as cell migration or axon outgrowth. Conceivably, better correlation of PG expression with developmental events could be achieved by comparing PG expression among regions of the brain that develop at distinctly different times.

The biochemical properties of PGs can also suggest functional roles. For example, integral membrane PGs are thought to mediate cell-cell and cell-substratum adhesion by associating with molecules such as NCAM (Cole et al., 1986) and fibronectin (Saunders and Bernfield, 1988). It would therefore be interesting to examine the binding of PGs such as M12 and M13 to neural cell adhesion molecules and molecules of the neural extracellular matrix.

PGs that are associated with the membrane fraction but do not exhibit hydrophobic partitioning may represent PGs of the extracellular matrix. This possibility was raised in connection with PGs such as M7, M8 and M9 that exhibit unusual gel filtration behavior suggestive of aggregation (Figure 1.3). Extracellular matrix PGs of the nervous system are currently thought to play a role in the storage of neurotrophic factors such as the fibroblast growth factors (Walicke,

1989), as well as in the localization of synapse-specific molecules such as acetylcholinesterase (Brandan et al., 1985), and in the modulation of neurite outgrowth (Muir et al., 1989; Snow et al., 1990a).

At present it is unclear whether M7, M8 and M9 aggregate with themselves, each other, or with non-PG proteins. It is noteworthy, however, that such behavior was observed when dilute samples of PGs were analyzed (in Figure 1.3, PGs were applied at 17 μg protein/ml, implying that individual PG species were in the range of 1-70 nM), as well as when samples were chromatographed in moderately chaotropic buffers (in an experiment similar to that described in Figure 1.3, in which P0 membrane PGs were chromatographed in the presence of 6M urea and 0.75 M NaCl, broadly smeared elution was still observed for M7 and for 46 kd, 41 kd and 35 kd non-PGs [data not shown]; these observations suggest that at least M7 participates in interactions of relatively high affinity).

Two membrane-associated PGs (M12 and M13) were found to be linked to glycosyl-phosphatidylinositol (GPI) anchors. So far, GPI-linked PGs have only been detected on the surfaces of hepatocytes, Schwann cells, and ovarian granulosa cells (Ishihara et al., 1987; Carey and Evans, 1989; Yanigashita and McQuillan, 1989). Since M12 and M13 are relatively abundant brain PGs it is possible that they, along with NCAM-120 and Thy1, are among the major GPI-linked constituents of neural cell surfaces. Currently, the physiological role of GPI-anchors is not understood, although it has been pointed out that many GPI-linked proteins are thought to be involved in cell adhesion or cell signalling and that shedding of GPI-linked molecules can be triggered by cell-associated PI-PLC, with the concomittant production of diacylglycerols (Low and Saltiel, 1988). Interestingly, the properties of S9, a PG of the soluble fraction, are sufficiently similar to those of M12 to suggest that the former may represent a shed form of the latter.

In summary, the mammalian brain, a structure that contains a diverse set of developmentally important proteins capable of binding GAGs and PGs, apparently also contains a diverse set of developmentally regulated heparan sulfate and chondroitin sulfate PGs. Uncovering the functions of these PGs will require identifying both the

cells that express them and the molecules that bind them. In this regard, it will be important to determine whether any of the PGs described here correspond to neural PGs that have been defined immunochemically (e.g. NG2 [Levine and Card, 1987; Stallcup and Beasley, 1987], Cat301[Zaremba et al., 1989], a HSPG of PC12 cells [Matthew et al., 1985]), neural PGs that have been described in other species (e.g. TAP-1[Carlson and Wight, 1987], cytotactin-binding PG[Hoffman et al., 1988]) or PGs found in tissues outside the central nervous system.

Acknowledgements

The authors would like to acknowledge Grant Joslin, Magdalena Lofstedt and Gary Gruberth for technical assistance, Matthias Lee for assistance in preparing proteoglycan fractions and for sharing preliminary data on velocity sedimentation analysis of PGs, and Vonya Perham for typing of the manuscript. The authors are grateful to Lisa Plantefaber and Frank Solomon for their helpful comments on the manuscript. This work was supported by grants from the Whitaker Health Sciences Fund and the National Science Foundation. M. Herndon is the recipient of NRSA pre-doctoral support.

REFERENCES

Akeson, R.A., and S.L. Warren. 1984. The adhesion of rat embryonic CNS neurons to complex extracellular matrices is heparin sensitive. J. Cell Biol. 99:172a.

Aquino, D.A., R.U. Margolis, and R.K. Margolis. 1984. Immunocytochemical localization of a chondroitin sulfate proteoglycan in nervous tissue. II. Studies in developing brain. J. Cell Biol. 99:1130-1139.

Bordier, C. 1981. Phase separation of integral membrane proteins in triton X-114 solution. J. Biol. Chem. 256:1604-1607.

Brandan, E., M. Maldonado, J. Garrido, and N.C. Inestrosa. 1985. Anchorage of collagen-tailed acetylcholinesterase to the extracellular matrix is mediated by heparan sulfate proteoglycans. J. Cell Biol. 101:985-992.

Bretscher, M.S. 1985. Heparan sulphate proteoglycans and their polypeptide chains from BHK cells. EMBO J. 4:1941-1944.

Burkart T., and U.N. Weismann. 1987. Sulfated glycosaminoglycans (GAG) in the developing mouse brain: quantitative aspects on the metabolism of total and individual sulfated GAG in vivo. Devel. Biol. 120:447-456.

Carbonetto, S., M.M. Gruver, and D.C. Turner. 1983. Nerve fiber growth in culture on fibronectin, collagen, and glycosaminoglycan substrates. J. Neurosci. 3:2324-2335.

Carey, D., and D.M. Evans. 1989. Membrane anchoring of heparan sulfate proteoglycans by phosphatidylinositol and kinetics of synthesis of peripheral and detergent-solubilized proteoglycans in Schwann cells. J. Cell Biol. 108:1891-1897.

Carlson, S.S., and T.N. Wight. 1987. Nerve terminal anchorage protein one (TAP-1) is a chondroitin sulfate proteoglycan: biochemical and electron microscopic characterization. J. Cell. Biol. 105:3075-3086.

Clemetson, K.J., D. Beinz, M.L. Zahno, and E.F. Luscher. 1984. Distribution of platelet glycoproteins and phosphoproteins in hydrophobic and hydrophilic phases in Triton X-114 phase partition. Biochim. Biophys. Acta. 778:463-469.

Cole, G.J., D. Schubert, and L. Glaser. 1985. Cell-substratum adhesion in chick neural retinal depends upon protein-heparan sulfate interactions. J. Cell Biol. 100:1192-1199.

Coster, L., I. Carlstedt, S. Kendall, A. Malmstrom, A. Schmidtchem, and L-A. Fransson. 1986. Structure of proteoheparan sulfates from fibroblasts: confluent and proliferating fibroblasts produce at least three types of proteoheparan sulfates with functionally different core proteins. J. Biol. Chem. 261:12079-12088.

Cunningham, D.D., W. E. VanNostrand, D.H. Farrell, and C.H. Campbell. 1986. Interactions of serine proteases with cultured fibroblasts. J. Cellular Biochem. 32:381-291.

Damon, D.H., P.A. D'Amore, and J.A. Wagner. 1987. Sulfated glycosaminoglycans modify growth factor-induced neurite outgrowth in PC12 cells. Soc. Neurosci. Abstr. 13:1606.

Eronen, I. T. Mononen, and I. Mononen. 1985. Isolation and partial characterization of keratan sulphate from human brain. Biochim. Biophys. Acta 843:155-158.

Gloor, S., K. Odink, J. Guenther, H. Nick, and D. Monard. 1986. A glia-derived neurite promoting factor with protease inhibitory activity belongs to the protease nexins. Cell 47:687-693.

Gordon, H., and Z.W. Hall. 1989a. Glycosaminoglycan variants in the C2 muscle cell line. Devel. Biol. 135:1-11.

Gordon, H., and Z.W. Hall. 1989b. Agrin does not induce ACHR clusters in a variant muscle cell. Soc. Neurosci. Abstr. 15:1352.

Hassell, J.R., J.H. Kimura, and V.C. Hascall. 1986. Proteoglycan core protein families. Ann. Rev. Biochem. 55:539-567.

He, H-T., J. Barbet, J-C. Chaix, and C. Goridis. 1986. Phosphotidylinositol is involved in the membrane attachment of NCAM-120, the smallest component of the neural cell adhesion molecule. EMBO J. 5:2489-2494.

Herndon, M.E., and A.D. Lander. 1989. Developmental changes in expression of brain proteoglycans in the rat. J. Cell Biol. 109:234a.

Hoffman, S., K.L. Crossin, and G.M. Edelman. 1988. Molecular forms, binding functions, and developmental expression patterns of cytotactin and cytotactin-binding proteoglycan, an interactive pair of extracellular matrix molecules. J. Cell Biol. 106:519-532.

Ishihara, M., N.S. Fedarko, and H.E. Conrad. 1987. Involvement of phosphatidylinositol and insulin in the coordinate regulation of proteoheparan sulfate metabolism and hepatocyte growth. J. Biol. Chem. 262:4708-4716.

Kato, M., Y. Oike, S. Suzuki, and K. Kimata. 1985. Selective removal of heparan sulfate chains from proteoheparan sulfate with a commercial preparation of heparitinase. Anal. Biochem. 148:479-484.

Kiang, W-L., R.U. Margolis, and R.K. Margolis. 1981. Fractionation and properties of a chondroitin sulfate proteoglycan and the soluble glycoproteins of brain. J. Biol. Chem. 256:10529-10537.

Kidokoro, Y., and Y. Hirano. 1988. Heparin and heparan sulfate inhibit

nerve-induced ACh receptor accumulation. Soc. Neurosci. Abstr. 14:514.

Klinger, M.M., R.U. Margolis, and R.K. Margolis. 1985. Isolation and characterization of the heparan sulfate proteoglycans of brain. J. Biol. Chem. 260:4082-4090.

Laemmli, U.K. 1970. Cleavage of structural proteins during the assembly of the head of bacteriophage T4. Nature 227:680-685.

Lander, A.D. 1987. Molecules that make axons grow. Molecular Neurobiol. 1:213-245.

Lander, A.D. 1989. Understanding the molecules of neural cell contacts: emerging patterns of structure and function. Trends in Neurosci. 12:189-195.

Lander, A.D., M.K. Lee, and M.E. Herndon. 1988. Proteoglycans of the developing and mature rat brain. J. Cell Biol. 107:160a.

Levine, J.M., and J.P. Card. 1987. Light and electron microscopic localization of a cell surface antigen (NG2) in the rat cerebellum: association with smooth protoplasmic astrocytes. J. Neurosci. 7:2711-2720.

Lindahl, U., L. Thunberg, G. Backstrom, J. Riesenfeld, K. Nordling, and I. Bjork. 1984. Extension and structural variability of the antithrombin-binding sequence in heparin. J. Biol. Chem. 259:12368-12376.

Linker, A., and P. Hovingh. 1972. Heparinase and heparitinase from flavobactera. Methods. Enzymol. 28:902-910.

Lobb, R.R., J.W. Harper, and J.W. Fett. 1986. Purification of heparin-binding growth factors. Anal. Biochem. 154:1-14.

Lories, V., H. DeBoeck, G. David, J-J. Cassiman, and H. VanDenBerghe. 1987. Heparan sulfate proteoglycans of human lung fibroblasts: structural heterogeneity of the core proteins of the hydrophobic cell-associated forms. J. Biol. Chem. 262:854-859.

Lories, V., J-J. Cassiman, H. VanDenBerghe, and G. David. 1989. Multiple distinct membrane heparan sulfate proteoglycans in human lung fibroblasts. J. Biol. Chem. 264:7009-7016.

Low, M.G., and A.R. Saltiel. 1988. Structural and functional roles of glycosyl-phosphatidylinositol in membranes. Science 239:268-275.

Low, M.G., and P.W. Kincade. 1985. Phosphatidylinositol is the membrane anchoring domain of the Thy-1 glycoprotein. Nature 318:62-64.

Marcum, J.A., C.F., Reilly, and R.D. Rosenberg. 1987. Heparan sulfate species and blood vessel wall function. *In* Biology of Proteoglycans. T.N. Wight and R.P. Mecham, eds. Academic Press, Orlando. 301-343.

Margolis, R.K., R.U. Margolis, C. Preti, and D. Lai. 1975a. Distribution and metabolism of glycoproteins and glycosaminoglycans in subcellular fractions of brain. Biochem. 14:4797-4804.

Margolis, R.U., R.K. Margolis, L.B. Chang, and C. Preti. 1975b. Glycosaminoglycans of brain during development. Biochem. 14:85-88.

Matthew, W.D., R.J. Greenspan, A.D. Lander, and L.F. Reichardt. 1985. Immunopurification and characterization of a neuronal heparan sulfate proteoglycan. J. Neurosci. 5:1842-1850.

Morris-Kay, G.M. and B. Crutch 1982. Culture of rat embryos with beta-D-xyloside: evidence of a role for proteoglycans in neurulation. J. Anat. 134:491-506.

Muir, D., E. Engvall, S. Varon, and M. Manthorpe. 1989. Schwannoma

cell-derived inhibitor of the neurite-promoting activity of laminin. J. Cell Biol. 109:2353-2362.

Neufeld, G., D. Gospodarowicz, L. Dodge, and D.K. Fujii. 1987. Heparin modulation of the neurotrophic effects of acidic and basic fibroblast growth factors and nerve growth factor on PC12 cells. J. Cell. Physiol. 131:131-140.

Oohira, A., F. Matsui, M. Matsuda, Y. Takida, and Y. Koboki. 1988. Occurence of three distinct molecular species of chondroitin sulfate proteoglycan in the developing rat brain. J. Biol. Chem. 263:10240-10246.

Perris, R., and S. Johansson. 1987. Amphibian neural crest cell migration on purified extracellular matrix components: A chondroitin sulfate proteoglycan inhibits locomotion on fibronectin substrates. J. Cell Biol. 105:2511-2521.

Ratner, N., D. Hong, M.A. Lieberman, R.P. Bunge, and L. Glaser. 1988. The neuronal cell-surface molecule mitogenic for Schwann cells is a heparin-binding protein. Proc. Natl. Acad. Sci. USA. 85:6992-6996.

Ratner, N., R.P. Bunge, and L. Glaser. 1985. A neuronal cell surface heparan sulfate proteoglycan is required for dorsal root ganglion neuron stimulation of Schwann cell proliferation. J. Cell Biol. 101:744-754.

Ripellino, J.A., and R.U. Margolis. 1989. Structural properties of the heparan sulfate proteoglycans of brain. J. Neurochem. 52:807-812.

Ruoslahti, E. 1989. Proteoglycans in cell regulation. J. Biol. Chem. 264:13369-13372.

Sanes, J.R. 1989. Extracellular matrix molecules that influence neural development. Ann. Rev. Neurosci. 12:491-516.

Saunders, S., and M. Bernfield. 1988. Cell surface proteoglycan binds mouse mammary epithelial cells to fibronectin and behaves as a receptor for interstitial matrix. J. Cell Biol. 106:423-430.

Saunders, S., M. Jalkanen, S. O'Farrell, and M. Bernfield. 1989. Molecular cloning of syndecan, an integral membrane proteoglycan. J. Cell Biol. 108:1547-1556.

Schaffner, W., and C. Weissman. 1973. A rapid, sensitive, and specific method for the determination of protein in dilute solution. Anal. Biochem. 56:502-514.

Schubert, D., and M. LaCorbiere. 1982. The specificity of extracellular glycoprotein complexes in mediating cellular adhesion. J. Neurosci. 2:82-89.

Schubert, D., M. LaCorbiere, and F. Esch. 1986. A chick neural retina adhesion and survival molecule is a retinol-binding protein. J. Cell Biol. 102:2295-2301.

Schubert, D., M. LaCorbiere, T. Saitoh, and G. Cole. 1989. Characterization of an amyloid b precursor protein that binds heparin and contains tyrosine sulfate. Proc. Natl. Acad. Sci. USA. 86:2066-2069.

Schubert, D., N. Ling, and A. Baird. 1987. Multiple influences of a heparin-binding growth factor on neuronal development. J. Cell Biol. 104:635-644.

Snow, D.M., V. Lemman, D.A. Carrino, A. Caplan, and J. Silver. 1990. Sulfated proteoglycans present in astroglial barriers during development in vivo inhibit neurite outgrowth in vitro. Expl. Neurol. 109:111-130.

Snow, D.M., D.A. Steindler, and J. Silver. 1990. Molecular and cellular characterization of the glial roof plate of the spinal cord and optic tectum: A possible role for a proteoglycan in the development of an axon barrier. Devel. Biol. 138:359-376.

Stallcup, W.B., and L. Beasley. 1987. Bipotential glial precursor cells of the optic nerve express the NG2 proteoglycan. J. Neurosci. 7:2737-2744.

Swanson, M.L., R.K. Keast, M.L. Jennings, and J.E. Pessin. 1988. Heterogeneity in the human erythrocyte Band 3 anion-transporter revealed by Trtiton X-114 phase partitioning. Biochem. J. 255:229-234.

Volk, T., and B. Geiger. 1986. A-CAM: A 135 kD receptor of intercellular adherens junctions. I. Immunoelectron microscopic localization and biochemical studies. J. Cell Biol. 103:1441-1450.

Walicke, P.A. 1988. Interactions between basic fibroblast growth factor (FGF) and glycosaminoglycans in promoting neurite outgrowth. Expl. Neurol. 102:144-148.

Walicke, P.A. 1989. Novel neurotrophic factors, receptors, and oncogenes. Ann. Rev. Neurosci. 12:103-126.

Wang, Y-J., and H.R. Mahler. 1976. Topography of the synaptosomal membrane. J. Cell Biol. 71:639-658.

Werz, W., G. Fischer, and M. Schachner. 1985a. Glycosaminoglycans of rat cerebellum: I. Quantitative analysis of the main constituents at postnatal day 6. J. Neurochem. 44:900-906.

Werz, W., G. Fischer, and M. Schachner. 1985b. Glycosaminoglycans of rat cerebellum: II. A developmental study. J. Neurochem. 44:907-910.

Woods, A., J.R. Couchman, and M. Hood. 1985. Heparan sulfate proteoglycans of rat embryo fibroblasts. J. Biol. Chem. 260:10872-10879.

Wray, W., T. Boulikas, V.P. Wray, and R. Hancock. 1981. Silver staining of proteins in polyacrylamide gels. Anal. Biochem. 118:197-203.

Yanagishita, M., and D.J. McQuillan. 1989. Two forms of plasma membrane-intercalated heparan sulfate proteoglycan in rat ovarian granulosa cells: labeling of proteoglycans with a photoactivatable hydrophobic probe and effect of the membrane anchor-specific phospholipase C. J. Biol. Chem. 264:17551-17558.

Zaremba, S., A. Guimaraes, R.G. Kalb, and S. Hockfield. 1989. Characterization of an activity-dependent, neuronal surface proteoglycan identified with monoclonal antibody Cat-301. Neuron 2:1207-1219.

Table 1.1. DEAE Purification of a Proteoglycan-Enriched Fraction from Postnatal Day 0 Rat Brain.

	Membrane-associated Proteoglycans[a] mg protein/g brain (wet weight)	Soluble fraction-associated Proteoglycans[b] mg protein/g brain(wet weight)
Crude homogenate	7.4 ± 2.1[c]	15.6 ± 2.5
DEAE Column pools:		
Flow through	3.6 ± 1.5	4.2 ± 0.65
Buffer D	0.84 ± 0.10	1.4 ± 0.02
Buffer E	1.00 ± 0.35	10.9 ± 6.1
Buffer F	0.02 ± 0.022	0.049 ± 0.007
PG fraction	0.01 ± 0.004[c]	0.015 ± 0.0045

See text for description of purification procedure. Numbers shown are mean values ± range based on two independent preparations([b]), or mean ± standard deviation for four independent preparations ([a]). [c] = only three determinations were available for these data points.

Table 1.2. Recovery of Proteoglycans from Embryonic, Newborn, and Adult Rat Brain.

Brain subcellular fractions	Crude homogenate	Proteoglycan Fraction	Recovery
	mg protein/g brain (wet weight)	μg protein/g brain (wet weight)	%of crude homogenate protein
Membrane fractions:			
Embryonic (day 18)[a]	2.62	8	0.30
Newborn (postnatal day 0)[c]	7.41	10	0.13
Adult (> 6 weeks)[b]	16.9	20	0.12
Soluble fractions:			
Embryonic (day 18)[a]	10.5	12	0.11
Newborn (postnatal day 0)[c]	15.6	14.5	0.09
Adult (> 6 weeks)[b]	35.0	15	0.04

Numbers shown are mean values from one([a]), two ([b]), or three ([c]) independent preparations.

Table 1.3. Fractionation of ^{125}I-proteoglycans mixed with crude homogenate.

Purification step	Percent input cpm
Labelled PGs + crude homogenate	100%
DEAE Column Pools:	
Flow through	4.7%
Buffer D	0.9%
Buffer E	2.1%
Buffer F	1.0%
PGs recovered (Buffer G):	
Peak (38ml)	39.2%
Tail (500ml)	8.5%
Not recovered	43.6%

Radioiodinated PGs purified from postnatal day 0 (P0) membrane preparation (300 ng, 1.24×10^7 cpm) were added to a fresh P0 membrane preparation (52 mg protein) and subjected to DEAE-Sephacel fractionation (50 ml column volume) as outlined in the text, except that buffers C through F contained 0.5% CHAPS instead of Triton X-100. Values shown are the percent of initial radioactivity that was recovered in the protein peaks eluted at the indicated steps. For discussion, see text.

Figure 1.1. SDS-PAGE analysis of proteoglycan preparations from postnatal day 0 rat brain. Purified and radioiodinated samples were subjected to enzymatic digestion, as described in the text, and analyzed on 5-15% exponential gradient gels run under non-reducing conditions. Samples derived from a membrane preparation (A) and from the soluble fraction of brain (B) are shown. (+) and (-) symbols indicate whether a sample was treated with an enzyme. Molecular weight markers are shown to the left of each gel, while arrowheads at right identify putative PG core proteins mentioned in Tables 1.4 and 1.5. Asterisks mark non PG proteins routinely found in these preparations.

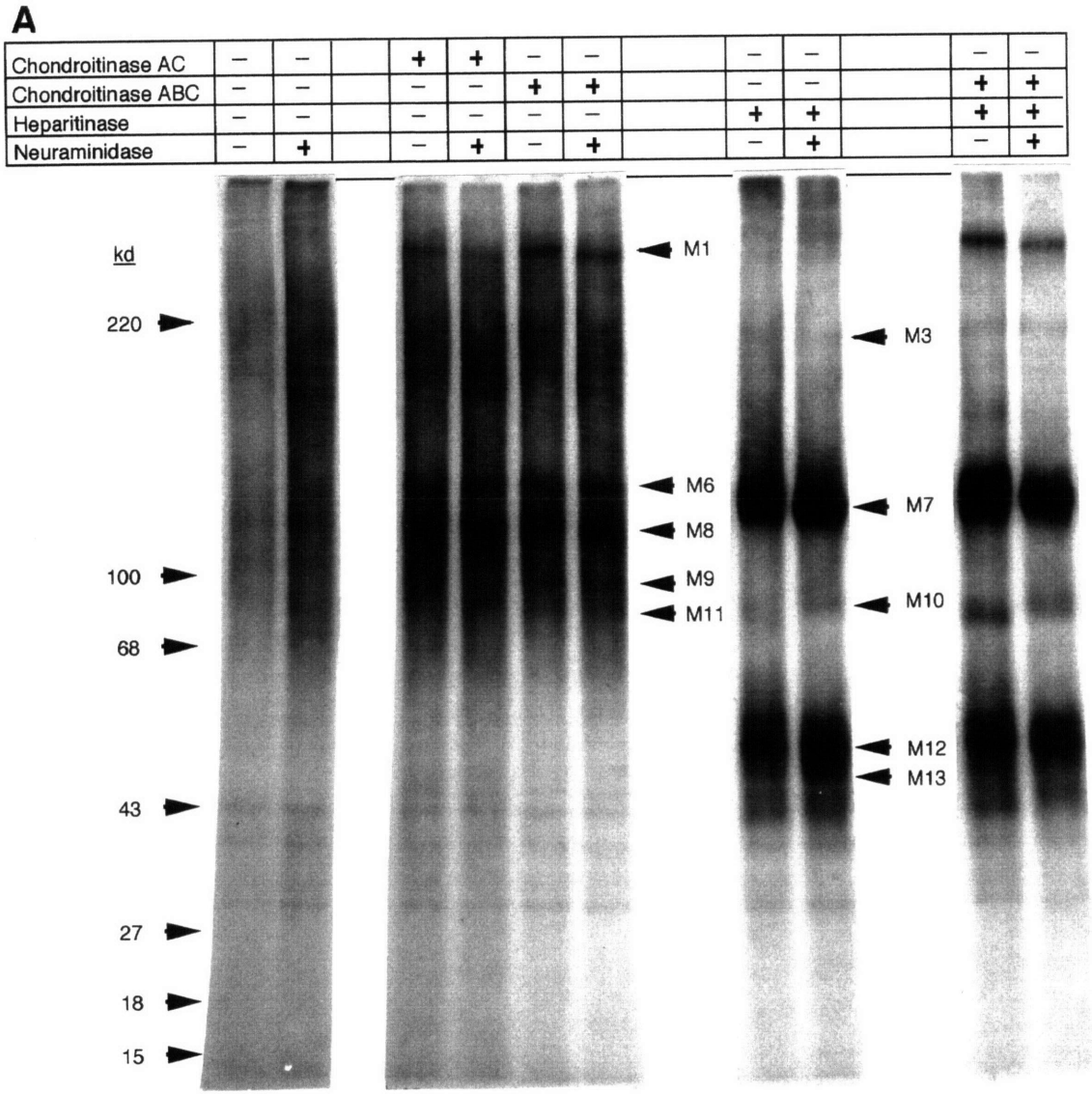
A
Chondroitinase AC
Chondroitinase ABC
Heparitinase
Neuraminidase
kd
220
100
68
43
27
18
15
M1
M3
M6
M7
M8
M9
M10
M11
M12
M13

B

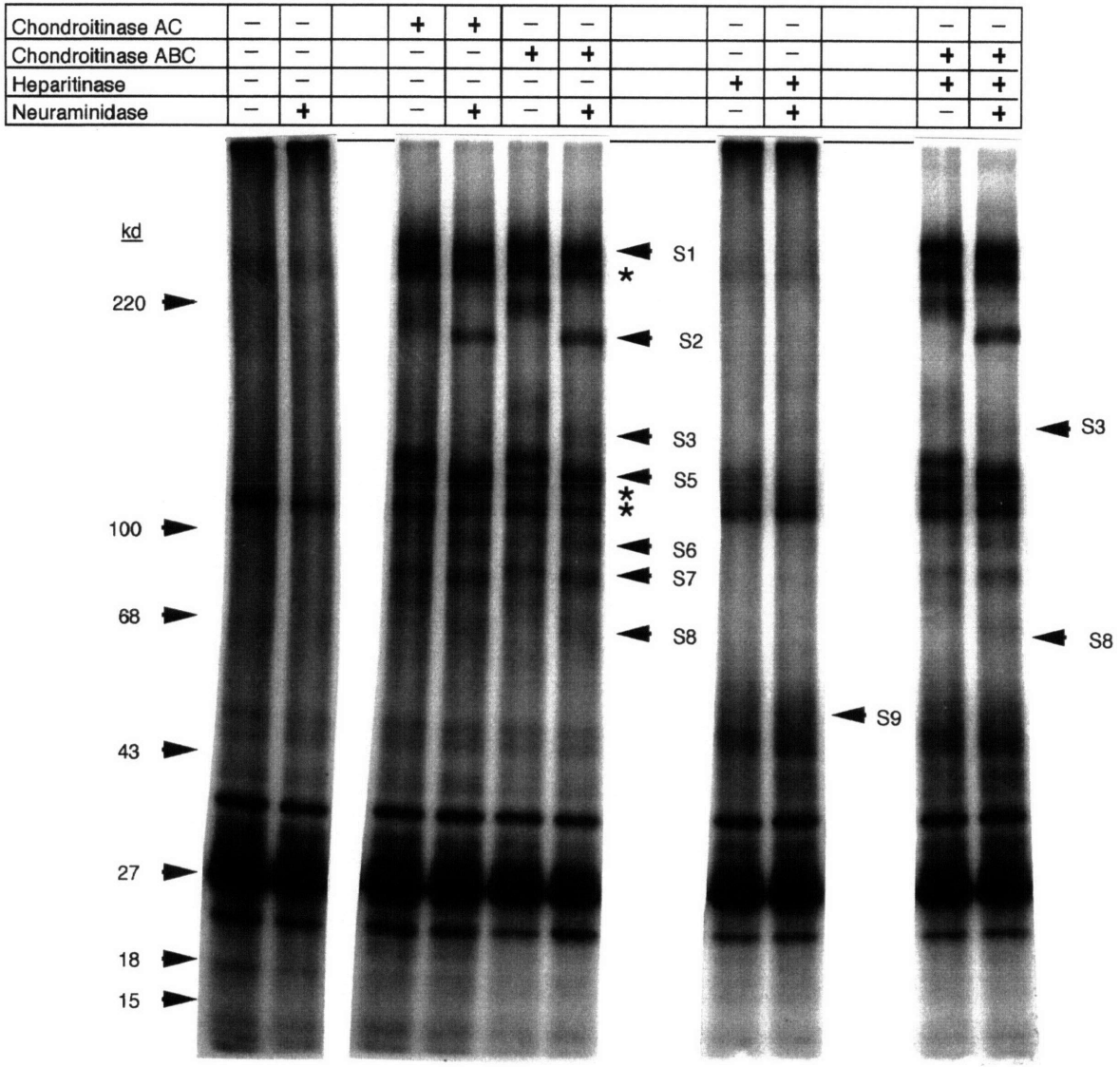
Chondroitinase AC
Chondroitinase ABC
Heparitinase
Neuraminidase
kd
220
100
68
43
27
18
15
S1
S2
S3
S5
S6
S7
S8
S9
S3
S8

Figure 1.2. Comparison of PG core protein expression in embryonic, newborn, and adult rat brain. Equivalent cpm of radioiodinated samples from embryonic day 18 (E18), postnatal day 0 (P0), and adult (Ad) rat brain were subjected to enzymatic digestion and analyzed by SDS-PAGE under non-reducing conditions on 10% gels. (+) and (-) symbols indicate whether a sample was treated with an enzyme. PGs from membrane fractions are shown in panel A , while PGs from soluble fractions are shown in panel B. Molecular weight markers are shown to the left of each gel. Arrowheads to the right of gels identify putative PG core proteins (see Tables 1.4 and 1.5).

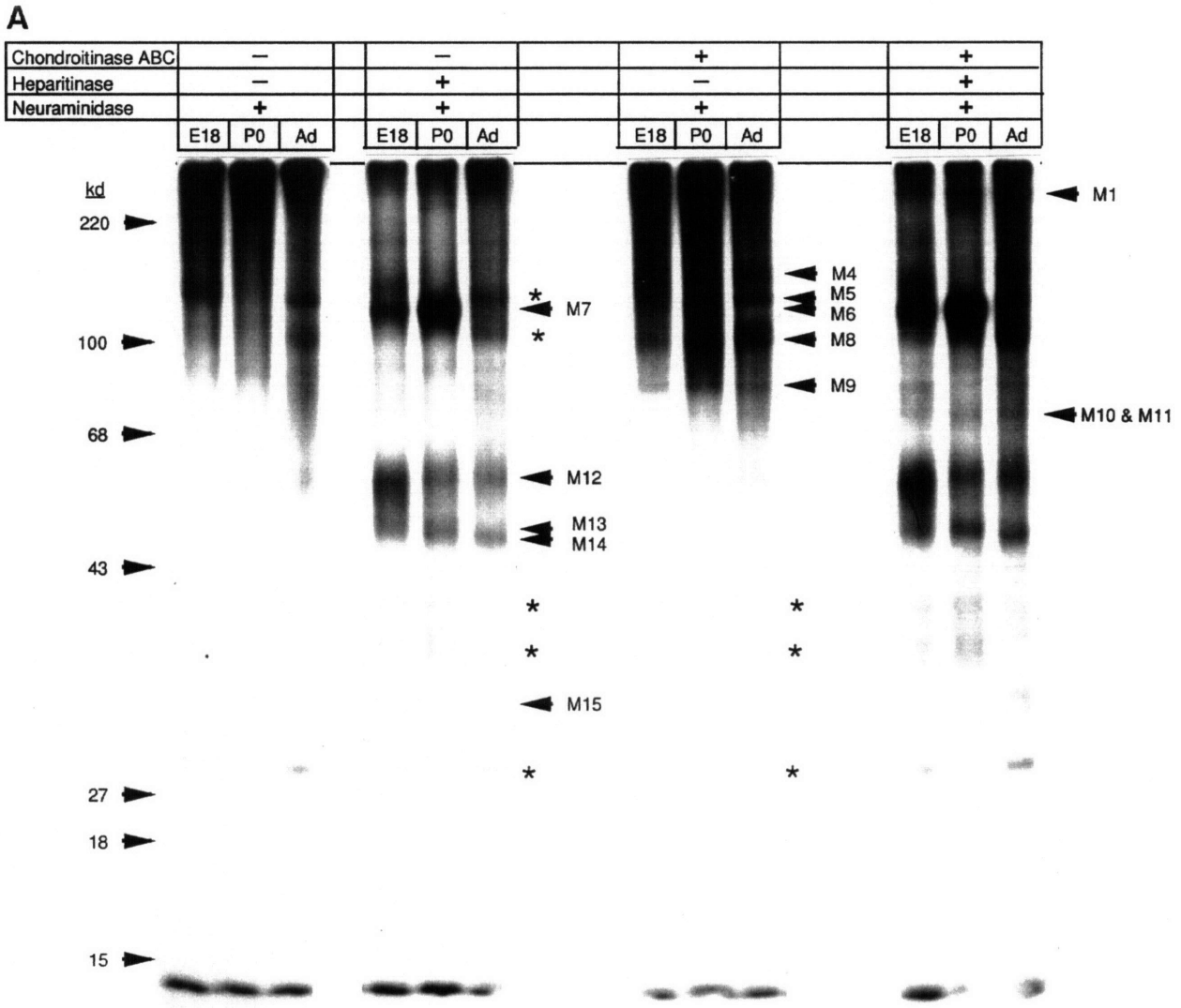
A
Chondroitinase ABC
Heparitinase
Neuraminidase
E18
P0
Ad
kd
220
100
68
43
27
18
15
M1
M4
M5
M6
M7
M8
M9
M10 & M11
M12
M13
M14
M15

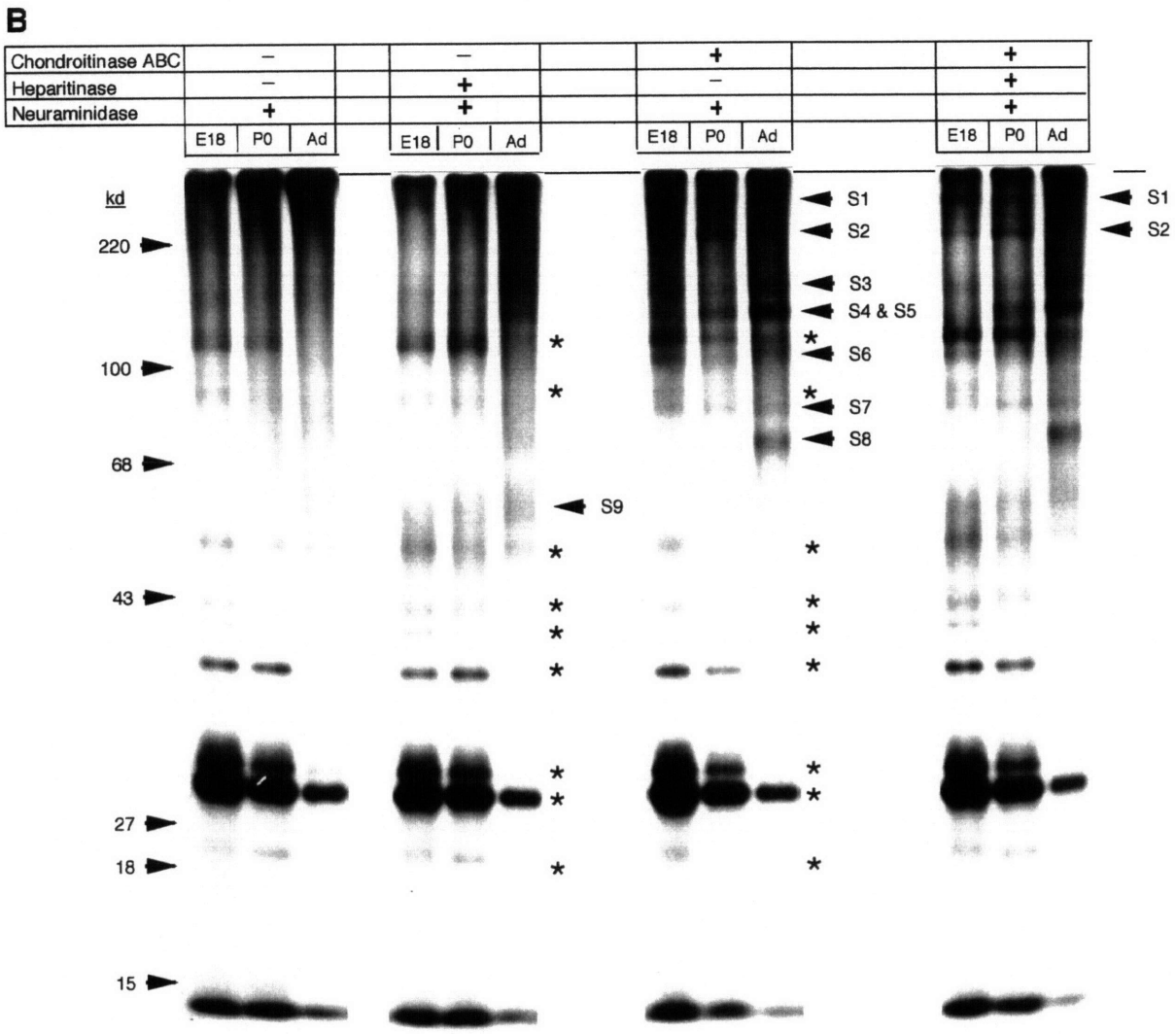
B
Chondroitinase ABC
Heparitinase
Neuraminidase
E18
P0
Ad
kd
220
100
68
43
27
18
15
S1
S2
S3
S4 & S5
S6
S7
S8
S9

Table 1.4. Proteoglycans of the Membrane Fraction.

Designation	GAG Type	Apparent M_r of Core Protein				DEAE Elution	Relative Abundance
		Non-reduced		Reduced			
		-N'dase	+N'dase	-N'dase	+N'dase	(M NaCl)	E18 P0 Adult
M1	ChS	440kd	420kd	440kd	415kd	0.5	
M2	ChS	330kd	270kd	270kd	260kd		
M3	HeS	230kd	230kd	n.s.	n.s.		
M4	ChS	162kd	160kd	170kd	n.s.		
M5	ChS	140kd	140kd	150kd	135kd		
M6	ChS	135kd	135kd	140kd	145kd		
M7	HeS	145kd	130kd	145kd	135kd	0.46	
M8	ChS	130kd	120kd	120kd	115kd		
M9	ChS	85kd	85kd	90kd	85kd	0.43	
M10	HeS	75kd	77kd	75kd	80kd		
M11	ChS	75kd	75kd	85kd	80kd		
M12	HeS	60kd	59kd	67kd	65kd	0.41	
M13	HeS	48kd	50kd	57kd	55kd	0.42	
M14	HeS	n.s.	49kd	n.s.	51kd		
M15	HeS	35kd	35kd	39kd	39kd		
M16	HeS	n.s.	n.s.	25kd	25kd		

^{125}I-labeled membrane-associated proteoglycans from embryonic day 18 (E18), postnatal day 0 (P0), and adult rat brain were subjected to SDS-gel analysis after enzymatic treatments. Electrophoretic bands that appear in response to either chondroitinase or heparitinase treatment are taken as evidence of chondroitin sulfate (ChS) or heparan sulfate (HeS) PGs, respectively (see text). Putative PGs are listed in descending order of apparent core protein M_r, as determined from 5%, 10%, and 5-15% reducing and non-reducing SDS polyacrylamide gels. Changes in apparent core protein M_r in response to digestion with neuraminidase (N'dase) from *Arthrobacter ureafaciens* are also noted. Identical results were seen with neuraminidase from *Clostridium perfringens* (not shown). In a few cases, electrophoretic bands were very faint or were obscured by other bands, and an accurate M_r could not be determined; in these instances the core protein is described as "not seen" (n.s.). Information on the relative abundances of PG species was obtained by comparing SDS-gel analyses of equivalent cpms of PGs from each developmental stage. Horizontal bars of four different widths have been used to convey a qualitative ranking of PGs into those that are of very high ( ), high ( ), moderate ( ), and low ( ) abundances, as determined from autoradiograms such as those in figure 2. Data on salt gradient elution profiles are also presented for several abundant PGs. These results, which reflect analysis of P0 material only, are expressed as the NaCl concentration at which the peak of eluted material is found.

Table 1.5. Proteoglycans of the Soluble Fraction.

Designation	GAG Type	Apparent M_r of Core Protein				DEAE Elution	Relative Abundance
		Non-reduced		Reduced			
		-N'dase	+N'dase	-N'dase	+N'dase	(M NaCl)	E18 P0 Adult
S1	ChS	500kd†	400kd	n.d.	n.d.	0.53	
S2	ChS	235kd	215kd	230kd	195kd		
S3	ChS	165kd	155kd	180kd	165kd	0.45	
S4	ChS	140kd	135kd	160kd	155kd		
S5	ChS	140kd	130kd	155kd	150kd	0.45	
S6	ChS	110kd	110kd	115kd	115kd		
S7	ChS	93kd	90kd	100kd	100kd		
S8	ChS	85kd	80kd	87kd	80kd		
S9	HeS	63kd	60kd	60kd	60kd	0.41	

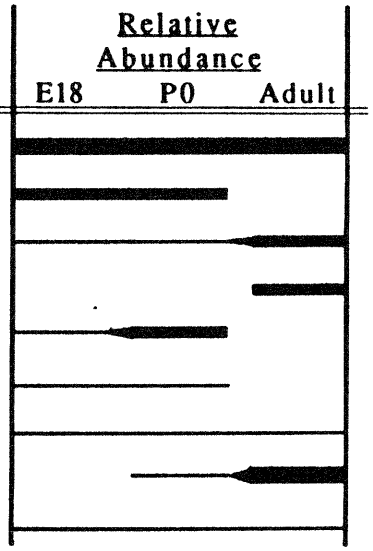

^{125}I-labeled soluble fraction proteoglycans from embryonic day 18 (E18), postnatal day 0 (P0), and adult rat brain were subjected to SDS-gel analysis after enzymatic treatments. For explanation, see legend to Table 14. n.d. = not determined (gels appropriate for accurate M_r determination in this range were not done). † = Estimation of kd based on extrapolation from molecular weight standards and therefore should be considered only a rough estimate.

Figure 1.3. Gel filtration analysis of membrane-associated PGs. Radioiodinated P0 membrane-associated PGs were subjected to gel filtration as described in text. Samples of each column fraction were subjected to 5-15% SDS-PAGE (non-reducing), either before (A) or after (B) digestion with neuraminidase, heparitinase, and chondroitinase ABC. V_0 and V_t were at fractions 27 and 50, respectively. Column fraction numbers are indicated at top. Molecular weight markers are shown to the left of each gel, while arrowheads at right identify putative PG core proteins mentioned in Table 1.4. Bands identified by asterisks (*) in panel A represent non-PG proteins that exhibit fractionation behavior suggestive of aggregation. Several non-PG proteins that do not exhibit this behavior are marked in panel A with diamonds (<>). Although the same non-PG proteins are present in panel B, only the PG core proteins have been marked. For further discussion, see text.

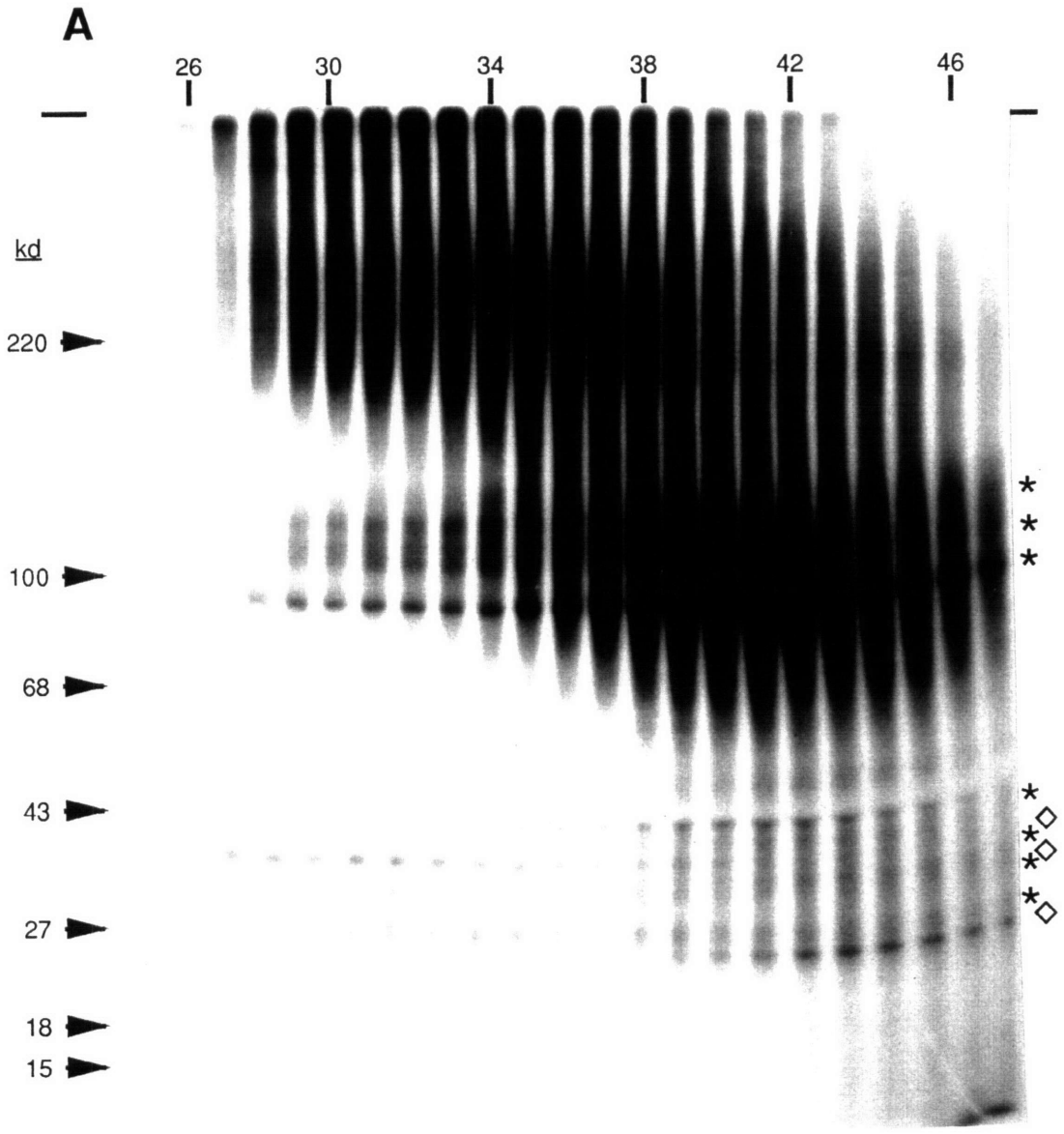
A
26
30
34
38
42
46
kd
220
100
68
43
27
18
15

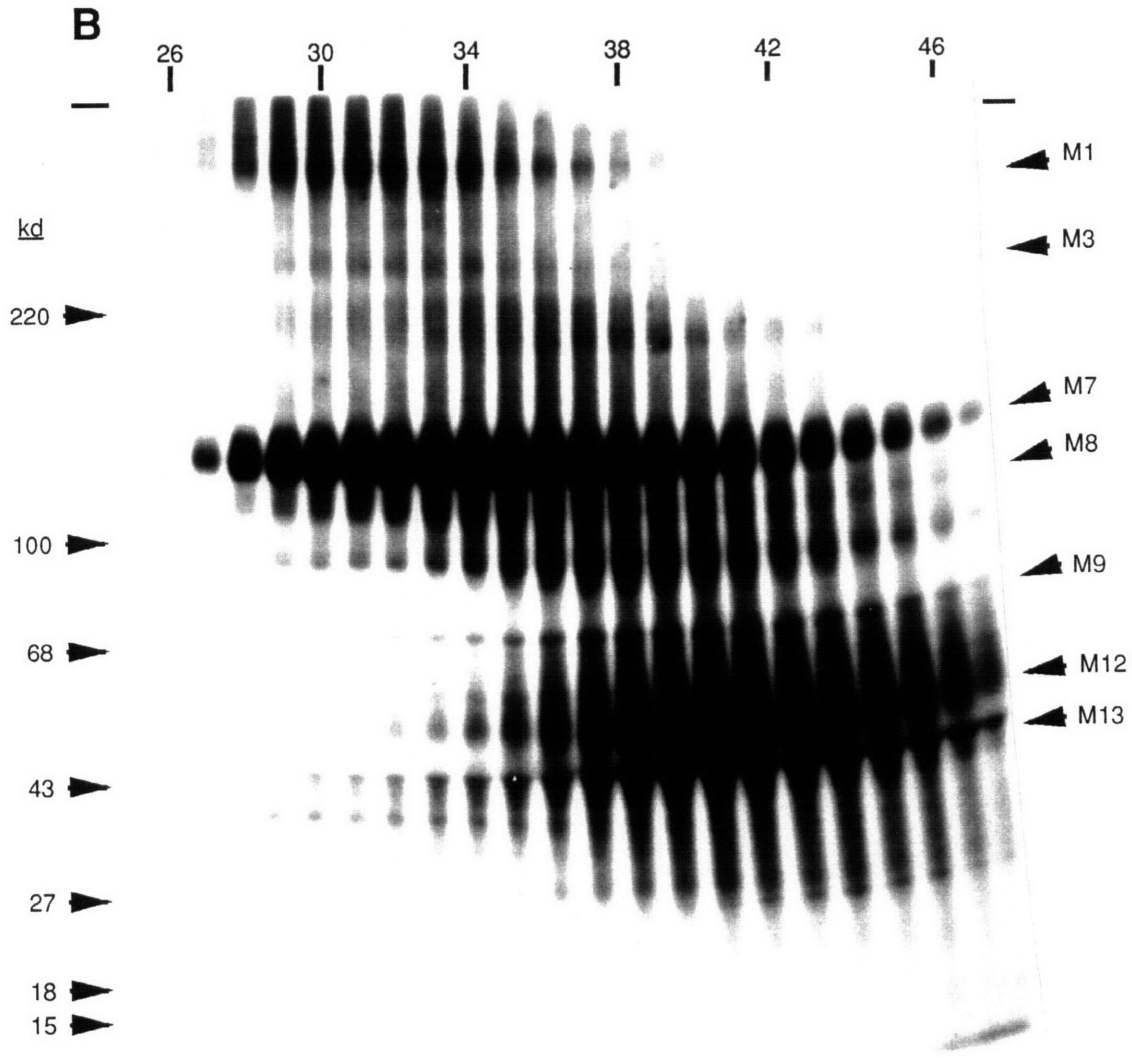
B
26
30
34
38
42
46
kd
220
100
68
43
27
18
15
M1
M3
M7
M8
M9
M12
M13

Figure 1.4. Triton X-114 phase partitioning of membrane-associated PGs. Radioiodinated membrane-associated PGs from embryonic day 18 (E18), postnatal day 0 (P0), and adult (Ad) brain were subjected to Tx114 partitioning as described in the text. Detergent-enriched (DET) and aqueous (AQ) phases of partitioning were subjected to non-reducing 5-15% SDS-PAGE before (-) and after (+) digestion with neuraminidase, heparitinase, and chondroitinase ABC ("triple digestion"). Molecular weight markers are shown to the left of each gel. Some proteins exhibit slightly altered mobility in DET lanes, presumably due to high concentrations of Tx114 in these samples. Although the figure shows results from a single gel, lanes marked DET represent threefold longer exposures than AQ lanes. In general, molecules that partitioned into detergent phases did not do so quantitatively. This was particularly true of intact PGs. In contrast, detergent partitioning of PG-cores (following GAG lyase digestion) tended to be more efficient (cf. Figure 1.5), consistent with the widely held view that highly hydrophilic moieties (such as GAG chains or other carbohydrates) hinder partitioning into detergent phases (cf. Clemetson et al.,1984; Volk and Geiger, 1986). Alternatively, biphasic partitioning can reflect the existence of distinct forms of a single protein, as has been suggested for human erythrocyte Band 3 protein (Swanson et al., 1988).

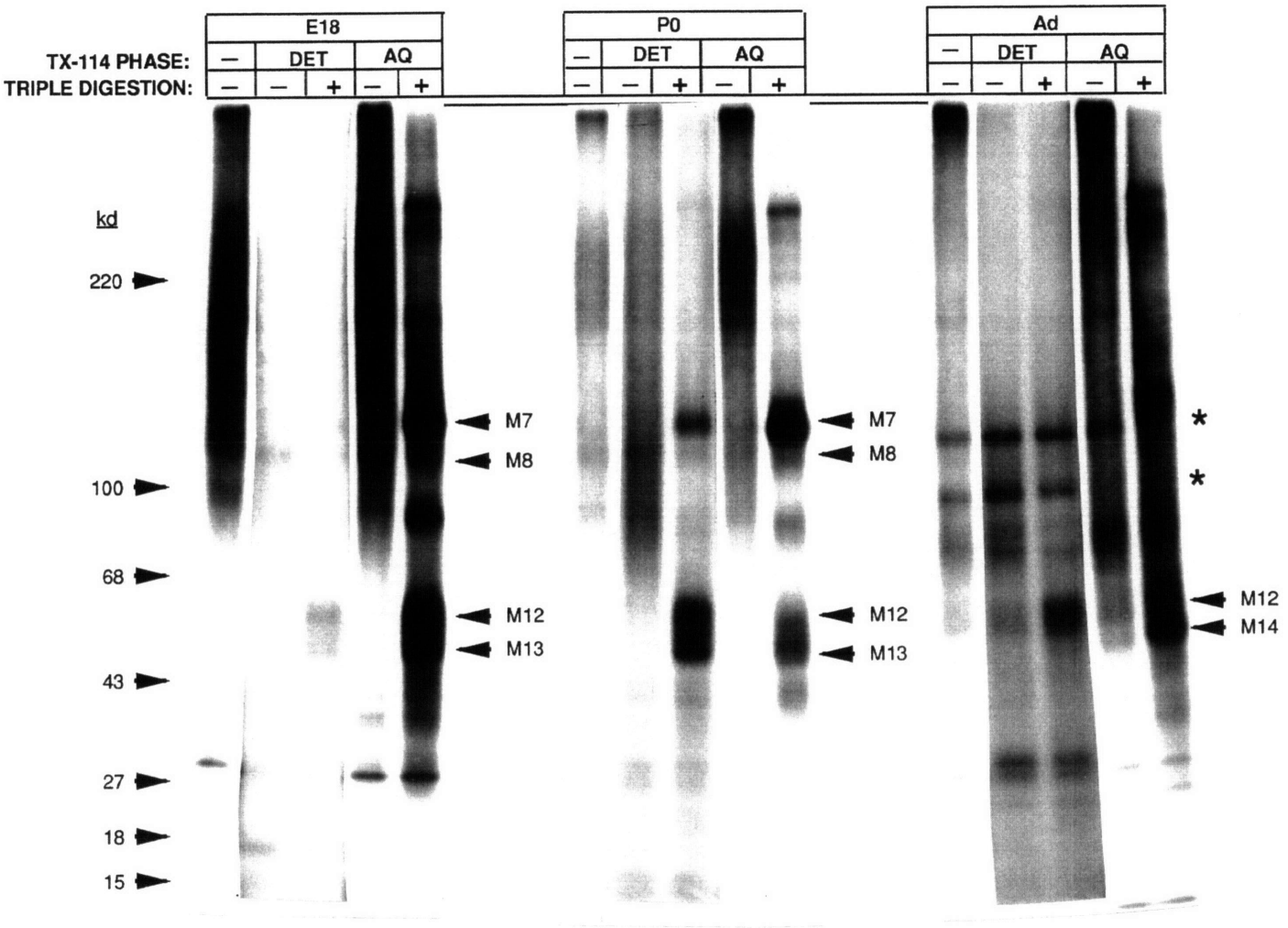
E18
P0
Ad
TX-114 PHASE:
TRIPLE DIGESTION:
—
DET
AQ
+
kd
220
100
68
43
27
18
15
M7
M8
M12
M13
M14
*
*

Figure 1.5. Glycosyl-phosphatidylinositol- (GPI-) linked PGs.
Radioiodinated membrane-associated PGs from embryonic day 18 (E18), postnatal day 0 (P0), and adult (Ad) brain were digested with neuraminidase, then heparitinase and chondroitinase ABC either with (+) or without (-) the addition of PI specific phospholipase C (PI-PLC). Samples were then subjected to Tx114 partitioning, 5-15% non-reducing SDS-PAGE, and autoradiography as described in the text. Molecular weight markers are shown to the left of each gel. Some proteins exhibit slightly altered mobility in DET lanes, presumably due to high concentrations of Tx114 in these samples. Two major heparan sulfate PGs (M12 and M13) and a non PG protein found only in adult brain (M_r 100kd; lower asterisk) demonstrate a significant shift from detergent to aqueous phases when pre-treated with PI-PLC, indicating that these proteins are GPI-anchored membrane proteins. For further discussion see text.

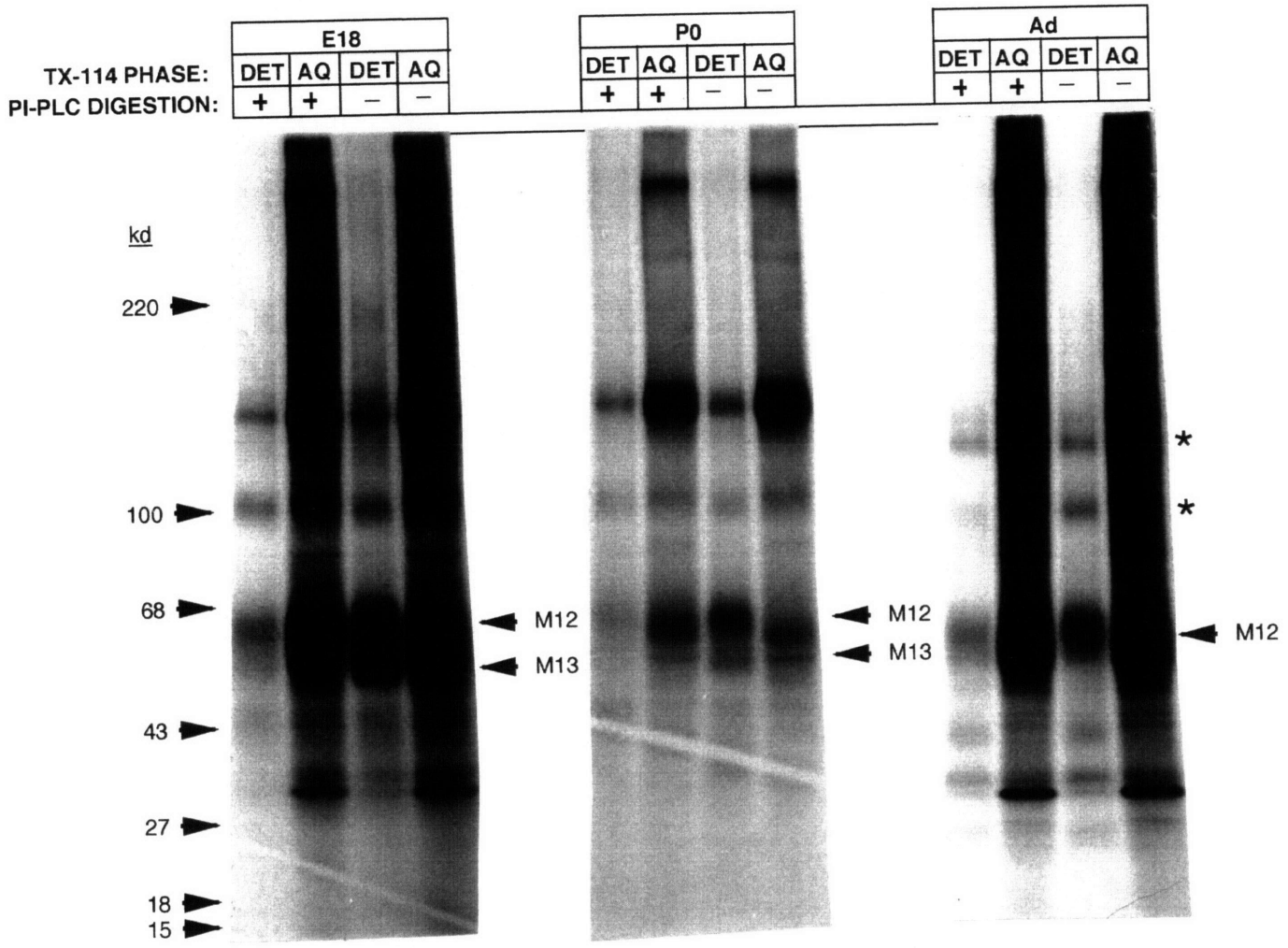
E18
P0
Ad
TX-114 PHASE:
PI-PLC DIGESTION:
DET AQ DET AQ
+ + – –
kd
220
100
68
43
27
18
15
M12
M13
M12
M13
M12
*
*

CHAPTER II

Neural Glycosaminoglycans and Proteoglycans Exhibit Distinct Affinities for Cell-Surface, Cell-Secreted, and Extracellular Matrix Molecules Expressed in the Brain.

INTRODUCTION

Many glycosaminoglycan (GAG) binding molecules that are involved in neural cell behaviors are known to bind heparin. For example, binding to heparin-sepharose has been demonstrated for FGF-1 (aFGF) and -2 (bFGF) (Lobb and Fett, 1984), laminin (Rao and Kefalides, 1990), and NCAM (Cole et al., 1985). In some cases, heparin binding has been quantified: FGF-1 and -2 dissociation constants have been estimated by various techniques to be in the range of 60-90 nM and 2-3 nM, respectively (Moscatelli, 1987; Lee and Lander, 1991); heparin solid-phase binding assay with NCAM gave a K_d of ~52 nM (Nybroe et al., 1989); and thrombin binding to heparin has been estimated at K_d = 6-10 μM (Olson et al., 1991). In a particularly illuminating study, San Antonio et al. (1993) used affinity coelectrophoresis (ACE) to fractionate heparin through laminin, fibronectin, and type I collagen, and measured re-binding of the fractions to all three extracellular matrix molecules, as well as to FGF-2 and thrombospondin-1. The results suggested that both specific sequences in heparin structure and specificity in protein GAG-binding domains are responsible for the wide range of affinities seen.

Besides being used in binding studies, heparin has been used to elucidate protein-GAG interactions in innumerable studies of protein function. In one of the best examples using a neurally expressed molecule, FGF-2, heparin has proved an invaluable tool for understanding molecular function at several levels: heparin has been used to elucidate 1) the dimerization of FGF-2 (Ornitz et al., 1992); 2) the hexasaccharide binding sequence in heparin responsible for modulating FGF-2 activity (Turnbull et al., 1992; Tyrrell et al., 1993); 3) a heparin binding domain in the FGF high affinity receptor (Kan et al., 1993); and 4) the requirement for heparin in receptor binding to FGF-2, and receptor dimerization and activation (Ornitz and Leder, 1992; Kan et al., 1993; Pantoliano et al., 1994; Roghani et al., 1994; Spivak-Kroizman et al., 1994; Ornitz et al., 1995).

Heparin, however, is not considered representative of most tissue GAGs. Structurally, heparin is 2-3 times more sulfated than the

related GAG heparan sulfate (HeS) (Gallagher and Walker, 1985) (it is precisely this high degree of modification of heparin that makes it so useful: heparin is generally believed to contain all possible combinations of HeS modifications in abundance), and while trisulfated disaccharides form the major structural unit of heparin, only 3% of HeS disaccharides are trisulfates (Turnbull and Gallagher, 1990). Further, heparin has a relatively uniform degree of sulfation along the chain length, while heparan sulfates have a domain structure comprised of alternating regions of low and high sulfation. The highly sulfated domains are also iduronate and iduronate-2-SO_4 rich, a feature that confers conformational flexibility to the molecule (Turnbull and Gallagher, 1991). These differences suggest that HeS and other tissue GAGs could behave differently in binding and function than does heparin. In fact, more than a few investigators have found this to be the case. For example, inhibition of agrin-induced acetylcholine-receptor aggregation was inhibited to a much greater extent by heparin than by HeS or ChS (Wallace, 1990). Aviezer et al. (1994b) found that the cell membrane HeS proteoglycans (HSPGs) syndecan-1, glypican, and syndecan-2/fibroglycan, immunopurified from human fetal lung fibroblasts, as well as various HeS preparations from bovine arterial tissue, not only failed to promote FGF-2 binding to its high affinity receptor, but also inhibited, in a dose dependent manner, the stimulation by heparin of FGF-2 receptor binding. On the other hand, the basement membrane HSPG perlecan is a potent promoter of FGF-2 binding to its receptor, an activity that is abolished by removal of perlecan's HeS chains with heparinase (Aviezer et al., 1994b). Examples such as these illluminate the value of examining GAG-protein interactions using the GAGs that are expected to be involved in vivo. By looking at the activity of GAGs and PGs purified from specific tissues, better insight into the specific ways cells use GAGs and PGs will be achieved.

Here, we have examined the binding of various neural and non-neural GAGs to a roster of heparin-binding proteins expressed in the brain. These proteins have been selected as significant neural representatives from three classes of molecules: Multidomain extracellular matrix glycoproteins included laminin-1, fibronectin, and thrombo-

spondin-1, each of which play roles in neural cell adhesion, migration, and/or axonal growth; NCAM and L1 are major cell-adhesion molecules expressed in the brain; and the serpin protease nexin-1 (PN-1), serine proteases thrombin and uPA, and the heparin-binding growth factor FGF-2 are all prominent cell-secreted molecules that influence neural cell behaviors (See Introduction chapter for details of the activities of each of these molecules). In some cases, binding to purified brain PGs was also measured. The results demonstrate several interesting and a few surprising features of GAG binding in the brain. Many of the GAG binding proteins tested showed both selectivity and specificity in binding, and the range of affinities seen was much broader than for heparin binding. Furthermore, PG binding to some of these molecules, though undoubtedly initiated by GAG binding, was found to be significantly stronger than the contribution of GAG binding alone.

MATERIALS AND METHODS

Materials

Several researchers generously provided molecules from their laboratories for the ACE experiments done here: Jack Lawler (Harvard Medical School, Boston,MA) provided human plasma thrombospondin-1; Denis Monard (Freidrich Miescher Institute, Basel, Switzerland) provided rat recombinant protease nexin-1 (produced in yeast); Four forms of mouse NCAM (untreated NCAM from adult and from postnatal [ages P0 to P7] mice, and endoneuraminidase treated forms of the same preparations) were provided on several occasions by Carl Lagenauer (Univ. of Pittsburgh School of Medicine, Pittsburgh, PA); Bob Rosenberg of MIT provided antithrombin III; and Jack Henken of Abbott Labs (Abbott Park, IL) provided human recombinant uPA (produced in E. coli). Other ACE substrates included: FGF-2, purified from bovine brain by the method of Lobb & Fett (Lobb and Fett, 1984); human plasma thrombin, provided by Enzyme Research Laboratories, Inc. (South Bend, IN); and laminin-1, purified from Engelbreth-Holm-Swarm (EHS) sarcoma according to published methods (Kleinman et al., 1982; Timpl et al., 1982). Protein concentrations for ACE gel stocks were determined by amino acid analysis (MIT Biopolymers Laboratory) of thrombin, fibronectin, uPA, protease nexin-1, NCAM, L1, antithrombin III, thrombospondin-1, and laminin-1 stocks; FGF-2 concentration was based on amido-black binding (see Chapter I).

Immunoprecipitated ^{125}I-labeled cerebroglycan and syndecan-3 from a postnatal day 0 rat brain growth cone preparation were kindly supplied by John Ivins (UCI, Irvine, CA). The syndecan-3 was precipitated using the mAb MSE-3 (Kim et al., 1994), while cerebroglycan was precipitated using the antipeptide polyclonal 521-2 (Litwack, 1995)

Sigma Chemical Co. supplied porcine intestinal heparin, bovine tracheal chondroitin sulfate, hyaluronic acid, heparinase II, insulin, transferrin, progesterone, putrescine, selenium, and tyramine. Shark chondroitin sulfate was from Fluka. Bovine kidney heparan sulfate and crystalline BSA were from ICN. Colominic acid was from Calbiochem. TX-114, TX-100, Sulfo SHPP, and Iodogen were from Pierce Chemical

Co. Chondroitinase ABC was from Seikagaku, USA. Affi-gel 10 matrix was suppled by Bio-Rad. All other reagents, including formulation of protease inhibitors, were the same as mentoned in Chapter I.

In Vitro Culture and $^{35}SO_4$ Labelling Of Brain Tissue

Dissections of E18 and PO brains and meninges removal was accomplished as outlined in Chapter I. Meninges free whole brains were cut into 1mm x 350 μm prisms with a McIlwain Tissue Chopper, then settled through HBSS (Gibco). Serum free, Sulfate free DMEM (SSF-DMEM) was formulated to GIBCO/BRL specifications for DMEM -- less sulfate -- using culture supplements and 10X Earle's Balanced Salt Solution from GIBCO. SSF-DMEM was supplemented ("labelling medium") to 50 μM with unlabeled Na_2SO_4,10 μg/ml insulin, 5 mg/ml crystalline BSA, 10 μg/ml transferrin, 20 nM progesterone, 100 μM putrescine, 30 nM selenium, and 100-250 mCi/ml $Na_2{}^{35}SO_4$ (Dupont/NEN). Labelling medium was added to tissue prisms at 20 ml per ml of tissue (settled volume) and cultured 16-20 hours in 5% CO_2, 37°C, with gentle gyratory rocking (Nutator).

Subcellular Fractionation and PG Purification

In most cases, labeled tissue was subjected to subcellular fractionation and membrane PGs were isolated as described in Chapter I. For the PG material used in the PN-affinity chromatography experiments, however, soluble and membrane-associated PGs were isolated together from E18 forebrain by homogenization of brain tissue directly into buffer B (Chapter I).

Radioiodination of PG Core Proteins

Radioiodination of PG core proteins was accomplished as in Chapter I.

Purification of GAGs From PGs

For ChS or HeS purification, GAG lyase digestion (completed as in Chapter I) preceded alkaline-borohydride cleavage of GAGs. For HeS purification, PGs were subjected to chondroitinase ABC at 0.05 -0.1 U/ml for 4-20 hours at 37°C, while adequate ChS purification

required sequential treatment of PGs with heparinase II (0.05U/ ml, 4-6 hr. 30°C) then heparitinase (4 μg/ml, 43°C, 4-20 hrs.). GAGs were cleaved from PG cores by alkaline-borohydride reaction, then concentrated by ethanol precipitation. Briefly, PG's were incubated at 45°C, 1 hour, in 90 mM NaOH and 9 mM $NaBH_4$, then the reaction quenched with the addition of a trace amount of phenol red followed by titration to pH ~7.0 using 5 M acetic acid. For ethanol precipitation, hyaluronic acid was added to 0.2 mg/ml then a 3.2 fold volume of 100% ethanol was added to the mixture and incubated at -20°C for at least one hour. Precipitates were collected by centrifugation at 13,000g for 30 min, 4°C, then briefly air dried. GAG pellets were resuspended in ACE electrophoresis buffer (50 mM MOPSO, 125 mM NaAcetate, pH 7.0; L&L, 1991).

Retinal HeS Prep

Eyeballs from embryonic day 18 Sprague Dawley rats were removed while submerged under DMEM medium (GIBCO). Retinas were detached from sclera and vitreous bodies in fresh medium, then transferred to SSF-DMEM (without BSA) and cut into pieces (~1 mm^3) using an electrochemically etched tungsten blade. Tissue pieces were then trypsinized (trypsin [GIBCO] added to 1 mg/ml for 20 minutes at 37°C). Trypsin digestion was halted with the addition of SBTI (GIBCO) to 1.4 mg/ml. Tissue was washed thrice with SSF-DMEM, then triturated well with a flame polished pasteur pipet. Cells were transferred to a small tissue culture plate and incubated 17 hours, 37°C, in labelling medium. Retinal cells were then harvested, washed thrice with cold HBSS by centrifugation, then the final pellet resuspended in buffer B (Chapter I, Methods and Materials) and placed in a sonicating water bath for 5 minutes. Insoluble material was pelleted out by centrifugation at 13.000g, 25 minutes, 4°C. The supernatent was used for HeS preparation as outlined above.

Radioiodination of Commercial GAG Preparations

Heparin and bovine kidney HeS were substituted with tyramine as described in San Antonio, et al.(1993). Bovine tracheal ChS and shark ChS were substituted with sulfo-SHPP: Briefly, 3 ml of 1 mg/ml

ChS, resuspended in O.15 M NaBorate pH8.5, was added to 330 µl Sulfo-SHPP (25 mg/ml in dimethylformamide) and incubated 4 hours at room temperature. The substituted ChS was dialyzed exhaustively against water, then the dialysate lyophilized and resuspended in 1 ml of H_2O.

For each substituted GAG, 3-10 µg of GAG in 50 µl of 0.25 M $NaPO_4$, pH 7.5 and 2-5 mCi of $Na^{125}I$ (NEN) were mixed in a 13 x 75 mm glass tube, that had previously been coated with 20 µg of Iodogen (50 µl of 0.4 mg/ml Iodogen in dichoromethane). ^{125}I-labeled GAGs were separated from free iodine by filtration over a 2 ml G-25 (Pharmacia) column that had been pre-blocked with 200 µg of crystalline BSA. For isolation of low molecular weight heparin (lM_r-heparin), ^{125}I-labeled heparin was further fractionated over a G-100 (Pharmacia) gel filtration column: the lM_r-heparin pool (Mr<6000) was isolated as the last 11% of the heparin peak to elute (San Antonio et al., 1993). All labeled GAGs were radioprotected with the addition of 0.25 mg/ml crystalline BSA, aliquotted, and stored at -80°C.

Affinity coelectrophoresis (ACE) and Analysis

Affinity co-electrophoresis (ACE) and its analysis was carried out essentially as described in Lim et al.(1991). ACE buffer was 50 mM MOPSO, 125 mM NaAcetate pH 7.0. For ACE of thrombospondin-1, 2mM calcium acetate was added to all buffers. Dried ACE gels were exposed in a phosphorimager cassette (Molecular Dynamics, Sunnyvale, CA), analyzed using ImageQuant Software (Molecular Dynamics) and quantified as described in San Antonio et al.(1993), using Microsoft Excel. Kaleidagraph (Synergy Software) was used to fit electrophoretic mobility data to equilibrium equations. Briefly, R values (retardation coefficient, the electrophoretic mobility of protein-bound GAG in a given lane normalized to the mobility of unbound GAG) were graphed with respect to the protein concentration for each lane and the resulting curve was fit to the equation:

$$R = \frac{R_\infty}{1 + (K_d/[P_{tot}]^n)}$$

where R_∞ = R value where the GAG is maximally shifted, K_d = Equilibrium dissociation constant, [G][P]/[G-P], for the reaction:

G (GAG) + P (protein) $\Leftrightarrow$ G-P (GAG-protein complex); $[P_{tot}]$ = Protein concentration in each lane of the ACE gel (at equilibrium, this value should actually be $([P_{tot}] - [G\text{-}P])$, but because GAG concentrations are so low under normal ACE conditions ($<0.1K_d$), the G-P term can be dropped from the equation); n = Number of protein molecules binding to each GAG molecule, i.e. order of binding mechanism.

Overruns (cases where the GAG electrophoreses out of the protein-containing zone of a particular lane) were compensated for using previously described methods (Lim et al., 1991).

All ACE gel results presented here have been fit to first order binding curves and these K_d values are reported. A second order binding equation will occasionally fit the data as well (see NCAM result, Table 2.3). Although several of the proteins tested for GAG binding contain multiple heparin binding domains, the K_d's given here represent binding to the protein as a whole. Because of weak GAG binding to some proteins, protein concentrations high enough to attain R_∞ or near R_∞ conditions were not possible. In these cases, R_∞ was estimated from the maximal shift seen when heparin is bound to the protein; if this R value was not available, the electrophoretic mobility of the top edge of the protein ligand *after* electrophoresis was normalized to unbound GAG mobility to calculate R_∞. For a cogent treatment of ACE analysis, see Lim et al. (1991).

RESULTS

The binding of brain HeS to the extracellular matrix glycoproteins fibronectin, laminin and thrombospondin-1, and to the cell secreted molecules PN-1, thrombin, uPA and bFGF shows a broad range of affinities.

Most interactions between HSPGs and other proteins in the extracellular domain are believed to be mediated by the HeS chains. Several heparin-binding extracellular matrix and secreted molecules that are implicated in cell developmental behaviors were chosen as candidates for possible binding by brain-derived HeS. To obtain dissociation constants for binding of the putative ligands to brain HeS, affinity co-electrophoresis (ACE) was used. Because the concentration of the protein ligand is constant throughout the binding assay, ACE allows measurements of even relatively weak equilibrium binding (provided that adequate protein concentrations can be achieved).

Brain HeS populations were derived from embryonic day 18 (E18) and postnatal day 0 (P0) rat brain membrane preparations. Freshly dissected brains (with meninges removed) were cut into 1mm x 300μm prisms and cultured for 16-20 hours in $^{35}SO_4$ supplemented medium. A membrane fraction was prepared from the cultured tissue, and PGs isolated by DEAE chromatography (as in Chapter I). HeS chains were purified by chondroitinase ABC treatment of PGs, followed by alkaline-borohydride cleavage and ethanol precipitation of the $^{35}SO_4$-HeS chains in the presence of hyaluronate as a carrier†.

Binding to the different protein ligands was measured using ACE. Figure 2.1 shows an example of the binding of P0 HeS to FGF-2: The phosphorimage of the ACE gel (panelA) shows that brain HeS exhibits robust binding to FGF-2. The faint band running at the bottom of the gel is incompletely digested ChS, as demonstrated by the absence of the band when this HeS preparation was further digested with chondroitinase (data not shown). Measurements of

---

† A carrier molecule was needed for adequate precipitation of the small amount of labelled GAGs in these preparations. Hyaluronate,was selected because it is a sulfate-free GAG and has a significantly lower charge density than HeS or ChS. Hyaluronate is therefore expected both to migrate behind and to not interfere with HeS or ChS binding during affinity coelectrophoresis. Glycogen, another commonly used ethanol precipitation carrier that is uncharged, appeared to selectively precipitate a subset of ^{125}I-labelled heparin molecules and was therefore not used (data not shown).

electrophoretic retardation in each of the FGF-2 lanes translates into an estimated K_d of 47 nM in units of FGF-2 concentration; see methods section for a description of ACE analysis.

Similar analysis was accomplished for the large multidomain extracellular matrix glycoproteins laminin, fibronectin, and thrombospondin-1, for the secreted proteases thrombin and uPA, and for the serine protease inhibitor protease nexin-1 (PN-1). Table 2.1 shows the equilibrium dissociation constants for P0 membrane-associated HeS binding to these molecules, ordered by strength of binding from top to bottom. Also shown are dissociation constants for binding of heparin to these proteins. Values for the binding of E18 HeS to these proteins were not significantly different from P0 HeS values (see tables 2.4 and 2.6 and the Discussion section).

The protein ligands demonstrated a very similar order of affinities for either brain HeS or heparin. However, heparin binding ranges from 1.75 to 16 fold stronger than HeS binding to these molecules. The range of affinities of the different proteins for brain HeS varies greater than 170 fold, with binding to PN-1 being the strongest and fibronectin the weakest. However, the range of heparin affinities for these molecules is more than 3 times narrower, varying only 54 fold.

In addition to binding brain heparan sulfate, a subset of molecules -- PN-1, uPA, thrombin, and thrombospondin-1 -- were found to bind brain chondroitin sulfate.

Another level of specificity in GAG-protein binding is the ability of a protein to recognize chondroitin sulfates (ChS) and well as heparan sulfates. When PN-1 was tested in ACE for binding to total GAGs purified from in vitro $^{35}SO_4$-labeled E18 brain, the GAGs split into two binding populations during electrophoresis (Figure 2.2 A). Treatment of the GAGs with either chondroitinase ABC or heparitinase to purify HeS or ChS respectively, and testing of the purified GAGs in PN-1 ACE demonstrated that the strong binding population in whole GAGs was HeS (K_d ~ 72 nM), while the faster migrating but weaker binding band was ChS (K_d ~ 287 nM) (Figure 2.2 B & C). Similarly, uPA, thrombin, and thrombospondin-1 were also found to bind to

brain ChS. Table 2.2 shows the equilibrium dissociation constants for the binding of P0 membrane-associated ChS to these molecules, ordered by strength of binding from top to bottom. Also shown for comparison are dissociation constants for binding of cartilage (bovine tracheal) ChS. ChS from E18 brain membrane preparations was not significantly different from that seen with P0 brain ChS (see tables 2.4 and 2.5 in discussion).

Like brain HeS, brain ChS exhibited a broad range of affinities for the molecules tested (139 fold change with respect to PN-1 affinity). The range for bovine tracheal ChS was smaller (35 fold change), though the order of strength of binding to the different ligands was the same. Brain ChS bound thrombospondin-1, PN-1, and thrombin somewhat better than did tracheal ChS (2.1, 3.0, and 4.2 fold increases, respectively), while binding to uPA was not significantly different (affinity of brain ChS was ~1.3 fold weaker than the affinity of tracheal ChS). The differences in binding between brain and tracheal ChS suggests that structural differences exist between the two molecules.

Subpopulations of brain HSPGs bear HeS chains with distinct affinities for PN-1.

When a particular PG exhibits different affinities for a given ligand, the differences may be accounted for by several means: 1) alterations in core protein structure, such as result from mRNA splicing variants, or glycosylation differences; 2) the number and 3) type of GAG chains expressed (e.g., HeS or ChS); or 4) changes in GAG structure. In order to determine if subpopulations of PGs with different affinities exist among brain PGs that bind to PN-1, PN-1 affinity chromatography was used to fractionate PGs from E18 forebrain. $^{35}SO_4$-labeled PGs were prepared from cultured whole E18 rat forebrain tissue, and a small fraction of the purified PGs were ^{125}I-labeled on their core proteins. ^{125}I-labeled PGs, $^{35}SO_4$-labeled PGs, and ^{125}I-labeled heparin were then applied to three identical PN-1 affinity columns run in parallel. Salt step elution was used to collect 6 pools from each column. The amount of radioactivity associated with each pool is shown in Figure 2.3.

To see which core proteins were associated with the salt steps, eluates from the column loaded with ^{125}I-labeled-PGs were subjected to GAG lyase digestions and SDS-PAGE. Figure 2.4 shows the SDS-PAGE result for the first three salt steps. The 0.15 M NaCl elution contained almost all of the CSPGs and was depleted for the HSPGs M12 [Chapter 1; now formally identified as glypican (Litwack et al., 1994)] and M13 [Chapter 1; now known as cerebroglycan (Stipp et al., 1994)], which were instead found in the higher salt elutions (0.3, 0.5 M NaCl steps are shown in fig 2.4; minor amounts of cerebroglycan and glypican were found in the 1.0, 1.5 and 3.0 M NaCl elutions, not shown).

The corresponding ^{35}S-labeled PG pools were chondroitinase ABC treated and subjected to alkaline borohydride cleavage to release HeS chains which were then tested in PN-1 ACE. Results show that the HSPG cores (mostly glypican and cerebroglycan) from progressively higher salt steps from the PN-1 column contained HeS chains of progressively higher affinities for PN-1 (figure 2.5).

In each HeS subpopulation, all of the HeS chains demonstrated the same binding to PN-1. Thus, the core molecules associated with each salt elution appear to bear HeS chains with a distinct affinity for PN-1. The range of affinities exhibited by the HeS chains in the different fractions was smaller than that seen by San Antonio et al.(1993), a study where heparin was fractionated by laminin-1, fibronectin and collagen I (2.5 rather than 5 to 30 fold;). However, in the experiment shown here, insufficient HeS was recovered in .75 M and higher salt fractions to test these HeS's in ACE -- the affinities of these minor HeS populations may have been even higher.

Retinal and brain membrane associated HeS showed little or no binding to the cell adhesion molecules NCAM and L1

NCAM is a heparin-binding cell-adhesion molecule that is highly expressed in the developing nervous system. When we tested the binding of E18 and P0 brain membrane-associated HeS preparations against mouse postnatal NCAM in ACE, the gel image showed a "flat-line" pattern with no measurable binding (data not shown). This result was surprising in light of a large body of evidence suggesting that HeS

and/or HSPGs are required for NCAM-mediated cell-cell adhesion, as well as cellular adhesion to NCAM substrates (Cole et al., 1985; Cole et al., 1986; Cole and Glaser, 1986b; Cole and Burg, 1989; Reyes et al., 1990; Kallapur and Akeson, 1992). Because many of these studies involved retinal cell adhesion, we next tested HeS preparations from E18 whole retina for binding to NCAM in ACE: Again, the gel image showed a "flat-line" pattern with no measurable binding (figure 2.6 A, and Table 2.6 in discussion). The same NCAM preparation demonstrated binding to heparin (K_d = 126 nM; Figure 2.6 B) with an affinity reasonably close to a previously reported value obtained using heparin-agarose binding [K_d = 52 nM; (Nybroe et al., 1989)]. The same retinal HeS preparation that showed no apparent binding to NCAM was seen to bind PN-1 with a K_d similar to that of brain HeS (Figure 2.6 C; seeTable 2.4).

In embryonic and early postnatal NCAM preparations, a significant fraction of the molecules are substituted with large amount of α2,8-polysialic acid [(Finne et al., 1983)]. This unusual N-linked glycan is thought to interfere with not only with the function of NCAM but of other cell surface receptors as well [(Rutishauser et al., 1988; Zhang et al., 1992)]. Like HeS, PSA is a polyanionic molecule. It seemed possible, therefore, that the PSA moieties on NCAM might bind to the heparin-binding region of NCAM, and thus account for the lack of retinal HeS binding seen here. To test this possibility, three other forms of NCAM were first tested in ACE: the adult form of NCAM, which has little PSA; endoneuraminidase (endo-N) treated postnatal NCAM (endo-N removes PSA); and endo-N treated adult NCAM. When tested for brain HeS binding, all three NCAM forms gave a flat-line pattern (data not shown; see Table 2.3 for K_d estimates). To test if the PSA moiety itself binds to NCAM, ^{125}I-labeled colominic acid, an E.coli produced polysialic acid, was tested in NCAM ACE. Again, a flat-line pattern was seen (ACE not shown; see Table 2.6). NCAM binding to other GAGs was also tested: Results showed no measurable NCAM binding to HeS from bovine kidney or to ChS from bovine trachea (ACE not shown; seeTable 2.6).

L1 is a cell-adhesion molecule that is structurally related to NCAM, and like NCAM, is found in the nervous system. L1-mediated

cell-cell adhesion appears to occur by homophilic binding between neurons and by heterophilic binding to an unidentified molecule in neural-glial cell interactions [reviewed in (Linnemann and Bock, 1989)]. Unlike NCAM, L1 molecules do not bear PSA chains and binding to heparin has not been shown for L1. When membrane-associated HeS from both E18 and P0 brain were tested for binding to L1, again, as with NCAM, the flat-line ACE patterns was seen (ACE not shown; see Table 2.3). GAGs from other sources (bovine tracheal ChS and bovine kidney HeS) also demonstrated no binding to L1 (ACE not shown; see Table 2.6). However, L1, like NCAM, bound heparin quite well (K_d = 108 nM; Figure 2.7).

The flat-line patterns seen here in ACE do not mean that the GAGs have no affinity for L1 or NCAM - they simply set a lower limit for possible dissociation constant values†. In ACE, if no electrophoretic shift is seen at a highest concentration tested, the K_d must be significantly higher than that concentration. Examination of ACE gels in which K_d's *are* obtainable can provide details about the protein concentration at which a shift first begins to appear, and how close that concentration is to the K_d value. Assuming that heparin ACE serves as a reasonable model for binding of other GAGs to a given ligand (vis-a-vis order of binding mechanism, for example), then we can define a minimum dissociation constant value , $K_{d,min}$:

$$K_{d,min} = C_{max} \times \frac{K_{d,hep}}{C_{nsm,hep}} \qquad (1)$$

where C_{max} = maximal concentration of ligand tested in the flat-line ACE; $K_{d,hep}$ = dissociation constant measured for heparin binding to the ligand; and $C_{nsm,hep}$ = "no shift maximum", the highest concentration of ligand tested in heparin ACE that exhibits no electrophoretic shift of the heparin.

In Figure 2.6 and Tables 2.3 and 2.6, $K_{d,min}$ values were calculated using this method. Brain HeS's have $K_{d,min}$ values greater than 3 μM for all types of NCAM, and greater than 2.5 μM for L1 (Tables 2.3 and 2.6). Although these $K_{d,min}$ values are within range of

† Because of difficulties in concentrating NCAM and L1, the ACE gels in this study had top concentrations of less than 260 nM.

K_d's measured for HeS binding to other molecules (e.g., fibronectin, thrombin, and uPA), the values also represent the strongest binding that is probable. In reality, HeS binding to L1 and NCAM may be much weaker.

Brain heparan sulfate proteoglycans exhibit affinities that are stronger than is attributable to single HeS chain binding.

The surprising result seen with NCAM and L1 binding to brain HeS suggests that GAG chains alone may be insufficient for PG binding to some heparin-binding molecules. We have tested the binding of several intact brain PGs to a few of the heparin-binding molecules used in this study. Both low and high affinities have been seen, suggesting that some contribution of core proteins to ligand binding may be important in the brain.

Before antibodies were available for immmunopurification of brain HSPGs, ^{125}I-labeled cerebroglycan and glypican were purified by Triton X-114 partitioning. Partitioning was accomplished as described in Chapter I, but with the additional step of washing of the detergent pellet to remove the HSPG M7. An example of cerebroglycan and glypican from E18 membrane-associated PGs partitioned by this method is seen in figure 2.8. When this cerebroglycan and glypican preparation was tested in fibronectin ACE, the material demonstrated strong binding and weak binding fractions (Figure 2.9 A). K_d's for these fractions are estimated to be 25 nM and 1 μM (exact measurements require knowledge of the mobility of the unbound material for each fraction, which is not distinguishable in these gels). Heparitinase pretreatment of the material abolished strong binding, while boiling in 0.1% SDS did not eliminate the high affinity component in the PG mixture (Figure 2.9, B and C, respectively). Laminin ACE testing of the same detergent phase showed a single fraction of high affinity (K_d estimated at ~10nM) (Figure 2.9 D). Detergent phase partitioned membrane PGs from newborn and adult brain demonstrated laminin ACE patterns identical to the embryonic material (data not shown).

Preparative ACE was used to isolate the PGs associated with high- and low-affinity binding to fibronectin. In preparative ACE, the

detergent phase of brain membrane PGs from three developmental ages, embryonic day 18, postnatal day 0, and adult, were run against 1000 nM fibronectin in a wide lane ACE format. After electrophoresis, each fibronectin lane was cut into 0.3 cm long fractions from top to bottom. The gel fractions were counted and "strong" and "weak" binding fractions pooled (Fig. 2.10). Material from each pool was digested with chondroitinase ABC and heparitinase and subjected to PAGE (figure 2.11).

Results demonstrate that in embryonic brain, cerebroglycan is found exclusively in the component that binds fibronectin strongly, while in newborn brain, only a portion of the cerebroglycan population and a previously unidentified PG (with an apparent core M_r that is slightly less than glypican's) exhibited high affinity for fibronectin. Adult brain, which contains no discernible cerebroglycan, had no strong binding component for fibronectin. Thus, a particular PG, cerebroglycan, exhibits two forms that have distinct affinities for fibronectin (a 40 fold difference in binding). Furthermore, expression of these forms appears to be developmentally regulated.

The PGs in the fibronectin strong binding pools (Figure 2.10) represented ~ 22% and 16% of the fractionated ^{125}I-labeled cerebroglycan and glypican (purified by detergent partitioning) in embryonic and newborn preparations, respectively. Because it is unlikely that detergent partitioning specifically selects for subpopulations of cerebroglycan and glypican, the strong binding pools should be representative of similar fractions of the actual PG populations in the brain. Also, cerebroglycan and glypican easily represent a major fraction of HSPGs in the brain (Chapter 1). Thus, a significant percentage of the brain HeS chains tested against fibronectin probably derive from these two PGs. Yet no HeS subpopulations with strong binding to either fibronectin or laminin were seen (data not shown). Thus, the affinity of these PGs to both fibronectin and laminin requires a binding contribution that is additional to single HeS chain binding.

The availability of antibodies to cerebroglycan and syndecan-3 (N-syndecan) enabled ACE analysis of immunopurified PGs. Testing against NCAM was unrevealing, because the PGs and the NCAM appear to have the same electrophoretic mobility in ACE (data not shown).

However, binding to thrombospondin-1 was quite informative. Figure 2.12 shows the result of thrombospondin-1 binding to immunopurified cerebroglycan (panel A), syndecan-3 (panel B), and E18 brain membrane-associated HeS (panel C). While the K_d's for binding of the PGs to thrombospondin-1 are in the same range as laminin and fibronectin binding to cerebroglycan and glypican, the differences between HeS chain binding and PG binding are not as large in the case of thrombospondin-1 as they are for laminin and fibronectin. The binding of cerebroglycan and of syndecan-3 to thrombospondin-1 were 5.45-fold and 3.75-fold stronger, respectively, than thrombospondin-1 binding to HeS alone. Binding of cerebroglycan to fibronectin and laminin, on the other hand, showed an estimated 300-fold and 90-fold increase over HeS binding. Interestingly, C. Stipp (1996) has shown that cerebroglycan immunopurified from growth cone preparations binds to laminin-1 ~1800-fold more strongly than does brain HeS.

DISCUSSION

To better understand the potential roles of PGs in brain development, HeS and ChS, were purified from two stages of brain development, E18 and P0, and tested for binding to a group of developmentally important molecules. The GAG binding molecules tested were members of three categories, extracellular matrix glycoproteins, cell-adhesion molecules, and cell-secreted molecules. and each has been shown to be important in neural development (see thesis introduction). The results show that brain HeS and ChS exhibit a broad range of affinities for these pericellular components. Most ligands demonstrated specificity both for type and strength of GAG binding. Finally, PG binding to ligands showed both dramatic increases over GAG binding and developmentally regulated changes in ligand affinity.

Uniformity in brain GAG populations

Affinity coelectrophoresis has been used both here and by others to separate GAG populations based on distinguishable binding to ligand molecules: ChS and HeS populations with as little as four-fold difference in K_d are distinguishable by eye as distinct bands (Figure 2.2); heparin species with very strong specific binding sequences, such as those that bind AT III, are also plainly separated from weak binding forms (Lee and Lander, 1991), whereas subpopulations of heparin that bind ligands with affinities varying smoothly over an order of magnitude are distinguished by a characteristic broad smearing pattern, especially at ligand concentrations that lie between the strong and weak binding K_d values (San Antonio et al., 1993).

Neither band separation nor smearing were seen in the ACE patterns of brain HeS or ChS bound to any of the ligands tested here. Instead brain HeS and ChS invariably displayed a single, relatively tight band in ACE. It would seem that brain GAG populations are very uniform in their binding character, at least vis-à-vis binding to particular molecules. There are, however, two caveats underlying this assessment. First and foremost, the brain GAGs used in this study were all prepared from cultured brain tissue. $^{35}SO_4$ label will only be found in GAGs synthesized during the twenty hour culture period;

thus, labeled GAG populations might not duplicate normally occurring species. Nonetheless, it is probable that many of these newly formed GAGs are representative of normal brain GAGs from the developmental ages used. Both E18 and P0 brain are still very active in both GAG synthesis and changes in GAG expression (Margolis et al., 1975a; Margolis et al., 1975b; Burkart and Weismann, 1987). The brain tissue was cultured in pieces that are relatively large (prisms roughly 1.0-5.0 mm x 1 mm x 0.35 mm), but small enough to prevent necrosis during the culture period (data not shown). Culture conditions were optimized for maximal incorporation of $^{35}SO_4$ into ethanol-precipitable GAGs, thus the tissue is not being sulfate-starved during culture (data not shown). Furthermore, Brauker et al., (1991), using a similar culture method for embryonic lung tissue, convincingly demonstrated that syndecan-1 from cultured tissue and from fresh tissue at different developmental ages exhibited the same changes in syndecan-1 molecular size, and that decreased HeS chain length accounted for these differences. It seems likely, therefore, that the cellular environment and the metabolic activity, at least for a majority of the cells in the brain sections, remain sound.

A second caveat with respect to the uniformity in brain GAG populations lies in the limits of detectability. In a GAG population that includes GAGs with a narrow range of affinities (which figure 2.2 demonstrates must be at least <4-fold different to be indistinguishable in ACE), statistically, the apparent K_d is expected to be a weighted average of the contributing K_d's (A. Lander, personal communication). If small enough subsets of cells in the brain express high affinity GAGs, these subspecies may go undetected in ACE. Minor strong binding subspecies of HeS or ChS that account for less than ~2% of counts, or very faint smears across an order of magnitude of binding are unlikely to be visualized. For example, figure 2.5 shows that the HSPGs eluted with increasing salt steps from a PN-1 affinity column contained HeS chains of increasingly stronger binding to PN-1. If this trend continues, it is possible that the HeS chains attached to the HSPGs in the highest salt steps (1.0, 1.5, and 3.0 M NaCl) had even higher affinities. These PGs represented less than 2% of the $^{35}SO_4$ counts applied to the column and provided insufficient HeS for ACE analysis.

As part of a larger GAG population, such a small fraction of GAGs might be missed in ACE, especially if there were any heterogeneity in binding. Interestingly, Rovelli et al. (1992) found that when heparin was fractionated by PN-1 affinity chromatography, the different fractions accelerated PN-1 anti-thrombin activity to the same extent; this is remarkably different than the case seen with strong-binding heparin activation of the related serpin AT III (Lam et al., 1976). It appears that stronger electrostatic binding by heparin does not necessarily correlate with an increase in function, at least in this case.

Another statistical feature of GAG binding in ACE is that the electrophoretic mobility shift of a GAG does not increase proportionally to the number of sites bound on the GAG chain (A. Lander, personal communication). Typically, ACE detects only the strongest binding site in a GAG chain, and chains with different numbers of strong-binding sites are predicted to give similar or identical K_d's in ACE. Yet, how many strong sites are in a chain may have significant biological relevance, especially with respect to effects on molecules, like many of those tested here, that have multiple heparin-binding domains.

Even if the detectability limitations for ACE are taken into account, the fact remains that the vast majority of E18 and P0 brain HeS and ChS molecules appear as discrete binding populations with respect to their affinities for many developmentally important brain molecules in three different categories of protein type: cell-adhesion molecules (L1 and NCAM), large multidomain extracellular matrix proteins (fibronectin, laminin, and thrombospondin-1), and smaller, secreted proteins (proteases uPA and thrombin, serpins PN-1 and AT III, and the growth factor FGF-2). Tables 2.4, 2.5 and 2.6 summarize the findings for GAG binding to each of these proteins. It is apparent from these results, that not only are P0 and E18 brain membrane-associated GAG populations relatively uniform in their binding to a given ligand, but like GAG types (i.e., HeS or ChS) from the two developmental stages are also very close to each other with respect to K_d values. Thus there appears to be little change in GAG structure, at least with respect to binding, during this developmental period. This suggests that changes in ligand-binding by the PGs that bear these

GAGs may be controlled at some other level -- increases in GAG chain length, changes in number or type of GAG chain attached to the core protein, or changes in level of PG expression (Chapter I), for example.

Selectivity in Brain GAG Populations

Despite uniformity in binding to a particular ligand, the HeS and ChS populations in the brain do express a great range in selectivity of binding. If we take heparin-binding to represent the strongest protein binding possible by a GAG (which has almost invariably been the case to date), then brain HeS binds some ligands quite strongly (e.g. brain HeS binds PN-1 only 1.75-fold weaker than heparin does), while brain HeS binds other ligands quite weakly (e.g., binding to laminin and to NCAM are 17-fold and 33-fold weaker than heparin-binding, respectively). The broad range of affinities seen, taken together with the differences in binding between HeS or ChS and heparin, is consistent with the idea that brain GAGs have structural specificity related to function.

Some brain heparin-binding proteins evidently select not to bind (or to bind quite weakly) to brain GAGs. The apparently low or absent affinity of NCAM and L1 for brain HeS -- indeed for all GAGs tested except heparin -- is, at first glance, a surprising result. After all, an HSPG with a core protein size of 120 kD appears to co-purify with NCAM isolated from chick retinal tissue (Cole and Burg, 1989), and HeS (50 μg/ml) abolishes retinal cell adhesion to NCAM coated surfaces (Cole et al., 1985)†. Even binding of the large neural CSPG neurocan to NCAM (K_d of ~1 nM in 50 mM NaCl) is reduced ~75% by chondroitinase treatment of the PG (Friedlander et al., 1994). These studies suggest that HeS, and even potentially ChS, could play roles in NCAM binding and function. There may be good reasons, however, for cell surface HeS in the brain to bind weakly, or not at all, to specific molecules in the extracellular environment. Low μM K_d's have also been seen for HeS binding to several other brain heparin-binding proteins: fibronectin (K_d = 7.4 μM), uPA (K_d = 2.3μM), and thrombin (K_d = 1 μM). And given the abundance of HSPGs and NCAM or L1 on

† In this study, HeS was from bovine lung, and if one assumes a M_r of 15 to 90 kD for the HeS chains, then 50 μg/ml HeS = 0.56 μM to 3.33 μM.

the surfaces of cells that express them [cf (Finne et al., 1983)], it may be that weak binding is preferable to strong. For example, if NCAM and L1 molecules were constantly bound by PGs, their abilities to mediate specific cell adhesion might be compromised.

Another level of selectivity was seen with four of the molecules tested: thrombospondin-1, thrombin, uPA, and PN-1 all bind not only to brain HeS, but also to brain ChS with K_d's for ChS that were less than ten fold weaker than HeS binding (Tables 2.4 and 2.5). Interestingly, these four proteins are all molecules that are known to interact with one another: (1) thrombospondin-1, a multidomain secreted glycoprotein, binds and inhibits the protease activity of uPA (Hogg et al., 1992); (2) thrombospondin-1 can participate in thio-disulfide exchange with another serine protease, thrombin, in a reaction that is accelerated if the thrombin is bound by the serine protease inhibitor PN-1 (Chang and Detwiler, 1992); and (3) both uPA and thrombin are substrates for PN-1 inhibition. The ability to bind both ChS and HeS provides more binding opportunities in the brain for these molecules. For instance, in the developing brain, "barriers" to migrating axons contain highly concentrated ChS (for review see (Silver, 1993)). In such regions, ChS concentrations are likely to exceed K_d values for uPA, thrombin, PN-1 and/or thrombospondin-1, potentially up- or down-regulating protein function. In addition, because most brain HSPGs are associated with membrane preparations (Chapter 1), uPA, thrombin, PN-1 and thrombospondin-1 would be likely to encounter increased concentrations of HeS at the cell surface compared to extracellular regions of the brain. Together with the localization of these GAGs, the difference in K_d's for HeS versus ChS binding by these proteins may in effect result in two discrete functionally different GAG populations in the brain.

Two other proteins, laminin and fibronectin, bound HeS, but had no measurable binding to ChS (Table 2.5). This selective binding for HeS in the brain should limit binding events for these molecules. As large extracellular matrix glycoproteins in the brain, laminin and fibronectin are found in an extracellular environment where ChS is the dominant GAG species [(Margolis et al., 1975a; Morris et al., 1987;

Fujita et al., 1989); Chapter 1, this thesis]. While the functional significance of this is not known, the conformational changes in fibronectin induced by HeS binding (Osterlund et al., 1985) suggests that selective binding to brain HeS, in a sea of ChS, may play a functional role for these molecules.

Strong vs. Weak Binding

In the everyday parlance of biochemists, high affinity binding is usually considered to be in the range of K_d ~ 10^{-9} to 10^{-12} M, e.g., that of polypeptide growth factors and strong antibodies. By this criterion, all GAGs are weak binders. In this study, heparin exhibited a range of K_d's in this study from ~ 10^{-7} to 10^{-8} M (FGF-2 to fibronectin). Brain GAGs varied from binding almost as strongly as heparin (K_d ~$3x10^{-8}$ M for PN-1 binding to HeS), to weak binding (K_d for ChS binding to uPA estimated to be ~$2.2x10^{-5}$). The importance of this broad range of affinities becomes more apparent when we examine other features of GAG, PG, and protein ligand structure. Perhaps the most significant aspect of GAG or PG binding to protein ligands is the potential for multimeric binding. Depending on the structure of the individual molecules, all three components, GAG, PG core protein and protein ligand, may contribute to the binding event, in some cases providing more than one binding site.

GAG chains present several ways to control GAG-ligand binding: First, GAG chains may express specific binding sequences. HeS is composed of alternating low and high sulfate content domains (average lengths of 18 and 5 disaccharides, respectively), with regular spacing along the HeS chain [reviewed in (Gallagher et al., 1992)]. Within either of the two domains may exist specific sequences for binding a given ligand. For instance, in the AT III pentasaccharide binding site in heparin, four of the five residues are sulfated (Rosenberg et al., 1978; Rosenberg and Lam, 1979). Disaccharide-binding sequences proposed for both FGF-1 and FGF-2 have multiple sulfates (Habuchi et al., 1992; Turnbull et al., 1992; Mach et al., 1993). And in this study, binding of brain HeS to PN-1 was seen to have an ionic component (figure 2.5) that is undoubtedly related to GAG sulfation.

Whether protein ligands bind specifically to the N-acetylated, low sulfate-containing domains in HeS has yet to be seen. However, the thrombospondin-1 monomer, in addition to having an N-terminal heparin-binding domain with characteristic clusters of basic amino acid residues (Lawler et al., 1992), is believed to contain up to two additional heparin-binding regions [(Guo et al., 1992; Lawler et al., 1992); see Introduction chapter for more details]. Neither of these putative heparin-binding sites contains consensus heparin-binding sequences (Cardin and Weintraub, 1989), suggesting that either region might interact with less-charged regions of HeS, such as the N-acetylated domains.

Besides control of GAG sequence, cells can also modify length of GAG chains. According to Gallagher (1992), heparan sulfates vary from 30 to 200 disaccharides (14 - 100 kD) in length. Thus, a cell might bear chains containing 1 to 8 highly sulfated domains on each chain. Because of the conformational flexibility of HeS chains (Turnbull and Gallagher, 1991), multiple binding sequences on a given GAG should allow positive cooperativity in binding to multisite ligands, such as fibronectin, thrombospondin-1, and laminin, provided the GAG chain is long enough to reach between the binding sites. Decreases in HeS chain length have been documented during epithelial cell and keratinocyte stratification, while changes in both ChS and HeS chain length have been seen in mesenchymal and epithelial cells during lung development (Sanderson and Bernfield, 1988; Brauker et al., 1991; Sanderson et al., 1992b).

Proteoglycan core proteins can be modified with respect to 1) number and type of GAG chains attached, 2) changes in level of proteoglycan expression (see Chapter I), and 3) changes in core protein structure due to mRNA splicing variants or carbohydrate attachment. Each of these means provides an opportunity for cellular control of PG-protein ligand binding. The primary structures of most of the PG core proteins sequenced to date contain multiple potential GAG attachment sites. Thus a PG that bears a single GAG chain in one instance, might express two in another, effectively doubling the "reach" of the GAG part of the molecule. Syndecan-1 provides the best documented example of how a particular core protein may bear either

ChS, HeS, or both, depending on the cell type, tissue, or developmental stage. For example, changes in the ratio of ChS to HeS chains expressed on the syndecan-1 core is associated with morphological changes in mammary gland epithelia (Sanderson and Bernfield, 1988) and TGF-β-induced differentiation of NMuMG cells (Rasmussen and Rapraeger, 1988). During morphological changes in other cell types, however, syndecan-1's ratio of ChS to HeS remains unchanged [e.g., keratinocyte stratification and differentiation of both B cells and lung alveoli epithelia (Sanderson et al., 1989; Brauker et al., 1991; Sanderson et al., 1992b)]. Thus, changes in both number and type of GAG provide a cellular strategy for affecting PG function.

In this study, intact HSPG binding to fibronectin, laminin, and thrombospondin-1 (Figures 2.7 - 2.12) were each increased above the level of binding seen with isolated HeS chains. During brain development, one of these PGs, cerebroglycan (as identified by its core protein), changes significantly with respect to its affinity for fibronectin (from $K_d \approx 25$ nM at E18 to mixed populations with K_d's ≈25 and 1000 nM at P0; Figures 2.5 - 2.8). Thus a particular PG shows a dramatic change in affinity during development that must be accounted for by differences in either core protein, GAG chains, or both. On the other hand, both cerebroglycan and glypican binding to laminin remains unchanged and strong during this developmental period ($K_d \approx 30$ nM). Therefore, there exists a subpopulation of cerebroglycan that has a weak affinity for fibronectin, yet exhibits no decreased binding to laminin. This is interesting in light of the results of San Antonio et al. (93) where subpopulations of heparin that bound fibronectin weakly also bound laminin weakly, and subpopulations that bound strongly to either molecule also bound strongly to the other. These data, together with the uniform and weak binding of E18 brain HeS to fibronectin, suggest that strong versus weak binding of cerebroglycan to fibronectin is not a feature of the HeS chains, but may involve changes in the number of GAG chains expressed or in the core protein itself.

How can we account for such large increases in PG over GAG binding to ligands? Because of the relationship $K_{eq} = 10^{-\Delta G/2.3RT}$, small changes in ΔG can have large effects on the equilibrium constant.

Thus, in principle, a small change in ligand-binding by a PG's core may be all that is required to transform weak binding into strong. For example, if an hypothetical HSPG that bears a single HeS chain exhibits an overall K_d of 25 nM ($K_a = 4x10^7 M^{-1}$) for fibronectin, and the purified chains have a K_d of 7 μM ($K_a = 1.4x10^5\ M^{-1}$) for fibronectin, the free energies of binding are ΔG_{PG} = -10.37 kcal/mole and ΔG_{HS} = -7.03 kcal/mole, respectively. The expected energy contribution by the binding of the core can be calculated using the intrinsic binding energy equation:

$$\Delta G_{i,core} = -RTlnK_{u,core} = -RTln(K_{a,PG}/K_{a,HS})^{\dagger}$$

which provides a value of $\Delta G_{i,core}$ = -3.34 kcal/mole (the difference between the two ΔG values above, as it should be). If we translate this value back to an intrinsic equilibrium constant, the value is $K_{i,core} = 2.86x10^2$. While this constant has no units (because the reaction is unimolecular) and does not relate to the K_a of core binding in the absence of HeS, it may serve an illustrative purpose: Compared to the K_{eq} values for HeS- and PG-binding ($K_a = 1.4x10^5\ M^{-1}$ and $K_a = 4x10^7\ M^{-1}$, respectively), $K_{i,core}$ is much smaller. Thus while the energetic contribution of second site binding may be relatively small, the effect on overall ligand-binding may be large in terms of the concentration of ligand required for binding. In fact, simply the presence of *any* protein moiety may be sufficient to increase GAG binding. An interesting (if painfully learned) result confirms how a relatively small, hydrophobic group can change GAG affinity: Initial measurements of bovine kidney HeS binding in this study were done using fluorescein-tagged HeS. For all ligands tested, the aromatic fluorescein group

---

† According to Creighton (1984), for multisite binding between two ligands, if each ligand has two binding domains, A and B. and if binding between the A domains occurs first, then binding between A sites is a bimolecular reaction, while subsequent binding between the B domains (second site binding) is unimolecular. The unimolecular equilibrium constant (also called the intrinsic binding constant) for second site binding, $K_{u,B}$, is related to the two bimolecular binding constants, $K_{a,AB}$ (overall ligand binding) and $K_{a,A}$ (binding of the A site) by the equation $K_{u,B} = (K_{a,AB}/K_{a,A})$. Thus, if the K_d's for the binding of one of the intact ligands and for one of its binding domains (in this case part A) is known, then the intrinsic binding constant for the second site can be calculated. The intrinsic binding energy, or the contribution to free energy of binding provided by the second site binding, is therefore:

$$\Delta G_{i,B} = -RTlnK_{u,B} = -RTln(K_{a,AB}/K_{a,A})$$

increased HeS affinities significantly, up to 14 fold above binding seen with tyraminated bovine kidney HeS (data not shown).

While the analysis above refers to the core protein in second site binding, another GAG chain, or even a second region of the same GAG chain (if it is long enough) could provide significant contributions to overall PG binding. In principle, the flexibility of HeS chains (and probably other GAG types) should increase the number of conformations available to the PG in binding, so that the effective concentrations of secondary binding sites, be they core protein or GAG, are high.

The data presented in this study suggest several roads of effort that might be followed. How PG structure relates to ligand binding should be addressed. The number, type and length of GAG chains, and how this relates to binding, using different transfected cell lines as a model system, for example, could contribute to our understanding of how GAG attachment is used by cells in response to specific ligands. Determination of core regions required for strong binding might be accomplished using PG deletion mutagenesis.

Another question that arises is one of functional significance: Does specificity of GAG binding relate to different effects on ligand function or cell-ligand interaction? The former is at least partly addressed in the next chapter. For the latter, expression of the same core protein in different, but related cell lines that express GAGs of distinct affinity for extracellular matrix glycoproteins, for example, might shed some light on how GAG binding per se affects cell adhesion, migration, or neurite outgrowth.

Acknowledgements

Thanks to Jon Ivins for supplying the immunoprecipitated cerbroglycan and syndecan-3, and for the instruction in retinal dissection and culture. John Slover and Tony Chang assisted with some of the affinity coelectrophoresis. My appreciation to Arthur for informative discussions about ACE analysis and what it all means. Finally, my heartfelt gratitude to Chris Stipp for help with the figure preparations during the eleventh hour.

REFERENCES

Aviezer, D., D. Hecht, M. Safran, M. Eisinger, G. David, and A. Yayon. 1994b. Perlecan, basal lamina proteoglycan, promotes basic fibroblast growth factor-receptor binding, mitogenesis, and angiogenesis. Cell 79:1005-1013.

Brauker, J.H., M.S. Trautman, and M. Bernfield. 1991. Syndecan, a cell surface proteoglycan, exhibits a molecular polymorphism during lung development. Dev. Biol. 147:285-292.

Burkart, T. and U.N. Weismann. 1987. Sulfated glycosaminoglycans (GAG) in the devloping mouse brain: Quantitative aspects on the metabolism of total and individual sulfated GAG in vivo. Dev. Biol. 120:447-456.

Cardin, A.D. and H.J.R. Weintraub. 1989. Molecular modeling of protein-glycosaminoglycan interactions. Arteriosclerosis 9:21-32.

Chang, A.C. and T.C. Detwiler. 1992. Reactions of thrombin-serpin complexes with thrombospondin. Arch. Biochem. Biophys. 299:100-104.

Cole, G.J. and M. Burg. 1989. Characterization of a heparan sulfate proteolglycan that copurifies with the neural cell adhesion molecule. Exp. Cell Res. 182:44-60.

Cole, G.J. and L. Glaser. 1986b. A heparin-binding domain from N-CAM is involved in neural cell-substratum adhesion. J. Cell Biol. 102:403-412.

Cole, G.J., A. Loewy, and L. Glaser. 1986. Neuronal cell-cell adhesion depends on interactions of N-CAM with heparin-like molecules. Nature 320:445-447.

Cole, G.J., D. Schubert, and L. Glaser. 1985. Cell-substratum adhesion in chick neural retinal depends upon protein-heparan sulfate interactions. J.B.C. 100:1192-1199.

Creighton, T. E. 1984. Proteins: Specificity of Interactions. (W. H. Freeman and Co., New York). pp. 360-380.

Finne, J., U. Finne, H. Deagostini-Bazin, and C. Goridis. 1983. Occurence of α2-8 linked polysialosyl units in a neural cell adhesion molecule. Biochem. Biophys. Res. Comm. 112:482-490.

Friedlander, D.R., P. Milev, L. Karthikeyan, R.K. Margolis, R.U. Margolis, and M. Grumet. 1994. The neuronal chondroitin sulfate proteoglycan neurocan binds to the neural cell adhesion molecules Ng-CAM/L1/NILE and N-CAM, and inhibits neuronal adhesion and neurite outgrowth. J. Cell Biol. 125:669-680.

Fujita, S., Y. Tada, F. Murakami, M. Hayashi, and M. Matsumura. 1989. Glycosaminoglycan-related eptitopes surrouning different subsets of mammalian central neurons. Neurosci. Res. 7:117-130.

Gallagher, J.T., J.E. Turnbull, and M. Lyon. 1992. Patterns of sulphation in heparan sulfate: polymorphism based on a common structural theme. Int. J. Biochem. 24:553-560.

Gallagher, J.T. and A. Walker. 1985. Molecular distinctions between heparan sulphate and heparin. Biochem. J. 230:665-674.

Guo, N., H.C. Krutzsch, E. Negre, V.S. Zabrenetzky, and D.D. Roberts. 1992. Heparin-binding peptides from the type I repeats of thrombospondin. J. Biol. Chem. 267:19349-19355.

Habuchi, H., S. Suzuki, T. Saito, T. Tamura, T. Harada, K. Yoshida, and K. Kimata. 1992. Structure of a heparan sulphate oligosaccharide that binds to basic fibroblast growth factor. Biochem. J. 285:805-813.

Hogg, P.J., J. Stenflo, and D.F. Mosher. 1992. Thrombospondin is a slow tight-binding inhibitor of plasmin. Biochemistry 31:265-269.

Kallapur, S.G. and R.A. Akeson. 1992. The neural cell adhesion molecule (NCAM) heparin binding domain binds to cell surface heparan sulfate proteoglycans. J. Neurosci. Res. 33:538-548.

Kan, M., F. Wang, J. Xu, J.W. Crabb, J. Hou, and W.L. McKeehan. 1993. An essential heparin-binding domain in the fibroblast growth factor receptor kinase. Science 259:1918-1921.

Kim, C.W., O.A. Goldberger, R.L. Gallo, and M. Bernfield. 1994. Members of the syndecan family of heparan sulfate proteoglycans are expressed in distinct cell-, tissue-, and development-specific patterns. Mol. Biol. Cell 5:797-805.

Kleinman, H.K., M.L. McGarvey, L.A. Liotta, P.G. Robey, K. Tryggvason, and G.R. Martin. 1982. Isolation and characterization of type IV procollagen, laminin, and heparan sulfate proteoglycan form the EHS sarcoma. Biochemistry 21:6188-6193.

Lam, L.H., J.E. Silbert, and R.D. Rosenberg. 1976. The separation of active and inactive forms of heparin. Biochem. Biophys. Res. Commun. 69:570-577.

Lawler, J., P. Ferro, and M. Duquette. 1992. Expression and mutagenesis of thrombospondin. Biochemistry 31:1175-1180.

Lee, M.K. and A.D. Lander. 1991. Analysis of affinity and structural selectivity in the binding of proteins to glycosaminoglycans: Development of a sensitive electrophoretic approach. P.N.A.S. 88:2768-2772.

Lim, W.A., R.T. Sauer, and A.D. Lander. 1991. Analysis of DNA-protein interactions by affinity coelectrophoresis. Meth. Enzymol. 208:196-210.

Linnemann, D. and E. Bock. 1989. Cell adhesion molecules in neural development. Dev. Neurosci. 11:149-173.

Litwack, E.D. (1995). Expression and function of proteoglycans in the nervous system: Massachusetts Institute of Technology).

Litwack, E.D., C.S. Stipp, A. Kumbasar, and A.D. Lander. 1994. Neuronal expression of glypican, a cell-surface glycosylphosphatidylinositol-anchored heparan sulfate proteoglycan, in the adult rat nervous system. J. Neurosci. 14:3713-3724.

Lobb, R.R. and J.W. Fett. 1984. Purification of two distinct growth factors from bovine neural tissue by heparin affinity chromatography. Biochem. 23:6295-6299.

Mach, H., D.B. Volkin, C.J. Burke, C.R. Middaugh, R.J. Linhardt, J.R. Fromm, D. Loganathan, and L. Mattson. 1993. Nature of the interaction of heparin with acidic fibroblast growth factor. Biochem. 32:5480-5489.

Margolis, R.K., R.U. Margolis, C. Preti, and D. Lai. 1975a. Distribution and metabolism of glycoproteins and glycosaminoglycans in subcellular fractions of brain. Biochem. 14:4797-4804.

Margolis, R.U., R.K. Margolis, L.B. Chang, and C. Preti. 1975b. Glycosaminoglycans of brain during development. Biochem. 14:85-88.

Morris, J.E., M. Yanagishita, and V.C. Hascall. 1987. Proteoglycans synthesized by embryonic chicken retina in culture: Composition and compartmentalization. Arch. Biochem. Biophys. 258:206-218.

Moscatelli, D. 1987. High and low affinity binding sites for basic fibroblast growth factor on cultured cells: Absence of a role for low affinity binding in the stimulation of plasminogen activator production by bovine capillary endothelial cells. J. Cell. Phys. 131:123-130.

Nybroe, O., N. Moran, and E. Bock. 1989. Equilibrium binding analysis of neural cell adhesion molecule binding to heparin. J. Neurochem. 52:1947-1949.

Olson, S.T., H.R. Halvorson, and I. Bjork. 1991. Quantitative characterization of the thrombin-heparin interaction. J.C.B. 266:6342-6352.

Ornitz, D.M., A.B. Herr, M. Nilsson, J. Westman, C.M. Svahn, and G. Waksman. 1995. FGF binding and FGF receptor activation by synthetic heparan-derived di- and trisaccharides. Science 268:432-436.

Ornitz, D.M. and P. Leder. 1992. Ligand specificity and heparin dependence of fibroblast growth factors 1 and 3. J. Biol. Chem. 267.

Ornitz, D.M., A. Yayon, J.G. Flanagan, C.M. Svahn, E. Levi, and P. Leder. 1992. Heparin is required for cell-free binding of basic fibroblast growth factor to a soluble receptor and for mitogenesis in whole cell. Mol. Cell. Biol. 12:240-247.

Osterlund, E., I. Eronen, K. Osterlund, and M. Vuento. 1985. Secondary structure of human plasma fibronectin: Conformational change induced by calf alveolar heparan sulfates. Biochemistry 24:2661-2667.

Pantoliano, M.W., R.A. Horlick, B.A. Springer, D.E.V. Dyk, T. Tobery, D.R. Wetmore, J.D. Lear, A.T. Nahapetian, J.D. Bradley, and W.P. Sisk. 1994. Multivalent ligand-receptor binding interactions in the fibroblast growth factor system produce a cooperative growth factor and heparin mechanism for receptor dimerization. Biochem. 33:10229-10248.

Rao, C.N. and N.A. Kefalides. 1990. Identification and characterization of a 43-kilodalton laminin fragment from the "A" chain (long arm) with high-affinity heparin binding and mammary epithelial cell adhesion-spreading activities. Biochem. 29:6768-6777.

Rasmussen, S. and A. Rapraeger. 1988. Altered structure of the hybrid cell surface proteoglycan of mammary epithelial cells in response to transformin growth factor-β. J. Cell Biol. 107:1959-1967.

Reyes, A.A., R. Akeson, L. Brezina, and G.J. Cole. 1990. Structural requirements for neural cell adhesion molecule-heparin interaction. Cell Regulation 1:567-576.

Roghani, M., A. Mansukhani, P. Dell'Era, P. Bellosta, C. Basilico, D.B. Rifkin, and D. Moscatelli. 1994. Heparin increases the affinity of basic fibroblast growth factor for its receptor but is not required for binding. J.C.B. 269:3976-3984.

Rosenberg, R.D., G. Armand, and L. Lam. 1978. Structure-function relationships of heparin species. Proc. Natl. Acad. Sci. 75:3065-3069.

Rosenberg, R.D. and L. Lam. 1979. Correlation between structure and function of heparin. Proc. Natl. Acad. Sci. 76:1218-1222.

Rovelli, G., S.R. Stone, A. Guidolin, J. Sommer, and D. Monard. 1992. Characterization of the heparin-binding site of glia-derived nexin/protease nexin-1. Biochemistry 31:3542-3549.

Rutishauser, U., A. Acheson, A.K. Hall, D.M. Mann, and J. Sunshine. 1988. The neural cell adhesion molecule (NCAM) as a regulator of cell-cell interactions. Science 240:53-57.

San Antonio, J.D., J. Slover, J. Lawler, M.J. Karnovsky, and A.D. Lander. 1993. Specificity in the interactions of extracellular matrix proteins with subpopulations of the glycosaminoglycan heparin. Biochem. 32:4746-4755.

Sanderson, R.D. and M. Bernfield. 1988. Molecular polymorphism of a cell surface proteoglycan: distinct structures on simple and stratified epithelium. Proc. Natl. Acad. Sci. USA 85:9562-9566.

Sanderson, R.D., M.T. Hinkes, and M. Bernfield. 1992b. Syndecan, a cell-surface proteoglycan, changes in size and abundance when keratinocytes stratify. J. Invest. Dermatol. 99:390-396.

Sanderson, R.D., P. Lalor, and M. Bernfield. 1989. B lymphocytes express and lose syndecan at specific stages of differentiation. Cell Regulat. 1:27-35.

Silver, J. (1993). Glial-neuron interactions at the midline of the developing mammalian brain and spinal cord. *In* Perspectives in Developmental Neurobiology, C. A. Mason, editor. (Gordon and Breach, Science Publishers S. A.). pp. 227-236.

Spivak-Kroizman, T., M.A. Lemmon, I. Dikic, J.E. Ladbury, D. Pinchasi, J. Huang, M. Jaye, G. Crumley, J. Schlessinger, and I. Lax. 1994. Heparin-induced oligomerization of FGF molecules is responsible for FGF receptor dimerization, activation, and cell proliferation. Cell 79:1015-1024.

Stipp, C.S. 1996. Identification, Molecular Cloning, and Characterization of Cerebroglycan, A Cell Surface Heparan Sulfate Proteoglycan of the Developing Rat Brain. PhD Thesis, Massachusetts Institute of Technology.

Stipp, C.S., E.D. Litwack, and A.D. Lander. 1994. Cerebroglycan: an integral membrane heparan sulfate proteoglycan that is unique to the developing nervous system and expressed specifically during neuronal differentiation. J. Cell Biol. 124:149-160.

Timpl, R., H. Rohde, L. Risteli, U. Ott, P.G. Robey, and G.R. Martin. 1982. Laminin. Meth. Enzymol. 82:831-838.

Turnbull, J.E., D.G. Fernig, Y. Ke, M.C. Wilkinson, and J.T. Gallagher. 1992. Identification of the basic fibroblast growth factor binding sequence in fibroblast heparan sulfate. J. Biol. Chem. 267:10337-10341.

Turnbull, J.E. and J.R. Gallagher. 1990. Molecular organization of heparan sulphate from human skin fibroblasts. Biochem. J. 265:715-724.

Turnbull, J.E. and J.T. Gallagher. 1991. Distribution of iduronate 2-sulphate residues in heparan sulphate. Biochem. J. 273:553-559.

Tyrrell, D.J., M. Ishihara, N. Rao, A. Horne, M.C. Kiefer, G.B. Stauber, L.H. Lam, and R.J. Stack. 1993. Structure and biological activities of a heparin-derived hexasaccharide with high affinity for basic fibroblast growth factor. J.C.B. 268:4684-4689.

Wallace, B.G. 1990. Inhibition of agrin-induced acetylcholine-receptor aggregation by heparin, heparan sulfate, and other polyanions. J. Neurosci. 10:3576-3582.

Zhang, H., R.H. Miller, and U. Rutishauser. 1992. Polysialic acid is required for optimal growth of axons on a neuronal substrate. J. Neurosci. 12:3107-3114.

Figure 2.1. Affinity Coelectrophoresis of P0 Brain Heparan Sulfate against FGF-2. Purified HeS from a preparation of membrane-associated proteoglycans from P0 rat brain were tested for binding to FGF-2 using affinity coelectrophoresis (ACE). Panel A: Phosphorimage of FGF-2 ACE gel. Concentrations of FGF (nM) are listed below the gel. The elecrophoretically shifted material is HeS; the faint band across the bottom is a trace amount of incompletely digested ChS (see text). Panel B: Calculation of affinity of HeS for FGF-2. Retardation coefficients for each protein lane were calculated and plotted against FGF-2 concentration (see Materials & Methods).

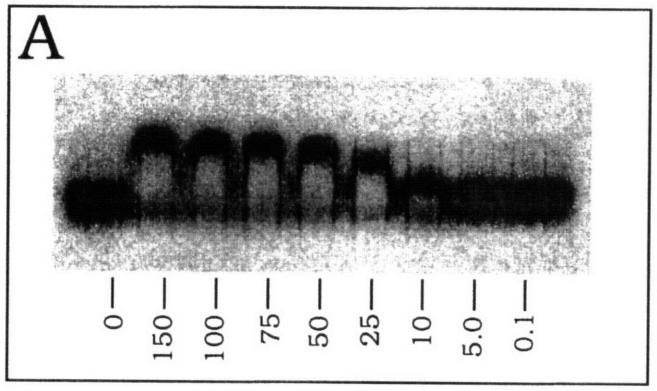
A
0
150
100
75
50
25
10
5.0
0.1

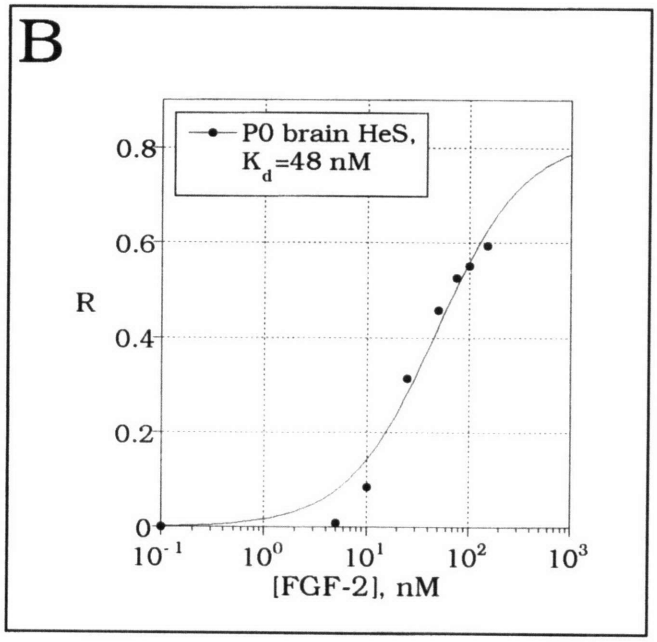
B
P0 brain HeS,
K_d=48 nM
0.8
0.6
R
0.4
0.2
0
10^-1
10^0
10^1
10^2
10^3
[FGF-2], nM

Table 2.1. Binding of Extracellular Matrix and Secreted Molecules to P0 Brain Membrane-Associated Heparan Sulfate and Heparin.

Ligand:	Type of molecule	K_d P0 brain membrane-associated HeS (nM ligand)	Fold decrease from PN-1 binding	K_d $1M_r$-heparin (nM ligand)
Protease nexin-1	serpin	35 nM	(1 X)	20 nM
FGF-2	growth factor	47 nM	1.3 X	9 nM
Thrombospondin-1	Multidomain ECM glycoprotein	180 nM	5 X	41 nM
Laminin	Multidomain ECM glycoprotein	891 nM	25 X	54 nM
Thrombin	serine protease	1025 nM	29 X	123 nM
uPA	serine protease	2310 nM	60 X	312 nM
Fibronectin	Multidomain ECM glycoprotein	6200 nM	177 X	486 nM

Equilibrium dissociation constants were derived from ACE analysis as described in text.

Figure 2.2. Affinity Coelectrophoresis of Protease Nexin-1 binding to Brain GAGs. ACE analysis of PN-1 binding to whole brain GAGs (A) from E18 rat brain membrane-associated PGs, purified HeS (B), and purified ChS (C), from the same GAG preparation. ChS and HeS are clearly distinguishable in the whole GAG ACE image. The concentration of PN-1 (nM) in each lane is shown below the gels. Equilibrium dissociation constants for HeS and ChS have been calculated from retardation coefficients for each protein lane, plotted against PN-1 concentration as shown in (D) (see Materials & Methods).

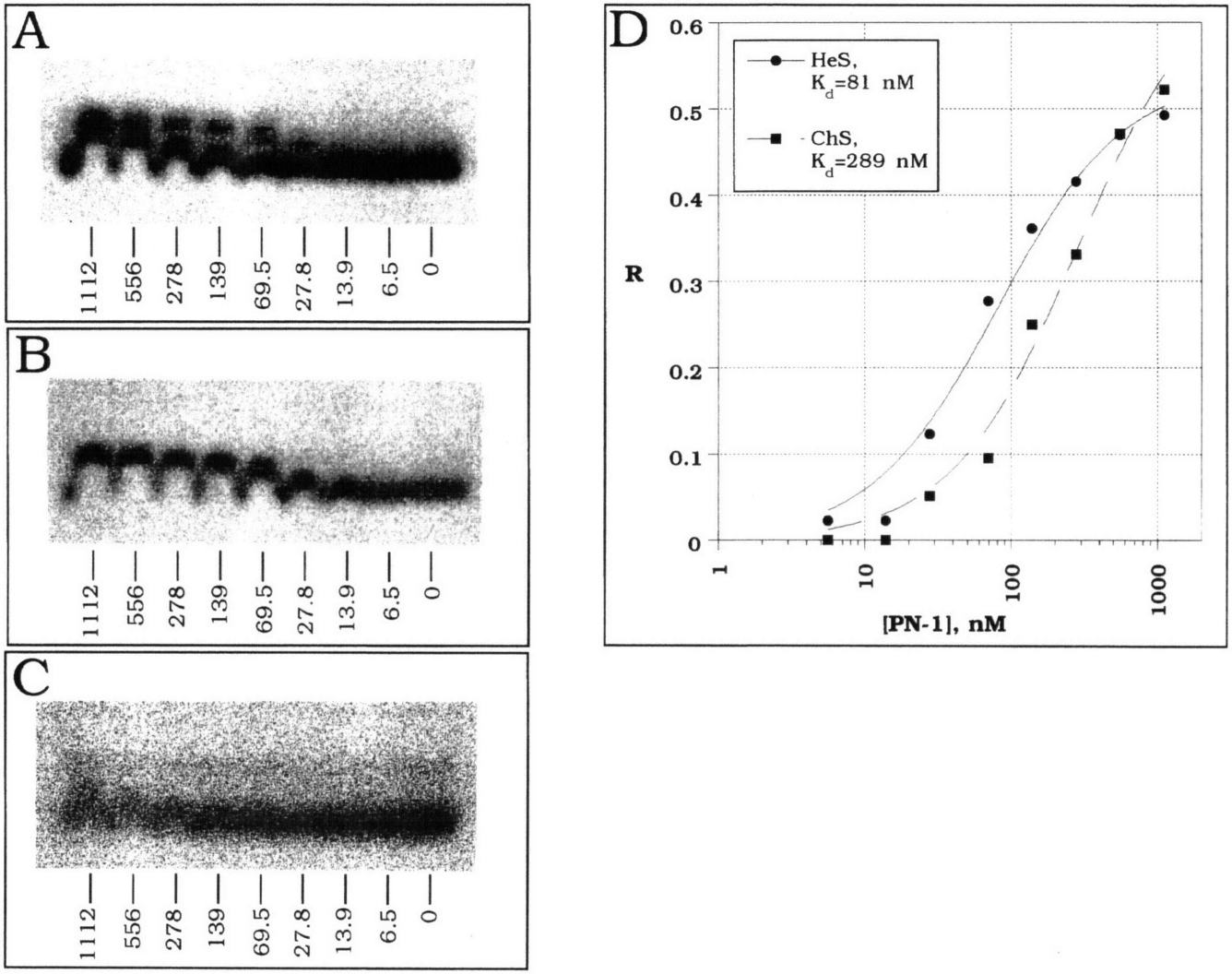
A
1112
556
278
139
69.5
27.8
13.9
6.5
0
B
1112
556
278
139
69.5
27.8
13.9
6.5
0
C
1112
556
278
139
69.5
27.8
13.9
6.5
0
D
HeS,
K_d=81 nM
ChS,
K_d=289 nM
R
0.6
0.5
0.4
0.3
0.2
0.1
0
1
10
100
1000
[PN-1], nM

Table 2.2. Binding of Extracellular Matrix and Secreted Molecules to P0 Brain Membrane-Associated Chondroitin Sulfate and Bovine tracheal Chondroitin Sulfate.

Ligand:	Type of molecule	K_d P0 brain membrane-associated ChS (nM ligand)	Fold decrease from PN-1 binding	K_d bovine tracheal ChS (nM ligand)
Protease nexin-1	serpin	158 nM	(1 X)	478 nM
Thrombospondin-1	Multidomain ECM glycoprotein	235 nM	1.5 X	487 nM
Thrombin	serine protease	2500 nM	16X	10.3 μM
uPA	serine protease	21.9 μM	139 X	17.1 μM

Equilibrium dissociation constants were derived from ACE analysis as described in text.

Figure 2.3. Protease Nexin-1 Affinity Chromatography of Brain Proteoglycans. $^{35}SO_4$-labeled and ^{125}I-labeled brain PGs from E18 forebrain (soluble + membrane-associated fractions) and ^{125}I-labeled $1M_r$-heparin were bound to Affi-gel coupled PN-1 in 0.15 M NaCl. PGs and heparin were eluted with 4x-column volume salt steps of 0.15 M, 0.3 M, 0.5 M, 1.0 M, 1.5 M, and 3.0 M. Percent of total recovered cpm associated with each salt elution are graphed here.

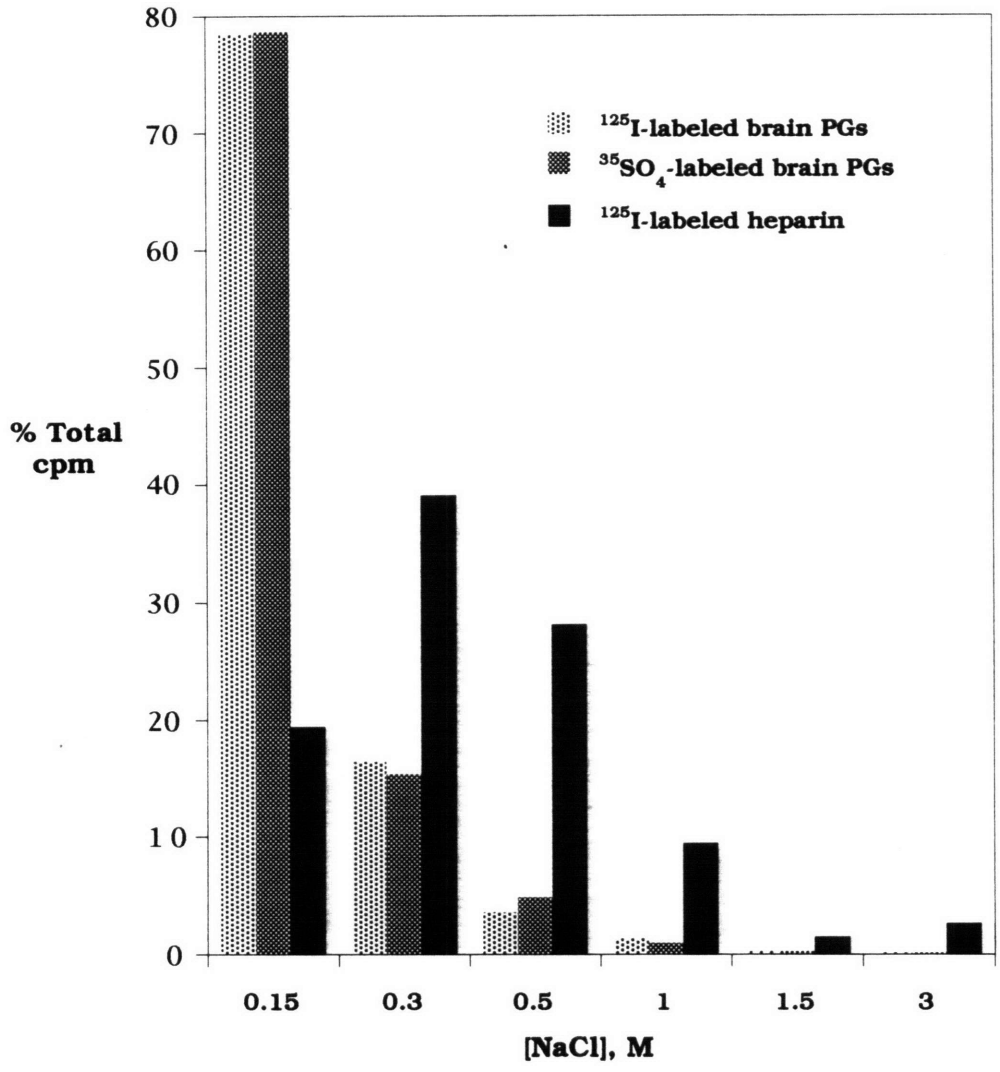
80
70
60
50
40
30
20
10
0
% Total cpm
125I-labeled brain PGs
35SO4-labeled brain PGs
125I-labeled heparin
0.15
0.3
0.5
1
1.5
3
[NaCl], M

Figure 2.4. SDS-PAGE of Proteoglycans Eluted during Protease-Nexin-1 Affinity Chromatography. ^{125}I-labeled PGs in salt-step elution pools from PN-1 affinity chromatography (0.15 M, 0.3 M, and 0.5 M NaCl) (figure 2.3), and total PGs, as a control, were either untreated (U) or treated with chondroitinase ABC (C), with heparitinase (H), or with both (CH), and then subjected to SDS-PAGE. Proteoglycan core proteins appear as bands that are present in the lyase treated lanes but absent in the accompanying untreated lane. Cerebroglycan (M13) and glypican (M12) cores are marked with arrowheads.

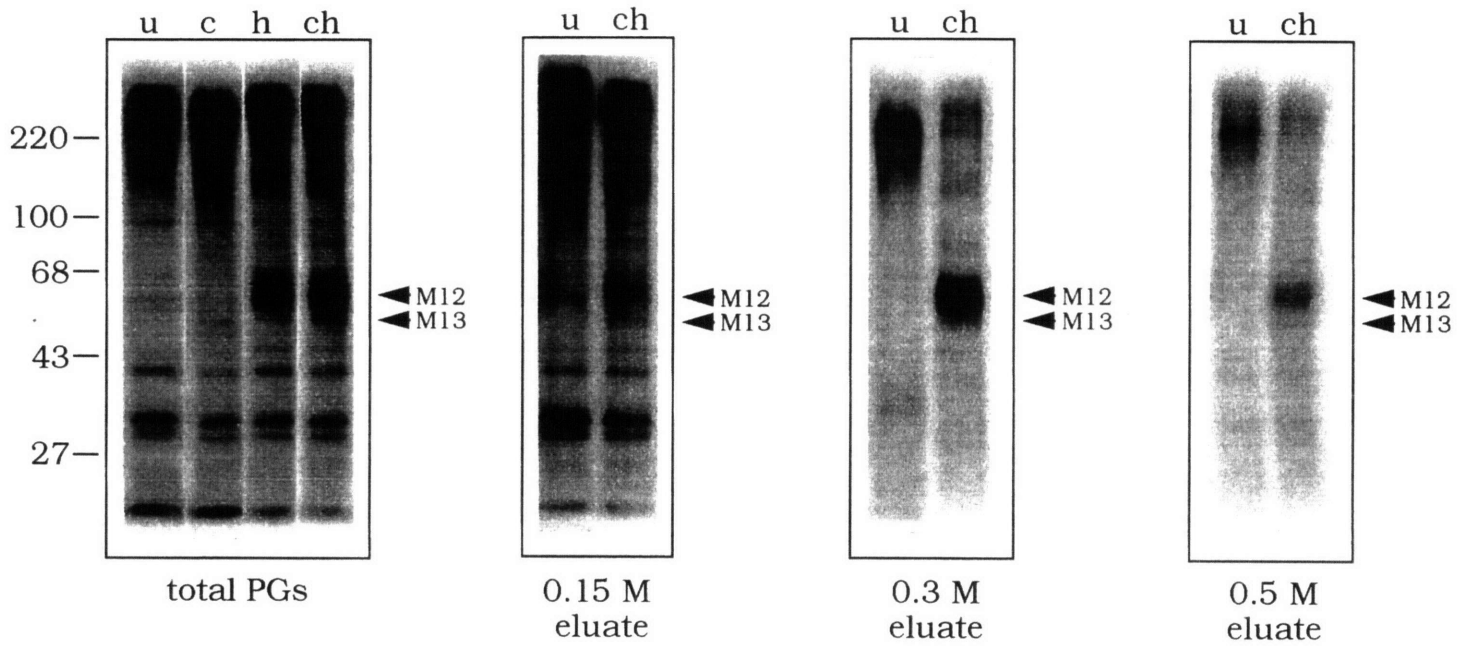
u c h ch
220
100
68
43
27
M12
M13
total PGs
u ch
M12
M13
0.15 M
eluate
u ch
M12
M13
0.3 M
eluate
u ch
M12
M13
0.5 M
eluate

Figure 2.5. Protease Nexin-1 Affinity Coelectrophoresis of Heparan Sulfate Chains Purified from PN-1-binding Brain Proteoglycans. ACE analysis was used to measure PN-1 binding to $^{35}SO_4$-labeled HeS chains purified from $^{35}SO_4$-labeled PGs that had been eluted during PN-1 affinity chromatography (Figure 2.3). Three different salt elutions from the PN-1 column are shown: (A) 0.15 M (column flow through), (B) 0.3 M, and (C) 0.5 M NaCl. The concentration of PN-1 (nM) in each gel lane is indicated below the gels. K_d's for each HeS subpopulation were calculated from retardation coefficients for each protein lane and plotted against PN-1 concentration, as shown in the graphs to the right of each gel (see Materials & Methods).

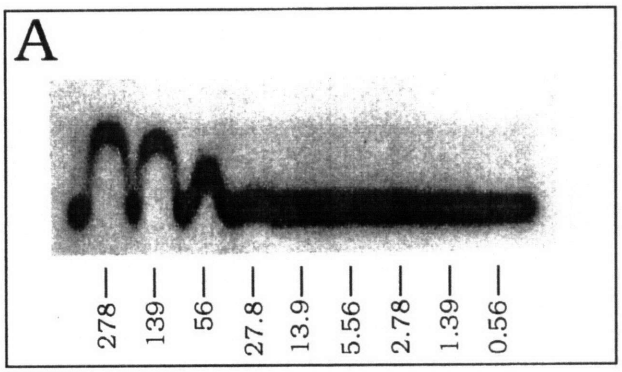
A
278
139
56
27.8
13.9
5.56
2.78
1.39
0.56

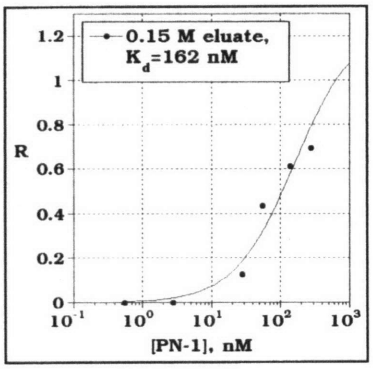
0.15 M eluate,
K_d=162 nM
R
[PN-1], nM

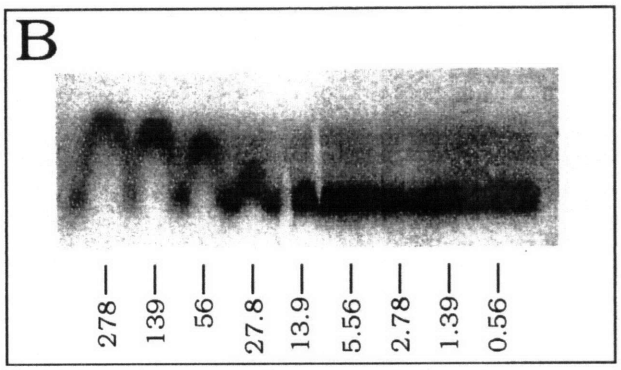
B
278
139
56
27.8
13.9
5.56
2.78
1.39
0.56

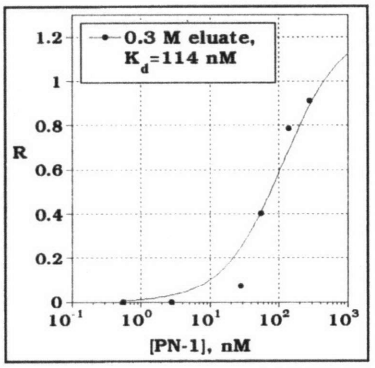
0.3 M eluate,
K_d=114 nM
R
[PN-1], nM

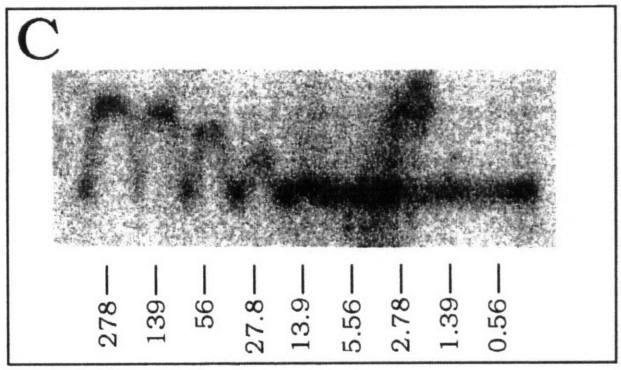
C
278
139
56
27.8
13.9
5.56
2.78
1.39
0.56

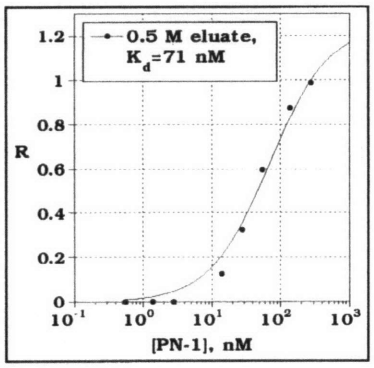
0.5 M eluate,
K_d=71 nM
R
[PN-1], nM

Figure 2.6 Affinity Coelectrophoresis of the Cell Adhesion Molecule, NCAM. ACE phosphorimages and analysis for early postnatal NCAM binding to E18 retinal-associated $^{35}SO_4$-labeled HeS (A) and ^{125}I-labeled $1M_r$-heparin (B). The same retinal HeS was tested for PN-1 binding as a positive control (C). The "flat-line" pattern seen in panel A is indicative of no measurable binding -- see text for discussion of the estimate of K_d. The concentration of PN-1 or NCAM (nM) in each gel lane is indicated below the gels. Equilibrium dissociation constants for the gels in panels B and C have been calculated from retardation coefficients for each protein lane, plotted against protein concentration, as shown in the graphs to the right of each gel (see Materials & Methods).

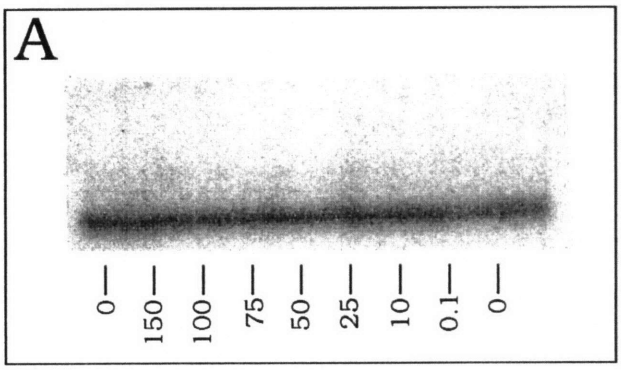

retinal HeS vs. NCAM;

No binding detected.

$K_{d_{min}} \geq 2.1\ \mu M$

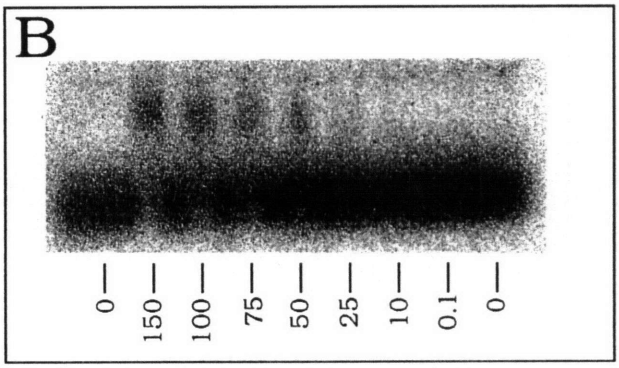

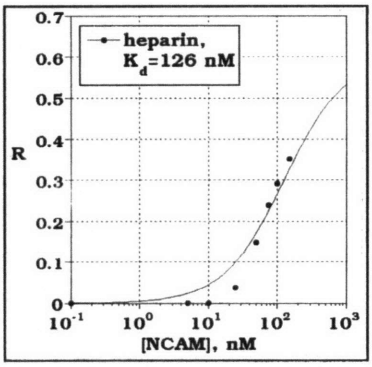

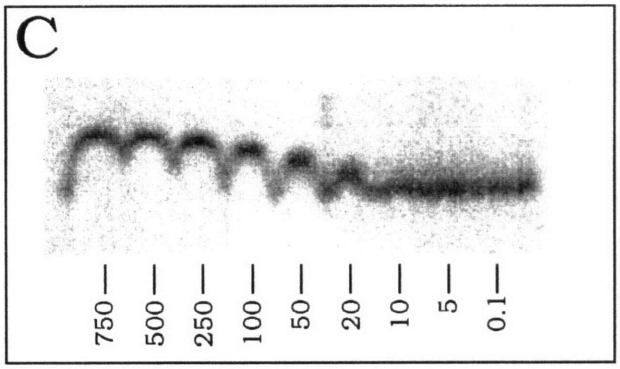

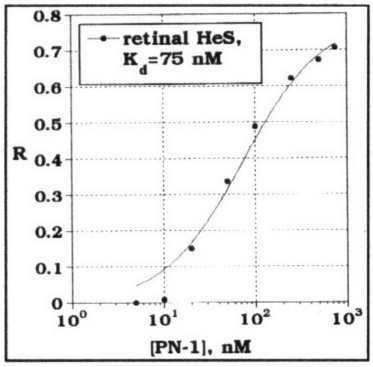

Table 2.3. NCAM and L1 Binding to Heparin and P0 Brain Membrane-Associated Heparan Sulfate.

		K_d $1M_r$-heparin (nM ligand)	K_d P0 brain membrane-associated HeS (nM ligand)
Postnatal NCAM (PSA +)	untreated	144 nM (1°)[a] 133 nM (2°)[b]	no binding seen [c] $K_{d,min} \cong 3150$ nM
	Endo-N treated	88 nM (1°)[a] 107 nM (2°)[b]	no binding seen [c] $K_{d,min} \cong 4680$ nM
Adult NCAM (PSA −)	untreated	104 nM (1°)[a] 110 nM (2°)[b]	no binding seen [c] $K_{d,min} \cong 5250$ nM
	Endo-N treated	119 nM (1°)[a] 85 nM (2°)[b]	no binding seen [c] $K_{d,min} \cong 5280$ nM
L1	(untreated)	144 nM (1°)[a] 133 nM (2°)[b]	no binding seen [c] $K_{d,min} \cong 2750$ nM

Equilibrium dissociation constants were derived from ACE analysis as described in text.

[a] = first order binding mechanism assumed in K_d derivation.

[b] = second order binding mechanism assumed in K_d derivation.

[c] = no measurable binding was seen in ACE; see text for method of calculating $K_{d,min}$.

Figure 2.7. Affinity Coelectrophoresis of the Cell Adhesion Molecule, L1. ^{125}I-labeled lM_r-heparin was tested for binding to L1 using affinity coelectrophoresis (ACE). Panel A: Phosphorimage of L1 ACE gel. Concentrations of L1 (nM) are listed below the gel. Panel B: Calculation of affinity of lM_r-heparin for L1. Retardation coefficients for each protein lane were calculated and plotted against L1 concentration (see Materials & Methods).

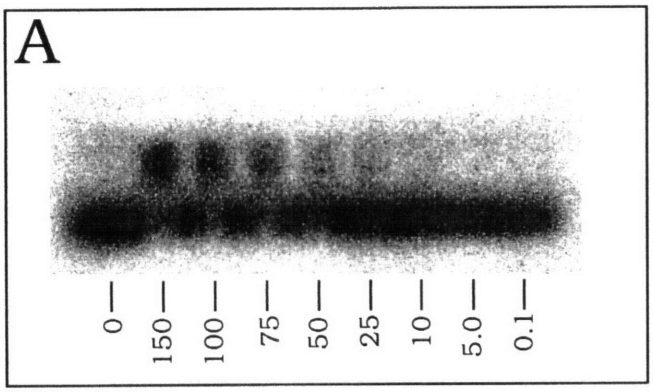
A
0
150
100
75
50
25
10
5.0
0.1

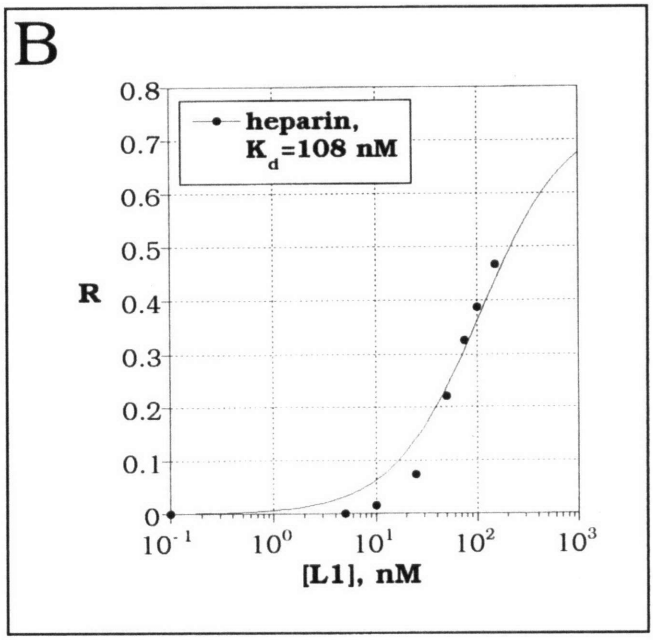
B
heparin,
K_d=108 nM
R
0.8
0.7
0.6
0.5
0.4
0.3
0.2
0.1
0
10^-1
10^0
10^1
10^2
10^3
[L1], nM

Figure 2.8. SDS-PAGE of Triton X-114 Partitioned Membrane-Associated Proteoglycans from Embryonic Day 18 Brain.
Autoradiographic image of membrane-associated PGs from E18 brain that were ^{125}I-labeled and subjected to Triton X-114 phase partitioning (see text). Unpartitioned material (total PGs), detergent phase (detergent) and aqueous phase (aqueous) of partitioned material was either digested with chondroitinase ABC and heparitinase (+) or left undigested (-), then subjected to SDS-PAGE. Proteoglycan core proteins appear as bands that are present in the lyase treated lanes but absent in the accompanying untreated lane. Core proteins of cerebroglycan (M13) and glypican (M12) (which are both GPI-tailed HSPGs; see chapter I), are marked with arrowheads. Molecular weight markers are indicated at left.

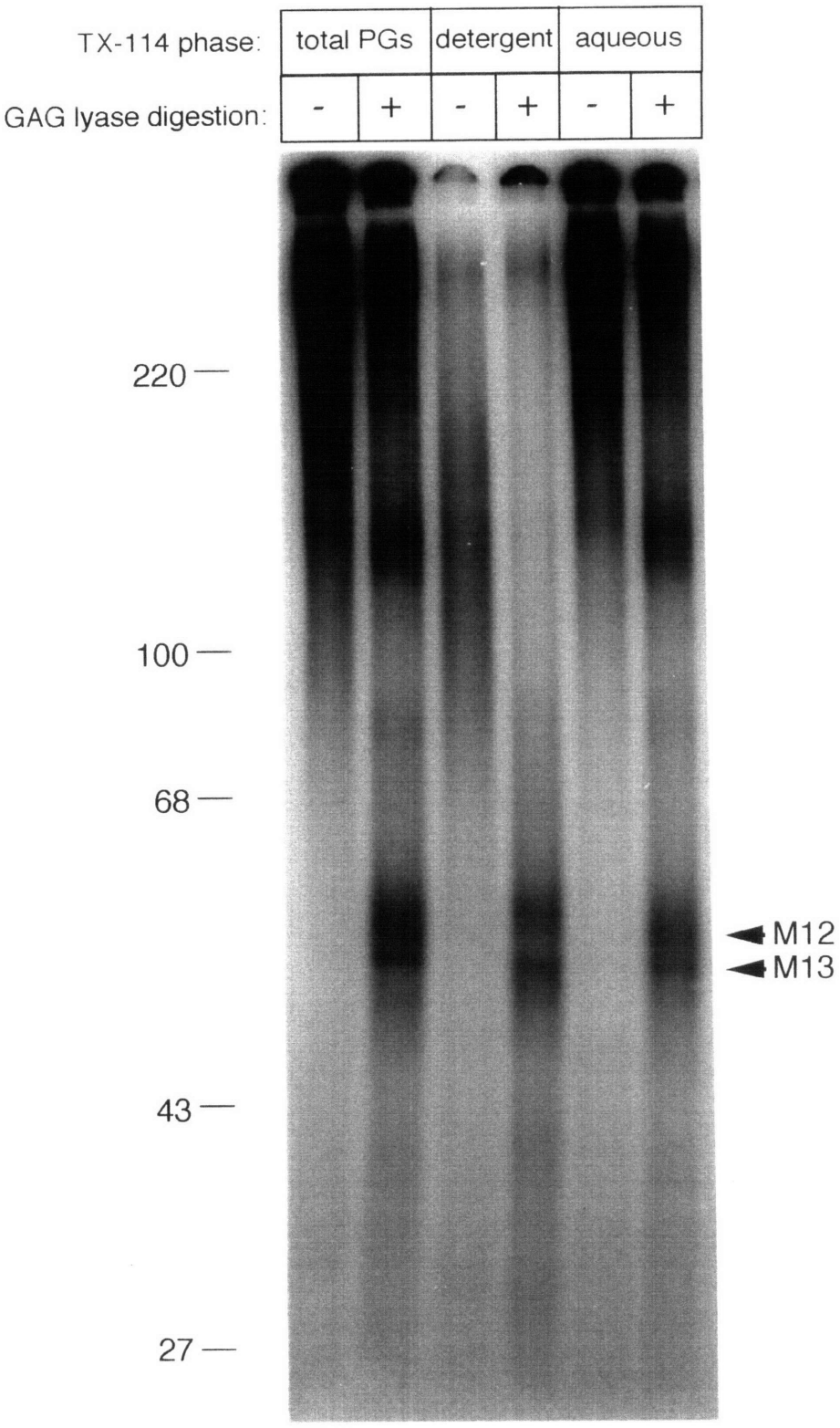
TX-114 phase:
total PGs
detergent
aqueous
GAG lyase digestion:
-
+
-
+
-
+
220
100
68
43
27
M12
M13

Figure 2.9. Affinity Coelectrophoresis of Extracellular Matrix Molecules Fibronectin and Laminin binding to Brain Proteoglycans. Fibronectin was tested for binding to detergent partitioned, ^{125}I-labeled PGs, cerebroglycan and glypican, from E18 brain (figure 2.8 and text). ACE autoradiographs for binding of these PGs to fibronectin and laminin are shown in panels A-C and D, respectively. In panel A, untreated PGs were tested for fibronectin binding, while PGs in panel C were pretreated by boiling in 0.1% SDS before electrophoresis. Strong and weak binding subfractions of the PGs are denoted by upper and lower arrows, respectively, in panels A and C. Heparitinase treatment of PGs (panel B) abolishes any visible fibronectin binding. See text for discussion and estimates of K_d's.

A
0
10
20
50
100
200
500
1000
0
B
0
10
20
50
100
200
500
1000
0
C
0
10
20
50
100
200
500
1000
0
D
0
5
10
25
50
75
100
150
250

Figure 2.10. Isolation of Cerebroglycan and Glypican Subpopulations that bind fibronectin strongly and weakly. TX-114 detergent partitioned ^{125}I-labeled GPI-tailed HSPGs from E18, P0 and adult brain membrane-associated PG preparations were fractionated by electrophoresis through agarose gels containing 1 μM fibronectin. Gels were then cut into 0.3 cm fractions perpendicular to the direction of electrophoresis and counted. Fibronectin strong binding pools (FN-S) were recovered from all three preparations as the three fractions corresponding to the first peak seen in the E18 prep (fractions 2-4), while fibronectin weak binding pools (FN-W) were from the three fractions corresponding to the highest part of the second peak (fractions 9-11).

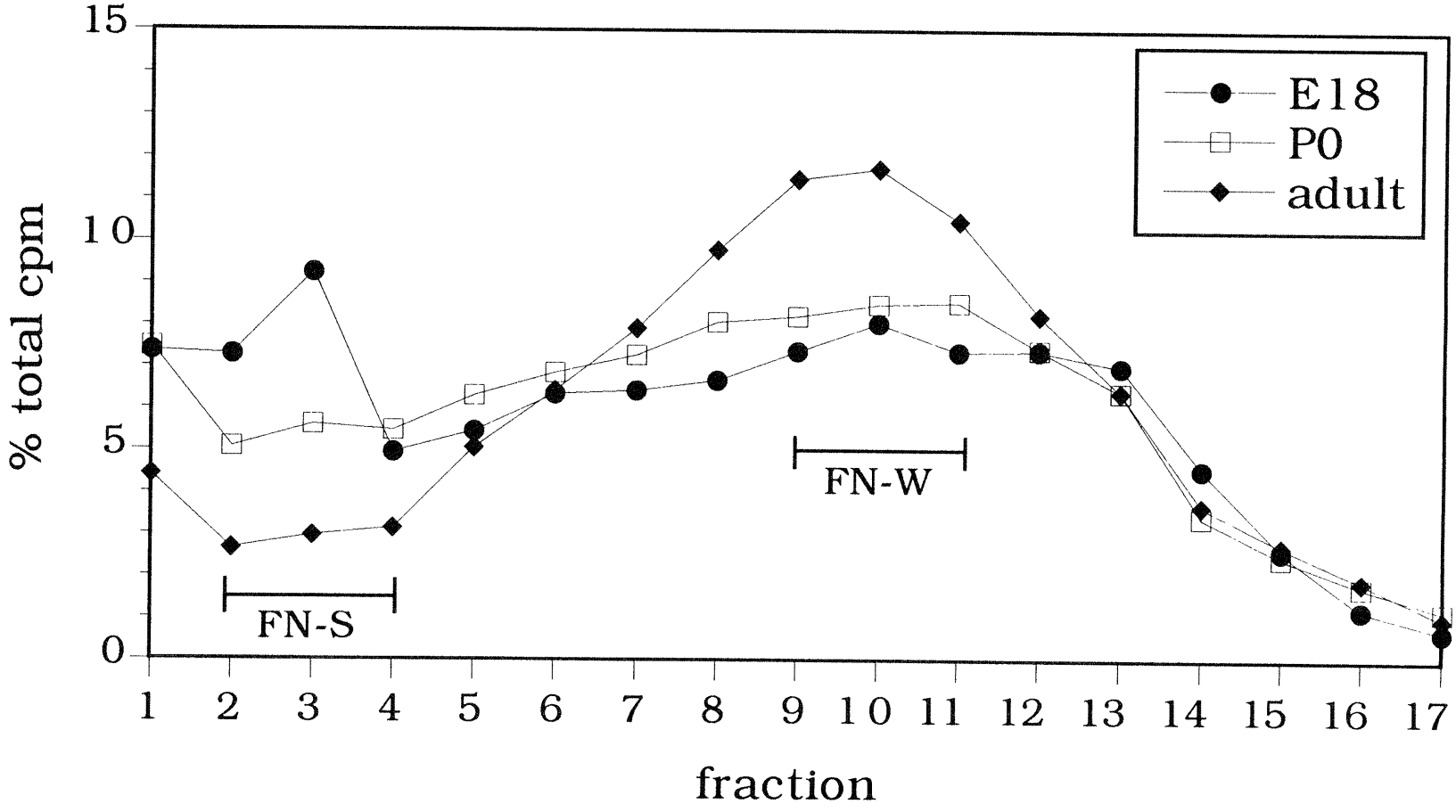
15
10
5
0
% total cpm
E18
P0
adult
FN-S
FN-W
1
2
3
4
5
6
7
8
9
10
11
12
13
14
15
16
17
fraction

Figure 2.11. SDS-PAGE Analysis of Fibronectin Strong- and Weak-binding Brain Proteoglycans. E18, P0, and adult GPI-tailed HSPGs that bind fibronectin strongly or weakly (Figure 2.10) were analyzed by SDS-PAGE on 9% mini-gels. Unfractionated control PGs (C), and equivalent volumes of strong (S), and weak (W) binding PG fractions were treated with chondroitinase ABC and heparitinase before electrophoresis. For E18 PGs, cerebroglycan (open arrowhead) is found almost exclusively in the high affinity pool, while for P0 brain, cerebroglycan is abundant in both pools (in adult brain, cerebroglycan is absent). Glypican (closed arrowhead) is most abundant in the weak fractions for E18 and P0. The fibronectin strong-binding fraction from P0 brain contains a small amount of a previously unidentified HSPG (*) with a slightly smaller core protein size than glypican.

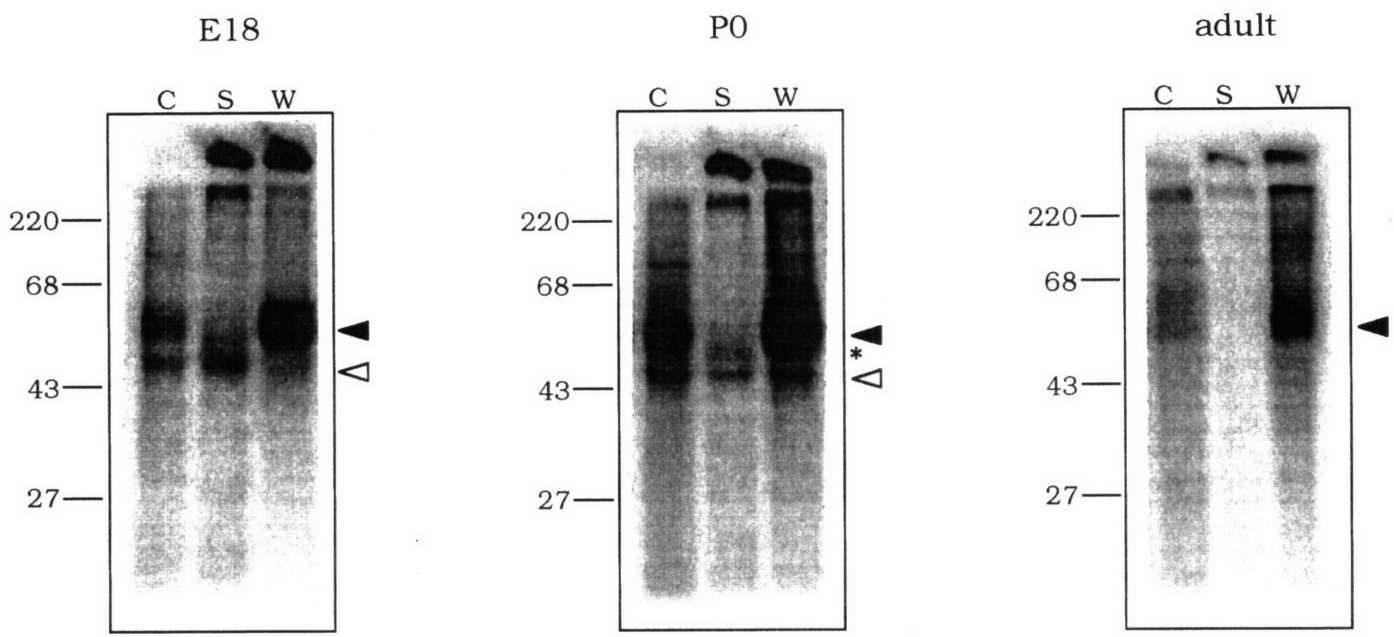
E18
C S W
220
68
43
27
P0
C S W
220
68
43
27
*
adult
C S W
220
68
43
27

Figure 2.12. Affinity Coelectrophoresis of Immunopurified Cerebroglycan and Syndecan-3 binding to Thrombospondin-1. ACE analysis was used to measure thrombospondin-1 binding to ^{125}I-labeled, immunopurified cerebroglycan (A) and syndecan-3 (B). Also shown is binding of E18 membrane-associated HeS chain binding to thrombospondin-1 (C). The concentration of thrombospondin-1 (nM) in each lane is indicated below the gels. Equilibrium dissociation constants were calculated from retardation coefficients for each protein lane and plotted against thrombospondin-1 concentration as shown in the graphs to the right of each gel (see Materials & Methods).

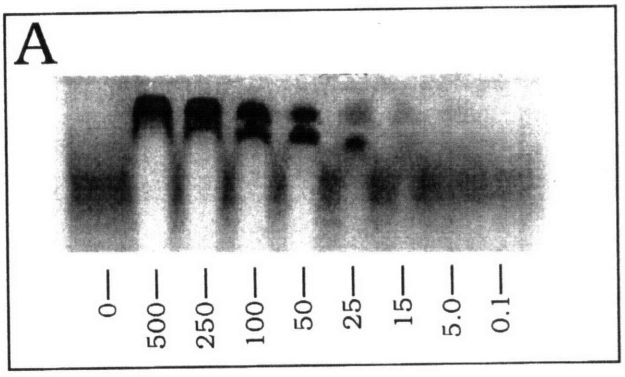
A
0
500
250
100
50
25
15
5.0
0.1

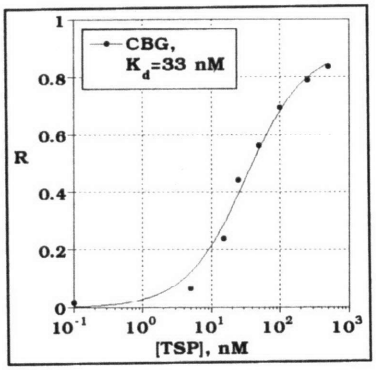
CBG,
K_d=33 nM
R
[TSP], nM

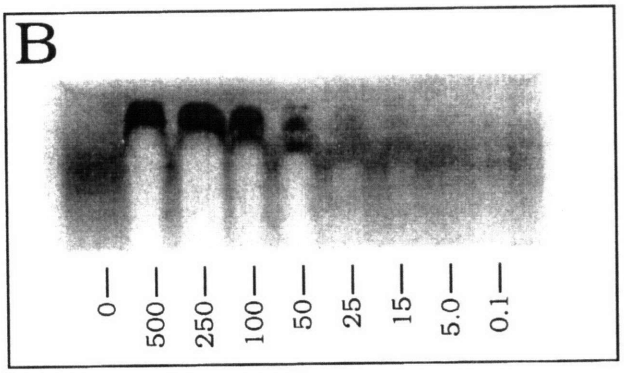
B
0
500
250
100
50
25
15
5.0
0.1

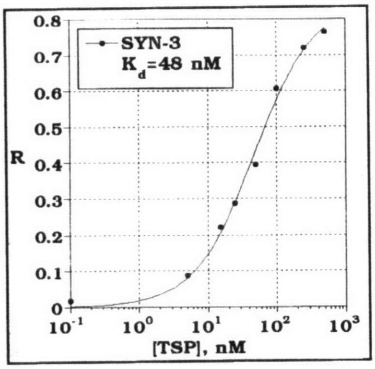
SYN-3
K_d=48 nM
R
[TSP], nM

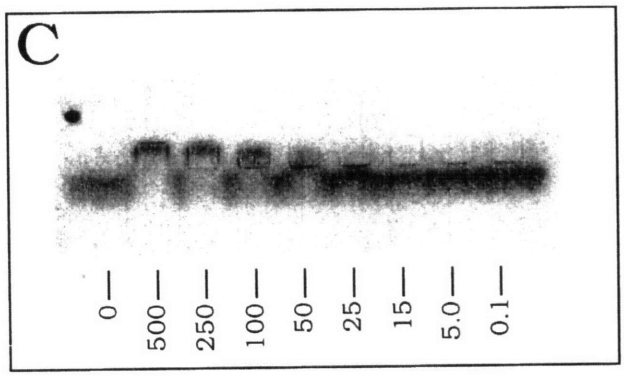
C
0
500
250
100
50
25
15
5.0
0.1

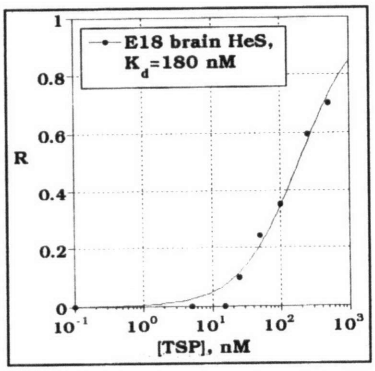
E18 brain HeS,
K_d=180 nM
R
[TSP], nM

Table 2.4. Equilibrium Dissociation Constants for GAG binding to Secreted Molecules.

GAG:	Protease Nexin-1	uPA	Thrombin	Anti-thrombin III	FGF-2
$1M_r$-Heparin, porcine intestinal	20 nM[e]	312 nM[b]	123 nM[c]	16 nM[h]	16 nM[b]
HeS, E18 rat brain membrane-associated	68 nM[b]	2790nM[a]	582 nM[a]	no binding[g] $K_{d,min}$ = 10 μM C_{max} =896 nM	n.d.
HeS, P0 rat brain membrane-associated	35 nM[a]	n.d.	n.d.	n.d.	47 nM[a]
HeS, P0 rat brain soluble fraction	101 nM[a]	2310 nM[a]	1025 nM[a]	n.d.	n.d.
HeS, bovine kidney	62 nM[a]	n.d.	1710 nM[a]	n.d.	170 nM[a]
ChS, E18 rat brain membrane-associated	223 nM[b]	16.4 μM[a]	4410 nM[a]	no binding[g] $K_{d,min}$ = 10 μM C_{max} =896 nM	n.d.
ChS from P0 rat brain membrane-associated	158 nM[a]	n.d.	n.d.	n.d.	no binding[g] $K_{d,min}$ = 13.5 μM C_{max} =150 nM
ChS, P0 rat brain soluble fraction	239 nM[a]	21.9 μM[a]	2500 nM[a]	n.d.	n.d.
ChS, bovine tracheal	478 nM[d]	17.1 μM[a]	10.3 μM[a]	n.d.	no binding[g] $K_{d,min}$ = 13.5 μM C_{max} =150 nM
ChS, shark cartilage	425 nM[a]	n.d.	n.d.	n.d.	n.d.

Equilibrium dissociation constants were derived from ACE analysis as described in text. All values listed are based on the assumption of first order binding mechanism; a = K_d value is from a single determination; b, c, d, e = K_d value is mean of two, three, four, or five determinations, respectively; f = soluble fraction refers to initial homogenization of brain tissue with buffered isotonic sucrose (see Chapter 1); g = no measurable binding in ACE. $K_{d,min}$ is determined as outlined in text. C_{max} = maximal concentration of ligand tested in ACE; h = K_d value reported in Lee & Lander (1991); n.d. = no determination was made.

Table 2.5. Equilibrium Dissociation Constants for GAG binding to Large Multidomain Extracellular Glycoproteins.

GAG:	Fibronectin	Laminin-1	Thrombospondin-1
$1M_r$-Heparin, porcine intestinal	486 nM[c]	54 nM[a]	41 nM[b]
HeS, E18 rat brain membrane-associated	7.4 μM[a]	886 nM[a]	180 nM[a]
HeS, P0 rat brain membrane-associated	6.2 μM[a]	891 nM[a]	180 nM[a]
HeS, bovine kidney	34.4 μM[a]	790 nM[a]	262 nM[a]
ChS, E18 rat brain membrane-associated	n.d.	no binding[g] $K_{d,min}$ = 977 nM C_{max} =181 nM	235 nM[a]
ChS from P0 rat brain membrane-associated	n.d.	no binding[g] $K_{d,min}$ = 977 nM C_{max} =181 nM	235 nM[a]
ChS, bovine tracheal	no binding[g] $K_{d,min}$ = 179 μM C_{max} =3650 nM	no binding[g] $K_{d,min}$ = 1.1 μM C_{max} =200 nM	487 nM[a]
ChS, shark cartilage	no binding[g] $K_{d,min}$ = 127 μM C_{max} =2600 nM	no binding[g] $K_{d,min}$ = 1.1 μM C_{max} =200 nM	648 nM[a]

Equilibrium dissociation constants were derived from ACE analysis as described in text. All values listed are based on the assumption of first order binding mechanism; a = K_d value is from a single determination; b, c, d, e = K_d value is mean of two, three, four, or five determinations, respectively; g = no measurable binding in ACE. $K_{d,min}$ is determined as outlined in text. C_{max} = maximal concentration of ligand tested in ACE; n.d. = no determination was made.

Table 2.6. Equilibrium Dissociation Constants for GAG binding to the Cell Adhesion Molecules, NCAM and L1.

	L1	Postnatal NCAM (PSA +)		Adult NCAM (PSA -)	
GAG:		Untreated	Endo N Treated	Untreated	Endo-N treated
$1M_r$-Heparin, porcine intestinal	108 nM[a]	144 nM[c]	88 nM[a]	104 nM[a]	119 nM[a]
HeS, E18 retina	n.d.	no binding[g] $K_{d,min}$ = 2100 nM C_{max} =150 nM	n.d.	n.d.	n.d.
HeS, E18 rat brain membrane-associated	no binding[g] $K_{d,min}$ = 2750 nM C_{max} =250 nM	no binding[g] $K_{d,min}$ = 3360 nM C_{max} =240 nM	n.d.	no binding[g] $K_{d,min}$ = 5250 nM C_{max} =250 nM	n.d.
HeS, P0 rat brain membrane-associated	no binding[g] $K_{d,min}$ = 2750 nM C_{max} =250 nM	no binding[g] $K_{d,min}$ = 3150 nM C_{max} =225 nM	no binding[g] $K_{d,min}$ = 4680 nM C_{max} =260 nM	no binding[g] $K_{d,min}$ = 5250 nM C_{max} =250 nM	no binding[g] $K_{d,min}$ = 5280 nM C_{max} =220 nM
HeS, bovine kidney	n.d.	n.d.	n.d.	no binding[g] $K_{d,min}$ = 5250 nM C_{max} =250 nM	no binding[g] $K_{d,min}$ = 5280 nM C_{max} =220 nM
ChS, bovine tracheal	no binding[g] $K_{d,min}$ = 460 μM C_{max} = 42 nM	n.d.	n.d.	n.d.	n.d.
Colominic Acid, E. coli	no binding[g] $K_{d,min}$ = 1760 μM C_{max} =160 nM	no binding[g] $K_{d,min}$ = 2240 μM C_{max} =160 nM	n.d.	n.d.	n.d.

Equilibrium dissociation constants were derived from ACE analysis as described in text. All values listed are based on the assumption of first order binding mechanism; a = K_d value is from a single determination; b, c, d, e = K_d value is mean of two, three, four, or five determinations, respectively; g = no measurable binding in ACE. $K_{d,min}$ is determined as outlined in text. C_{max} = maximal concentration of ligand tested in ACE; n.d. = no determination was made.

Chapter III

Effects of Brain Glycosaminoglycans on Protease Nexin-1 Inhibition of Thrombin and Urokinase Plasminogen Activator

INTRODUCTION

Considering the structural diversity, expression patterns, binding properties, and abundance of glycosaminoglycans (GAGs) and proteoglycans in the brain, these molecules are expected to play significant functional roles in neural development. A growing body of evidence demonstrates that, in vitro at least, GAGs can affect a multitude of cell behaviors, including cell adhesion, cell proliferation and differentiation, axon outgrowth in neurons, cell migration and extracellular matrix organization [reviewed in (Ruoslahti, 1988; Wight et al., 1992; Lander and Calof, 1993)]. The vast majority of investigations in which GAGs have been used have relied on commercial GAG preparations (e.g., heparin from intestine, heparan sulfates derived from kidney or liver, and chondroitin sulfates purified from cartilage). No published studies to date have used GAGs purified from brain as in vitro reagents in either molecular or cellular functional assays. Yet the structures of both heparan and chondroitin sulfates from different tissues, indeed from different proteoglycans within a tissue, may vary significantly, suggesting that their functional aspects may also change in different tissues (Linker and Hovingh, 1973; Gallagher et al., 1986; Karamanos, 1992; Cheng et al., 1994; Deutsch et al., 1995). To assess possible functional roles for GAGs in the brain, we chose to examine the in vitro effects of GAGs purified from brain, as well as the effects of GAGs from non-neural sources, on the activities of a set of functionally related and developmentally important secreted molecules found in brain: the serine protease inhibitor, protease nexin-1 (PN-1) and two of its substrate serine proteases, urokinase plasminogen activator (uPA) and thrombin. These molecules were chosen because, in addition to their functional relatedness, each of these molecules is known to bind heparin, and each has potent effects on neural cell behaviors in vitro.

The serine protease inhibitor PN-1 (also known as glial-derived nexin), is expressed by both neural and glial cell lines in vitro (Wagner et al., 1991), and has been found in both the central and peripheral nervous systems throughout development (Mansuy et al., 1993). PN-1 is very abundant in the brain: Mansuy et al (93) reported ~4ng of PN-1 per 100μg of whole brain homogenate protein from age P0 to P14

mouse. This translates to PN-1 at 20 nM overall in the brain, and perhaps up to a tenfold higher concentration if the majority of the molecules are confined to extracellular regions. In vitro, PN-1 stimulates neurite outgrowth in neuroblastoma cells [(Monard et al., 1983); reviewed in (Cunningham, 1992)]; inhibits cerebellar cell migration in culture (Lindner et al., 1986); and reverses thrombin-mediated inhibition of astrocyte stellation (Cunningham, 1992).

The serine proteases thrombin and uPA are also neurally expressed molecules that have known effects on neural cell behaviors. While immunolocalization of thrombin protein in brain tissue is problematic due to its abundance in blood, both prothrombin mRNA and thrombin receptor mRNA expression patterns suggest that widespread and abundant expression of thrombin occurs throughout brain development (Dihanich et al., 1991; Weinstein et al., 1995). uPA mRNA is strongly expressed in both the peripheral and central nervous systems, where onset of expression occurs in all identifiable neurons early in development and is continued in the adult (Sumi et al., 1992; Dent et al., 1993).

In vitro, uPA appears to have varied effects on neural cell behaviors. For example, inhibition of uPA slows the migration of cultured cerebellar granule neurons (Moonen et al., 1992), while neurite outgrowth and growth cone lamellipodial activity in cultured sympathetic neurons are increased by antibodies that inhibit uPA activity (Pittmann et al., 1989). Thrombin exhibits concentration dependent effects: at sub-picomolar concentrations, thrombin inhibits astrocyte stellation in cultured astroglia, while at higher concentrations (>30 pM), neurite retraction occurs in cultured neuroblastoma cells and astrocyte mitosis is induced (Cavanaugh et al., 1990; Cunningham, 1992). Each of these thrombin activities is completely reversible by the addition of PN-1. Interestingly, while PN-1 is a potent inhibitor of uPA in medium from cultured neuroblastoma cells, cell-bound PN-1 appears unable to inhibit uPA (Wagner et al., 1991).

Inhibition of thrombin and uPA by PN-1 occurs by formation of a characteristic serpin-protease complex [reviewed in (Potempa et al., 1994)]. Serpins (*ser*ine *p*rotease *in*hibitors) are a class of protein

proteinase-inhibitors, whose members characteristically are single chain polypeptides of 41 to 43 kD M_r containing a proteinase susceptible loop at the protein surface that forms the reactive site. Cleavage of this loop by the proteinase causes transition from a stressed conformation to a heat-stable, relaxed form that continues to block the activity of the proteinase but also destroys future anti-protease activity on the part of the serpin; therefore, serpins are classified as suicide inhibitors. The serpin binds its target protease at the site of the protease-reactive serine, forming a long-lived complex. [For example, the antithrombin III-thrombin complex has a half life of 5.7 days (Bjork and Lindahl, 1982)]. This complex was previously considered to be a covalent acyl-enzyme intermediate. However, it is now generally believed that complex formation stops at a long-lived tetrahedral intermediate stage. This intermediate is converted to the covalent acyl form by denaturants such as heat and SDS. Thus, a generalized reaction scheme for serpin-proteinase reactions is:

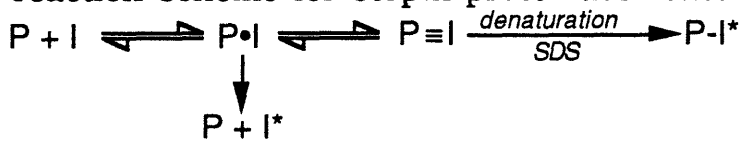

(1)

where P = Protease; I = inhibitor (serpin); P•I = noncovalently bound complex (Michaelis complex); P≡I = stable tetrahedral intermediate; I* = cleaved inactive inhibitor; and P-I* = denaturation induced acyl form of complex [from (Potempa et al., 1994)].

Serpins exhibit specificity of inhibition, inhibiting some proteases better than others. For example, Evans et al., (1991) report that PN-1 inhibits trypsin>thrombin>plasmin>factor Xa, with association constants ranging over 431 fold. Many serpins, including PN-1, antithrombin III, heparin cofactor II (HCII), type 1 plasminogen activator (PAI-1), and protein C inhibitor (PCI), bind to the glycosaminoglycan heparin, and in some cases other GAGs as well. Heparin-binding can dramatically increase inhibition by these serpins. And because heparin-binding accelerates serpin activity toward particular proteases to different extents, GAG-binding can effectively change the specificity of the serpin. For example, in the absence of heparin, the level of antithrombin inactivation for four of its substrates is thrombin≈factor Xa>plasmin≈factorIXa, with a 140-fold range in

association constants. Heparin addition, however, changes the rate of association of antithrombin with its substrates so that it binds thrombin>factor IXa≈factor Xa>>plasmin with more than 400-fold difference in k_{assoc} (Jordan et al., 1980b).

GAGs are believed to accelerate serpin-protease reactions by either or both of the following mechanisms [reviewed in (Bjork and Lindahl, 1982)]:

(1) Allosteric activation of the serpin: GAG-binding induces a conformational change that activates the serpin toward the protease. This type of activation is probably responsible for GAG-accelerated inhibition by GAG-binding serpins of proteases that do not bind GAGs [e.g., antithrombin inhibition of factor Xa (Jordan et al., 1980b; Streusand et al., 1995)].

(2) Ternary complex model: GAG-binding by both the serpin and the protease incresases the rate of complex formation by facilitating two dimensional diffusion of the serpin and/or the protease toward each other along the GAG [e.g., inhibition of thrombin by antithrombin, HCII, and PCI (Hoylaerts et al., 1984; Pratt et al., 1992)]. This model is also called a template model, as the GAG provides a template upon which the complex can form.

Inhibition of proteases by serpins may, of course, involve both mechanisms. This is generally held to be the case for antithrombin inhibition of thrombin, although the relative contribution of each mechanism remains in debate (Pratt et al., 1992; Streusand et al., 1995).

In order to understand better the functional roles that nervous system GAGs may play in serpin-protease reactions we have carried out studies of PN-1 inhibition of thrombin and uPA in the presence of GAGs purified from newborn rat brain. Binding of PN-1, thrombin, and uPA to both brain GAGs and non-neural GAGs was measured by affinity co-electrophoresis (ACE). Also, we report the use of a new technique, reverse ACE, for determination of protein-to-GAG binding affinities in terms of GAG concentration. PN-1 inhibition of uPA was oppositely affected by the presence of GAGs than was thrombin inhibition by PN-1. The results are presented in view of current models of GAG acceleration of serpin-protease reactions.

MATERIALS AND METHODS

Materials

Denis Monard (Freidrich Miescher Institute, Basel, Switzerland) generously provided rat recombinant protease nexin-1 (produced in yeast) while human recombinant uPA (high molecualr weight form, produced in E. coli) was the gift of Jack Henken of Abbott Labs (Abbott Park, IL). Human plasma thrombin was supplied by Enzyme Research Laboratories, Inc. (South Bend, IN). All protein concentrations were determined by amino acid analysis (MIT Biopolymers Laboratory).

Sigma Chemical Co. supplied porcine intestinal heparin, bovine tracheal chondroitin sulfate, uronic acid, and heparinase II. Shark chondroitin sulfate was from Fluka. Bovine kidney heparan sulfate and crystalline BSA were from ICN. Chondroitinase ABC was from Seikagaku, USA. Heparitinase was the same material mentioned in chapter I. Protease inhibitors and protease cocktail formulation were the same as mentoned in Chapter I.

Purification of neonatal brain heparan and chondroitin sulfates

A collection of brain soluble fractions from an estimated total of 240 g of postnatal day 0 (P0) Sprague-Dawley rat brains (prepared according to methods outlined in Chapter I and stored up to five years at -80°C) were used as a source of unlabelled P0 brain GAGs. Soluble fraction proteoglycans were prepared by DEAE-Sephacel chromatography as outlined in chapter I. GAGs were cleaved from PG cores by alkaline-borohydride reaction: PG's were incubated at 45°C, 3 hours, in 90 mM NaOH and 9 mM $NaBH_4$, then the reaction quenched with the addition of ammonium formate to 0.45 M and HCl to 90 mM. The reaction mixture was then diluted to I = 0.1 M with 50 mM Tris-HCl, pH $8.0^{(4°C)}$ and re-applied to a 10 ml DEAE-Sephacel column. The column was washed with 200 ml 0.1 M NaCl, 6 M Urea, 50 mM Tris-HCl, pH $8.0^{(4°C)}$, and then with 100 ml 50 mM Tris-HCl, pH $8.0^{(4°C)}$. GAGs were eluted with 30 ml 0.75 M NaCl, 50 mM Tris-HCl, pH $8.0^{(4°C)}$, and collected as a single pool. GAG concentration in the eluate was determined to be 380 μg/ml (yield 11.4 mg), using the uronic acid assay outlined below. For HeS purification from P0 brain GAGs, chondroitin ABC lyase digestion was carried out at 0.05 U/ml

for 15 hours at 37°C, while ChS was purified by treatment of GAGs with heparitinase (4 μg/ml, 43°C, 15 hrs). Both lyase digestions were done in the presence of protease inhibitor cocktail. Lyase treated HeS and ChS were concentrated by ethanol precipitation by adding a 3.2 fold volume of 100% ethanol and incubating at -20°C for 20 hr. Precipitates were collected by centrifugation at 12,000 g for 30 min, 4°C, then briefly air dried. GAG pellets were resuspended in 200 μl of 0.15 M NaCl, 50 mM Tris-HCl, pH $8.0^{(4°C)}$.

To assess purity of the HeS and ChS populations, GAGs were tested by digestion with the appropriate lyase using standard procedures (Chapter II) and subjected to PAGE and AzureA/Ammoniacal Silver staining according to the method of Lyon & Gallagher (1990). Untreated GAGs each appeared as broad, diffuse bands near the top of a 20% acrylamide gel, while treatment of HeS with heparitinase and treatment of ChS with chondroitinase ABC abolished the smears (data not shown).

Determination of GAG concentrations

GAG concentrations were determined by measurement of uronic acid content, using a microscaled version of the method of Filisetti-Cozzi and Carpita, (1991). This method improves over carbazole measurements of uronic acid by using the more sensitive m-hydroxydiphenyl (3-hydroxybiphenyl) as the colorimetric reagent, and by the addition of sulfamate during the reaction, which suppresses interfering color production by neutral sugars, including glucosamine and galactosamine. All reagents were prepared as outlined in Filisetti-Cozzi and Carpita (1991). Briefly, uronic acid standards ranging from 0.5 to 10 μg, and an estimated 3 to 6 μg of each GAG to be tested were each diluted to 100 μl in 10 mM sodium acetate buffer, pH 5.0, in acid washed 13x75 mm glass tubes. To each sample, 10 μl 4 M sulfamic acid/potassium sulfamate solution and 600 μl 75 mM sodium tetraborate in concentrated sulfuric acid were added. The samples were vortexed well and then placed in a boiling water bath for 20 min, with acid-washed marbles as caps. Tubes were then chilled in an ice bath. Next, at room temperature, 18 μl of 0.15% 3-hydroxybiphenyl was mixed into each tube. After 10 min, absorbance at 525 nm was

read. To calculate GAG concentrations, absorbances for GAG samples were compared to a standard curve drawn for the uronic acid sample absorbances. The uronic acid concentration for each GAG was then divided by 0.4 to give GAG concentration in μg/ml. This multiplier is based on the work of Linker & Hovingh (1973), and Turnbull and Gallagher, (1990), that shows that for heparan sulfate, at least, ~40% by weight is uronic acids.

Reverse ACE

Unlike ACE ("forward" ACE), in reverse ACE the labelled molecule at sub-K_d concentrations is not the PG or GAG, but the protein ligand. The name of the technique derives from the "reverse" set-up that is required to achieve equilibrium conditions during electrophoresis. Figure 3.1 diagrams the set-up and a typical post-electrophoretic pattern for reverse ACE. The reverse ACE gel is prepared and run identically to forward ACE [Chapter II; (Lee and Lander, 1991; Lim et al., 1991)] but with the following changes: 1) slot well and comb wells are reversed in orientation (Figure 3.1); 2) comb wells are filled with unlabeled GAG, at descending concentrations, embedded in agarose; 3) slot well is filled with labeled (usually by ^{125}I) protein ligand, also embedded in agarose; 4) electrophoresis continues until most of the GAG has passed through the region of the labeled protein. The gel is dried and imaged as usual.

Determination of the equilibrium dissociation constant, K_d, for reverse ACE is also quite similar to the method used with forward ACE, but with the following differences:

1) Electrophoretic mobility, instead of being measured from the physical top of the comb wells, is measured from the physical position of the slot well, with positive mobilities toward the cathode ("above" the slot) and negative mobilities toward the anode ("below" the slot). In most cases the ligand alone (i..e., unbound protein) has some slight mobility, either forward or reverse. If the unbound ligand does not move during electrophoresis, however, mobility determinations must be measured from either slightly above or below the slot, to prevent the value of "n", mobility of unbound ligand, from equalling zero.

2) R values (retardation coefficients) for each lane of the reverse ACE gel are calculated the same as for forward ACE ($R = [n - \mu]/n$, where μ = mobility of the protein-GAG complex at a given concentration of GAG and n = mobility of unbound protein ligand). By this convention, if unbound ligand migrates in the negative (anodal) direction, R values will be negative as well.

3) As with forward ACE, K_d values are derived by fitting graphs of R values versus associated GAG concentration values to:

$$R = \frac{R_\infty}{1 + (K_d/[G_{tot}]^n)} \qquad (2)$$

where R_∞ = R value where the protein ligand is maximally shifted, K_d = equilibrium dissociation constant, [G][P]/[G-P], for the following reaction:

G (GAG) + P (protein) $\Leftrightarrow$ G-P (GAG-protein complex);

$[G_{tot}]$ = GAG concentration in each lane of the ACE gel (in the general case, this value should actually be ($[G_{tot}]$ - [G-P]), but because labeled protein ligand concentrations are so low ($<0.1K_d$), the G-P term can be dropped from the equation); n = number of protein molecules that must bind simultaneously to each GAG molecule, i.e. order of binding mechanism. All K_d determinations done here were fit to first order binding.

4) Because ChS binding to some of the protein ligands tested was relatively weak, ChS concentrations high enough to attain R_∞ or near R_∞ conditions were not possible. In these cases, R_∞ was estimated as the R_∞ value for heparin-binding to the protein multiplied by the ratio of free ChS mobility over free heparin mobility, because the mobility of the GAG component appears to dominate GAG-protein complex mobility in reverse ACE (personal observation). In cases where R values were negative, estimated R_∞ values were of course also negative, and graphs were a flip-image of curves with positive R values.

Radioiodination of Protease nexin-1, Thrombin, and uPA

0.3, 0.5, and 4.0 nmoles of uPA, thrombin, and PN-1, respectively, each in 50 µl of 0.25 M $NaPO_4$, pH 7.5, and 3 mCi of

$Na^{125}I$ (NEN) were mixed in a 13 x 75 mm glass tube, that had previously been coated with 20 µg of Iodogen (50 µl of 0.4 mg/ml Iodogen in dichoromethane). Reactions were incubated for 4 minutes, then an additional 50 µl of 0.25 M $NaPO_4$, pH 7.5 was added. After 4 more minutes, the ^{125}I-labelled proteins were separated from free iodine by filtration over a 2 ml G-25 (Pharmacia) column that had been pre-blocked with 200 µg of crystalline BSA. Column buffer was 0.5X PBS (68.5 mM NaCl, 1.35 mM KCl, 4 mM Na_2HPO_4, 0.75 mM KH_2PO_4, pH 6.85). Labelled protein peaks were collected and radioprotected with the addition of 1.0 mg/ml crystalline BSA. ^{125}I-labelled thrombin and uPA were aliquotted and stored at -80°C, while ^{125}I-labelled PN-1 was stored at 4°C.

Kinetic Assays of PN-1 Inhibition of Thrombin and uPA

All kinetic assays involved measurements of the increase in absorbance at 405 nm due to ρ-nitroanilide release from cleavage of chromogenic peptide substrates tosyl-Gly-Pro-Arg-4-nitranilide (Chromozym TH, Cat # 838268, Boehringer Mannheim) or benzoyl-b-Ala-Gly-Arg-4-nitranilide (Chromozym U, Cat # 836583, Boehringer Mannheim) by thrombin or uPA, respectively. Reactions were carried out in assay buffer (50 mM Tris-HCl, pH $8.3^{25°C}$, 225 nM NaCl, 5 mg/ml crystalline BSA, 0.02% NaN_3) at room temperature (25°C). Absorbance increases at 405 nm were measured using a Perkin-Elmer Lambda 4B spectrophotometer and chart recorder. Effects of PN-1 addition to thrombin reactions and uPA reactions were determined both in the presence and absence of the following GAGs: porcine intestinal heparin, P0 rat brain soluble fraction ChS, and P0 rat brain soluble fraction HeS for both thrombin and uPA inhibition reactions, while thrombin inhibition reactions were also tested in the presence of bovine kidney HeS, bovine tracheal ChS, and shark ChS. Measurements from chart records included initial thrombin or uPA reaction slope in the absence of PN-1 and slopes at 20 or 60 sec intervals for thrombin or uPA, respectively, after addition of PN-1 with or without GAGs. For reactions containing GAGs, PN-1 was mixed with the polysaccharide at least 5 minutes prior to addition to the protease reaction. Addition of PN-1 (+/-GAGs) resulted in a 25% increase in

volume (from 400 to 500 µl), so the inhibition reaction slope for t = 0 ($Slope_{init}$) was calculated by multiplying initial reaction slopes by 0.8. Average time required for the mixing of PN-1 with the protease reactions was 8 seconds. Therefore, t = 0 of PN-1 inhibition reactions was set at 8 seconds after opening the spectrophotometer door. Initial O.D. value for t=0 was calculated by extrapolating backwards in time to t = 0 using O.D. values recorded after the door was closed and chart recording had begun (this was required because changes in the chart recorder offset occasionally occurred due to opening and closing of the door). In most cases back-extrapolation was accomplished by projecting the slope at the first measured interval back to t = 0; however, for curves with rapidly changing slopes, O.D. values for t = 0 were estimated by eye .

Kaleidagraph (Synergy Software) was used to fit data from each inhibition curve to the following equation:

$$OD = \frac{Slope_{init}}{P_o} \cdot \frac{1}{Q} \left[\ln \frac{1 - \frac{P_o}{I_o} e^{-[I_o - P_o]Qt}}{1 - \frac{P_o}{I_o}} \right] \qquad (3)$$

where OD = the O.D. value (arbitrary units) for each timepoint; $Slope_{init}$ = the initial slope of the protease reaction before PN-1 addition, corrected for subsequent volume changes; P_o = the initial molar concentration of protease; I_o = the initial molar concentration of inhibitor, PN-1†; t = timepoint in seconds; and Q is the apparent rate constant (see below and results).

Equation 3 is essentially an integration with respect to time of an equation for [P] as a function of time ($[P] = (Slope_{init}/Q)(1 - \exp(-Qt))$; cf., equation 2 in Stone and Hermans, (1995)), and was derived from the following reaction model:

---

† The I_o value was initially allowed to vary during curve fitting for reactions without GAGs in order to derive a corrected I_o value based on the real activity of PN-1 toward the protease. The $I_{o,corr}$ value was then fixed during subsequent curve fitting for reactions containing GAG and the same PN-1 concentration. This curve fitting method was required to compensate for the tendency of the curve fitting program to balance variables in two-variable curve fits (for example, GAG increases which caused increases in the apparent rate constant would also be reflected in an increased PN-1 concentration variable).

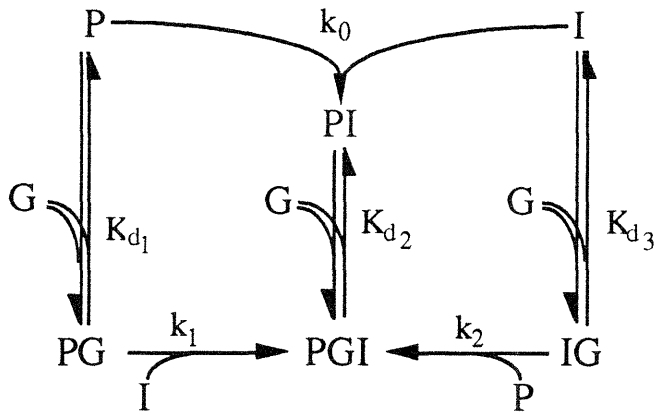

(4)

where P = protease (thrombin or uPA), G = GAG, and I= inhibitor (PN-1). Derivation of equation 3 is also based on the following assumptions: 1) that GAG binding to either P or I is rapid compared to the rates of other steps; 2) that initial concentration of GAG ($[G_o]$) is much higher than both $[P_o]$ and $[I_o]$, so that $K_{d1} = ([P][G_o])/[PG]$, $K_{d2} = ([PI][G_o])/[PGI]$, and $K_{d3} = ([I][G_o])/[IG]$; 3) that protease forms P and PG are equally active toward the peptide substrate, while forms PI and PGI are totally inactive; 4) that the slope at any time of OD v. time graphs is proportional to the amount of active protease; 5) that GAG-bound protease and GAG-bound inhibitor are not available to each other as reactants; and 6) that the cleavage of I and release of active P (see equation 1) occurs only to a negligible extent during the duration of the asssay under the buffer conditions employed (Olson, 1985; Stone and Hermans, 1995).

The three rate constants and two of the equilibrium dissociation constants found in equation (4), as well as the initial GAG concentration appear in the variable Q, the apparent rate constant for formation of inactive protease:

$$Q = \frac{k_0}{1 + \frac{[G_o]^2}{K_{d1}K_{d3}} + \frac{[G_o]}{K_{d1}} + \frac{[G_o]}{K_{d3}}} + \frac{k_1}{1 + \frac{K_{d1}}{K_{d3}} + \frac{K_{d1}}{[G_o]} + \frac{[G_o]}{K_{d3}}} + \frac{k_2}{1 + \frac{K_{d3}}{K_{d1}} + \frac{[G_o]}{K_{d1}} + \frac{K_{d3}}{[G_o]}} \quad (5)$$

See results section for simulations of changes that occur in Q as a function of GAG concentration. When no GAG is present, the reaction model is simply:

$$P + I \rightleftharpoons P\bullet I \longrightarrow P\text{-}I^* \qquad (6)$$

and Q reduces to k_0, the apparent first order rate constant, which includes all steps for the conversion of active P to the inactive form in the absence of GAG.

All of the mathematical modelling and derivations presented in the above section are the work of Arthur Lander.

Titration of PN-1 by uPA and Thrombin

Long term inhibition assays of 10 nM thrombin and 10 nM uPA, respectively, by protease nexin-1 were carried out using a broad range of PN-1 concentrations (0.1 nM to 1.0 μM). Protease substrate and buffer conditions were identical to those used in kinetic assays (above). 306 μl PN-1 in reaction buffer was mixed with 34 μl of 100 nM thrombin or uPA and incubated for four or five hours, respectively, at room temperature. 40 μl of protease substrate was then mixed into each inhibition reaction, incubated for a further 5 minutes at room temperature to allow color development, then quenched with 225 μl 50% Acetic Acid. Absorbance at 405 nm was measured using a Perkin-Elmer Lambda 4B spectrophotometer.

RESULTS

Both heparan and chondroitin sulfates bind to protease nexin-1, thrombin, and uPA with distinct affinities.

Heparin has substantial effects on the activity of the serpin antithrombin III: A subfraction of heparin molecules that bind strongly to antithrombin III will increase antithrombin's inhibition of thrombin up to 4000-fold [reviewed by (Bjork and Lindahl, 1982)]. This type of GAG-mediated acceleration has been found to take place with other serpin-protease combinations as well. In general, the effects of GAGs on serpin-protease reactions in vivo will depend on which GAGs bind these proteins, whether GAG and serpin are present in the same place, and what happens to serpin activity when GAG binding occurs. To test for GAG binding to the neurally expressed serpin protease nexin-1 (PN-1) and to the neural serine proteases thrombin and urokinase plasminogen activator (uPA), affinity coelectrophoresis (ACE, or "forward" ACE) was used (see methods in Chapter 2). For all three proteins, heparin (both low M_r and unfractionated forms) and various heparan and chondroitin sulfates were tested. Figure 3.2 shows ACE images for PN-1 binding to low M_r heparin, compared to antithrombin III binding to low M_r heparin. Unlike AT III, PN-1 did not selectively bind to a subpopulation of heparin. The ACE binding pattern, showing a single relatively tight GAG band, was seen with each protein ligand tested, PN-1, thrombin, or uPA, and for all GAG types tested (data not shown). Also, for each of the proteins, low M_r heparin and unfractionated heparin exhibited identical, single band ACE patterns (data not shown). These uniform binding patterns suggest that the majority of (if not all) molecules in each of these GAG population contain at least one binding site for each protein ligand.

Additionally, for uPA, thrombin and PN-1, each GAG-protein combination exhibits a distinct affinity (or at least a narrow range of affinities). Comparison of dissociation constants for each of the ACE analyses, shown in table 3.1, shows that PN-1 binds to each type of GAG more strongly than does either thrombin or uPA. All three molecules bound both neural and non-neural heparan sulfates and

chondroitin sulfates, and for each, binding to heparan sulfates was stronger than chondroitin sulfate binding.

Reverse Affinity Co-electrophoresis demonstrates that protease nexin-1, thrombin, and uPA each exhibit single affinities for heparin and chondroitin sulfate.

While "forward" ACE provides information about the protein concentration required for half maximal GAG binding, as well as whether there are subpopulations of GAGs with significant differences in K_d, any heterogeneity in the protein ligand is not discernible in forward ACE, where the observed K_d would be artificially raised by the presence of weaker or non-binding molecules in the protein preparation. Reverse ACE, on the other hand, provided two advantages for this study: it allowed verification that the proteins used in this study have single demonstrable affinities for heparin and chondroitin sulfate, and it allowed measurements of K_d in terms of GAG rather than protein concentration. This second feature provides useful information for interpreting the effects of GAGs on PN-1 and thrombin or uPA interactions (see kinetic analyses below).

Figure 3.3 shows representative reverse ACE gels of heparin and chondroitin-4-sulfate vs. ^{125}I-labelled protease nexin-1. PN-1 demonstrates a single binding isotherm in reverse ACE. A minor component of non-binding material in the gel may represent a fraction of the PN-1 that has decreased binding to heparin; however, a more likely interpretation is that it represents a fraction of the PN-1 that was damaged during the chloramine-T iodination procedure. Both ^{125}I-labelled thrombin and uPA demonstrated patterns similar to PN-1 in heparin and chondroitin-4-sulfate reverse ACE, with no significant GAG binding subpopulations seen (data not shown). Dissociation constants for reverse ACE analyses, both in terms of μg/ml and approximate nM GAG, are compiled in table 3.2. As with forward ACE, heparin and chondroitin sulfate each bind more strongly to PN-1 than to either of the proteases, thrombin or uPA. Also, each protein ligand bound heparin much more strongly than it bound the chondroitin-4-sulfate (heparin binding of 250 fold, 63 fold, and 40 fold stronger than Ch4S binding to PN-1, thrombin, and uPA, respectively).

Brain Glycosaminoglycans exert opposite effects on the inactivation of Thrombin and Urokinase Plasminogen Activator by Protease Nexin-1.

Inhibition of thrombin and uPA activity by PN-1 involves the stereotypical formation of a serpin-protease complex. Complex formation for PN-1 and many other serpins (including heparin cofactor II, protein C inhibitor, PAI I, and antithrombin III) is accelerated in the presence of heparin and often other GAGs (Evans et al., 1991; Pratt et al., 1992; Gebbink et al., 1993). The binding interactions demonstrated here in forward and reverse ACE suggest that both heparan and chondroitin sulfates from brain may affect PN-1 complex formation with uPA and thrombin.

A general model for the influence of GAG binding on serpin-protease interactions (equation4) predicts (given a small number of reasonable assumptions -- see Methods) that the rate of protease inactivation will depend on the dissociation constants for GAG binding to the serpin and its substrate protease, as well as three rate constants, k_1, k_2, and k_0: k_1, the rate constant for GAG-bound protease association with free inhibitor; k_2, for GAG-bound inhibitor binding to unbound protease; and k_0, for formation of complex in the absence of GAG. The influence of these five parameters may be lumped into a single variable, Q, which represents an apparent rate constant in the presence of GAG (equations 3 and 5). Predictions of how changes in GAG concentration affect Q have been simulated in figure 3.4. Using K_d's obtained by reverse ACE for uPA and PN-1 as estimates for K_{d1} and K_{d3}, respectively, these simulations predict that when either or both of the rate constants for formation of the GAG-bound protease-inhibitor complex, k_1 and/or k_2, are greater than k_0, the overall rate constant Q will rise then fall as a function of GAG concentration (Figure 3.4 A, B, and C). k_2 appears to have a more dominant effect on Q than does k_1: The effect of raising k1 100 fold over k0 has less effect on Q than does raising k2 the same amount (figure 3.4 A and B). No changes in the value of Q are seen when k_1 is varied from $k_1 = k_0$ down to $k_1 = 0$ (Figure 3.4 A). Yet the same lowering of the k_2 value shows Q curves falling off compared to Q for $k_1 = k_2 = k_0$. Examination of the equation for Q (equation 5) shows

that the expressions for the divisors of k_1 and k_2 are reciprocal with respect to the two K_d's. Thus the rate constant for the GAG-bound molecule that binds to the GAG more strongly (the inhibitor, in this case) exhibits more control over the overall rate of complex formation. As GAG concentration increase above a value roughly midway between the two Kds, the species IG and PG (equation 4) will begin to dominate the reaction. Because the model proposes that no productive interactions occur between IG and PG, Q decreases (figure 3.4 A, B, and C). Thus, the model used here predicts that a characteristic bell-shaped curve for GAG-acceleration is a consequence of the ternary complex model that has been proposed for several serpin-protease combinations, including antithrombin, PN-1, PAI-1, HCII, and PCI, each with thrombin; antithrombin with factor IXa; and PCI with protein C, uPA, and chymotrypsin (Jordan et al., 1980b; Pratt and Church, 1992; Pratt et al., 1992; Rovelli et al., 1992; Gebbink et al., 1993). Declining values of Q result from cases where GAG binding disfavors complex formation (when k_1 and/or k_2 are less than k_0).

PN-1-thrombin and -uPA complex formation were assessed using assays of each protease's activity toward peptide substrates in the presence of PN-1. First, end-point titration of PN-1 to thrombin and uPA was carried out: These experiments revealed that for both thrombin and uPA, a 3:1 molar ratio of PN-1 to protease concentrations was required for complete inactivation of the protease in four to five hours at room temperature (data not shown). In short term kinetic assays, thrombin was used at 1 nM protein, while uPA was used at 3 nM protein concentration: Proteases were mixed with 0.2 mM ρNA-conjugated peptide substrates in assay buffer and quickly transferred to a cuvette for spectrophotometric measurement of increases in absorbance due to substrate cleavage. Reaction progress was recorded on a chart recorder for 10 to 20 minutes. In the absence of PN-1, no measureable decrease in either thrombin or uPA activity was seen during the time period of the assays (data not shown).

Short term kinetic assays of PN-1 inhibition of the proteases, including a broad range of GAG concentrations, were used to measure GAG effects. In these assays, effects of PN-1 or PN-1 premixed with

GAGs on thrombin or uPA activity were measured by adding the serpin after the protease assay had proceeded for 2 to 3 minutes, so that the initial slope of each protease reaction could be measured before inhibition began. 50 nM PN-1 protein was added to thrombin reactions and 150 nM PN-1 protein was added to the uPA reactions. In the absence of GAGs, reactions using these PN-1 concentrations recorded mid-range in the chart record over the time of the assay. Thus, when GAGs were added along with the PN-1, either acceleration or deceleration of PN-1 inhibition could be immediately read on the chart recorder without changing settings. These PN-1 concentrations also represent ~17x the amount of PN-1 needed to completely inhibit each of the proteases in long term assays.

Figure 3.5 shows an example of a curve fit for data from kinetic assays of thrombin inhibition by PN-1, with and without added HeS. This HeS, from a newborn rat brain soluble fraction proteoglycan preparation, is seen to accelerate thrombin inhibition by PN-1, with the apparent rate constant, Q, increasing from 2.16 $x10^5$ $M^{-1}s^{-1}$, to 3.24 $x10^5$ $M^{-1}s^{-1}$, to 5.54 $x10^5$ $M^{-1}s^{-1}$ for 0, 10, and 100 μg/ml added HeS, respectively. By similar analysis, Q values from kinetic assays of both uPA and thrombin inhibition by PN-1 with the addition of heparin from 10^{-4} to 10 μg/ml, P0 rat brain soluble fraction ChS from 1 to 500 μg/ml, and P0 rat brain soluble fraction HeS from 1 to 1000 μg/ml were evaluated. Additionally, apparent rate constant values were obtained for thrombin inhibition reactions tested in the presence of bovine kidney HeS, bovine tracheal ChS, and shark ChS, each from 1 to 1000 μg/ml. Figure 3.6 shows the changes that occur to the apparent rate constant as GAG concentrations are varied for both thrombin and uPA inhibition by PN-1. Additionally, K_d values from the reverse ACE experiments described above are displayed in the graphs.

The effect of heparin on the inhibition of thrombin by PN-1 is one of dramatic acceleration of protease inhibition, starting at concentrations as low as 10 ng/ml. Whether the relationship of Q to GAG concentration eventually peaks and then falls off, as is predicted by the simulation of Q shown in figure 3.4, was not determined for heparin, which was only tested to 10μg/ml. However, a bell-shaped curve for PN-1 inhibition of thrombin in the presence of heparin has

been documented by others (Rovelli et al., 1992; Stone et al., 1994) using heparin concentrations higher than those tested here. All other GAGs tested for effects on PN-1 inhibition of thrombin, including both heparan and chondroitin sulfates from neural and non-neural sources, gave changes in the apparent rate constant indicative of GAGs that accelerate serpin-protease complex formation (Figure 3.6; and see figure 3.4 for k_1 and/or $k_2 > k_0$). Interestingly, the peak of acceleration for these GAGs occurs at roughly the same concentration and is increased similarly for each of these GAGs, regardless of heparan or chondroitin sulfate type.

Figure 3.6 also shows the effects of three GAGs, heparin, brain heparan sulfate, and brain chondroitin sulfate, on PN-1 inhibition of uPA. Intriguingly, PN-1 inhibition of uPA is affected by these GAGs in a way that is not predicted by the model in equation 4, or by simulations of changes in the apparent rate constant, Q. All three GAGs cause deceleration of the serpin-protease reaction initially, reminiscent of the prediction for k_1 and/or $k_2 < k_0$ (figure 3.4). However, the drop in PN-1 activity appears to plateau as the brain GAGs are increased, while PN-1 activity actually reverses and begins to increase as heparin concentrations rise. It has been reported that uPA protease activity is stimulated by heparin concentrations above 10 μg/ml (Andrade-Gordon and Strickland, 1986). However, short term kinetic assays of uPA activity in the absence of PN-1 showed that the addition of heparin across the range of concentrations used in the inhibition assays ($1x10^{-4}$ to 10 μg/ml), or the addition of 100 μg/ml of either brain chondroitin sulfate or heparan sulfate, had no effect on uPA activity toward its peptide substrate (data not shown)†. This supports the idea that the apparent reduction in PN-1 inhibition of uPA caused by the addition of GAGs is not an artifact of uPA stimulation by GAG, but is instead a genuine effect of GAG on the interaction between the serpin and its protease substrate.

The concentration ranges over which heparin and the two brain GAGs exert their effects on the uPA--PN-1 reaction are identical to the ranges where the thrombin--PN-1 reaction is affected. Therefore, just

---

† In these uPA assays, the values for [reaction slope after GAG addition/$slope_{init,corr}$] varied by no more than 1±0.035 at any of the conditions tested.

as a given GAG is increasing PN-1 inactivation of one protease, it is decreasing PN-1's inhibition of the other protease.

DISCUSSION

Heparin, and in some cases other glycosaminoglycans, are known to affect the interactions of particular serpin and serine protease combinations. To explore possible roles for brain GAGs in the regulation of such protein interactions, inhibition by the serpin protease nexin-1 (PN-1) of two substrate proteases, thrombin and urokinase plasminogen activator, was examinined. All three proteins were found to bind both heparan and chondroitin sulfates purified from brain tissue. Also, the in vitro inhibition of uPA and thrombin by PN-1 was found to be affected by brain GAGs. Together with evidence that all these molecules, PN-1, uPA, thrombin and GAGs, are abundantly expressed in the brain, the data presented here suggest an important role for GAG-mediated control of PN-1 interactions with thrombin and uPA in vivo.

Binding of PN-1, uPA, and thrombin to various GAGs was measured by affinity coelectrophoresis (ACE), which provides a measure of binding in terms of the protein concentration. Results showed that PN-1 bound each GAG type more strongly than did uPA or thrombin, while for each protein, heparan sulfates bound more tightly than did chondroitin sulfates. A new technique, reverse ACE, was used to obtain dissociation constant values in terms of GAG concentrations. The values for GAG binding to PN-1, thrombin, and uPA obtained from reverse ACE (Table 3.2), vary no more than four-fold from the "forward" ACE values (Table 3.1), differences that probably lie within experimental error. Measurement of GAG concentrations relied on measurement of uronic acid by 3-hydroxybiphenyl with potassium sulfamate rather than the more standard carbazole reactions. While this method is considered more reliable than the carbazole method (Filisetti-Cozzi and Carpita, 1991), deviations, if any, from uronic acid standard color production by specific GAG types that may occur has not been documented as it has for carbazole. Therefore, GAG concentrations reported, both in reverse ACE and in the inhibition assays, were based on direct comparisons with uronic acid standards. In any event, it is unlikely that the GAG concentration measurements were as reliable as the protein measurements used in the "forward" ACE determinations, which relied on amino acid

analysis. Thus while forward ACE K_d's are probably more accurate measurements of protein-GAG binding, the reverse ACE values are more valuable for comparison of GAG-protein binding to the GAG concentration effects seen in the kinetic assays of protease inhibition. Insufficient amounts of the brain GAGs were available for reverse ACE studies. However, in forward ACE, the range of K_d's for binding of the non-heparin GAGs to each of the proteins varied by ≤10-fold, with chondroitin-4-sulfate generally at the weak-binding end of the scale; thus, the reverse ACE K_d values for chondroitin-4-sulfate may provide a reasonable, if slightly high estimate of dissociation constants for binding of PN-1, thrombin, and uPA to the other non-heparin GAGs.

In short-term kinetic assays, thrombin inhibition by PN-1 was accelerated by the addition of any of the glycosaminoglycans tested (table 3.3; figure 3.6). In the case of the heparan and chondroitin sulfates both from brain and from non-neural sources, figure 3.6 shows that the pattern of acceleration is similar to predicted changes in Q, the apparent rate constant, for a model reaction (figure 3.4). The rise in Q with increasing amounts of GAG switches to a decline at a GAG concentration that lies between the K_d's for PN-1 and thrombin binding to chondroitin-4-sulfate. These bell-shaped curves, with the K_d values for serpin- and protease-heparin binding on the ascending and the descending arms of the curve, respectively, are consistent with a model in which ternary complex formation accounts for the GAG-mediated increase and subsequent decrease in PN-1 inhibition of thrombin. Several observations support a ternary complex model: (1) For the GAGs other than heparin, the shapes of the curves are generally similar to the shapes of curves predicted by equation 4 (Figure 3.4). In particular, the peaks of the acceleration curves lie between the K_d's for GAG binding to PN-1 and to thrombin, a feature predicted when both proteins are binding to the same GAG molecule to form a ternary complex (Jordan et al., 1980b; Streusand et al., 1995) (2) The five different non-heparin GAGs, including both chondroitin sulfates and heparan sulfates, accelerate PN-1 inhibition of thrombin to roughly the same extent (Figure 3.6), and all bind to either thrombin or PN-1 with affinities within the same order of magnitude (Table 3.1). This suggests that the binding of these GAGs

to PN-1 and to thrombin, and the resulting activation of PN-1 inhibition of thrombin, involves broad features of GAG structure common to all GAG types. (3) The decrease in PN-1 inhibition of thrombin seen at higher concentrations of GAG is predicted for a template model which requires both serpin and protease to bind to a single GAG molecule for a productive reaction to occur. At high concentrations of GAG, the effect of GAG binding is to separate the reactants from each other. While the data presented here support a template model, they do not rule out GAG-mediated allosteric activation of PN-1 inhibition of thrombin: The rise in Q values could be attributable to PN-1 activation due to GAG binding, while the subsequent decrease in Q might result from steric blocking of PN-1 access to thrombin due to increased thrombin GAG binding.

It should be noted that thrombin is known to contain two heparin binding sites [(Jordan et al., 1980a; Jordan et al., 1980b; Olson et al., 1991; Sheehan and Sadler, 1994)]. Olson et al. (1991) estimated that thrombin contains a strong binding site that accomodates a 3 disaccharide site in heparin, and binds with an intrinsic K_d of 6-10 μM heparin, while a second weaker binding site is estimated to bind heparin with an affinity that is about 100-fold weaker. Interestingly, the intrinsic K_d for thrombin binding to a 3-disaccharide heparin [~8 μM; (Olson et al., 1991)], corresponds to a K_d in terms of heparin by weight of ~5 μg/ml, and is in good agreement with the K_d for thrombin binding to heparin reported here (3 μg/ml; Table 3.2). While several individual point mutations (R to E or K to E) in the weaker thrombin heparin-binding site (exosite I) do not significantly reduce rates for heparin-mediated inhibition by antithrombin, similar point mutations in the strong binding site of thrombin (exosite II) show both reduced binding to heparin-agarose and reduced inhibition by antithrombin [(Sheehan et al., 1993; Sheehan and Sadler, 1994; Sheehan et al., 1994)]. On the other hand, heparin chains that are long enough to accomodate both heparin-binding sites in thrombin increase the anitithrombin inhibition rate constant 1000-fold over the change seen with single-site binding chains (25 vs. 5 disaccharides long, respectively) (Hoylaerts et al., 1984). This result is in good agreement with the finding by

Rosenberg and colleagues (Jordan et al., 1980b) that for the heparin-mediated inhibition of thrombin by antithrombin, theoretical predictions of changes in the initial reaction velocity match observed values best when the thrombin-heparin tertiary complex (TH_2) rather than the binary complex (TH_1) is assumed to be the form of thrombin that is least inhibited by antithrombin. Together, these results suggest that thrombin binding to heparin may involve cooperative binding of both heparin binding sites.

Because thrombin may be binding either to two separate GAG molecules or to a single GAG that wraps around to bind both heparin-binding sites, in theory, the inhibition model shown in equation 4 should contain an additional reaction loop to accomodate this stoichiometry. Such a loop would contain an additional rate constant (k_3 for PGG + I $\rightarrow$ PGGI) and two additional K_d's (K_{d4} for PG + G $\leftrightarrow$ PGG, and K_{d5} for PGI + G $\leftrightarrow$ PGGI). Inclusion of these variables would probably complicate the equation for Q significantly (equation 5). However, if we maintain the assumption that GAG-bound protease and GAG-bound inhibitor are unavailable to each other as reactants, then the new model is likely to predict that the association contant for binding between GAG-bound inhibitor and free protease (k_2) will still have the dominant effect on the overall rate constant of inhibition (Q), simply because the inhibitor binds the GAG much more strongly than does the protease (see figure 3.4). However, while the assumption that protease and inhibitor that are bound to separate GAG chains cannot interact simplifies the mathematical modelling, this assumption is actually not correct, but rather an overstatement of a predominant feature of ternary complex formation. This feature, that protease and inhibitor molecules that are bound to separate GAG chains are *less likely* to interact than are GAG-bound inhibitor and *free* protease molecules, accounts for the descending limb of the bell-shaped curve that is typical of GAG-mediated ternary complex fomation [cf., (Jordan et al., 1980b; Streusand et al., 1995)]. In the simplified model, rate of complex formation is predicted to continually decrease as the GAG concentration increases. In reality, as GAG concentrations enter ranges that are saturating for both protease and inhibitor, the apparent rate constant forms a plateau [cf., (Jordan

et al., 1980a; Pratt and Church, 1992)]. For heparin-mediated antithrombin-thrombin and antithrombin-factor IXa complex formations, these plateaus represent rate constants that are 700- and 680-fold higher, respectively, than rate constants in the absence of heparin (Jordan et al., 1980b). The formation of such plateaus might be accounted for by any of several mechanisms that would result in continued inhibition of the protease at high GAG concentrations. The best documented mechanism, for antithrombin at least, is an allosteric effect of heparin-binding that facilitates protease-inhibitor complex formation [cf., (Jordan et al., 1980b; Streusand et al., 1995)]. Second, direct complex formation between protease and inhibitor, each bound to a separate GAG chain, might occur at a constant low rate without invoking an allosteric effect. A third possibility is that competing binding sites in GAGs at high concentrations may induce facilitated "jumping" of the more weakly bound protease to other GAG chains, thus increasing the likelihood of its encounter with a GAG-bound inhibitor molecule.

The curve obtained for heparin-mediated effects of thrombin inhibition by PN-1 was not entirely typical for ternary complex formation (figure 3.6 A), since reaction rates continued to increase with heparin concentration above the K_d of heparin for thrombin. This may be attributable to the ionic strength of the buffer used in the kinetic assays, which was higher than that of the reverse ACE buffer used for measurements of GAG binding (I = 0.25 M and 0.15 M, respectively)†. These buffer conditions were selected because, for antithrombin at least, they have been shown to reduce the rate of cleavage and release of inactivated serpin [(Olson, 1985); see also equation 1]. Two previous studies reported that heparin-mediated PN-1 inhibition of thrombin produced a bell-shaped ternary complex curve, with heparin acceleration beginning at about 1.5 ng/ml, peaking at ~0.15 μg/ml heparin (300 to 530-fold above the control rate), and fully decelerated at ~15 μg/ml (Rovelli et al., 1992; Stone et al., 1994).

---

† The increase in the apparent rate constant beyond the K_d for heparin-thrombin binding is not due to any changes in thrombin protease activity caused by the heparin preparation used, because heparin concentrations up to 1 mg/ml showed no effect on thrombin activity toward the peptide substrate (data not shown).

Thus, the K_d's for heparin binding to PN-1 and to thrombin measured here (0.077 and 3.0 μg/ml, respectively) would fall on the ascending and descending arms of these curves. The thrombin K_d value reported here (3.0 μg/ml) is in good agreement with published values of ~6.3 μg/ml (Streusand et al., 1995) and ~5.0 μg/ml (Jordan et al., 1980b). Also, heparan sulfate proteoglycans that eluted from PN-1 affinity columns at 0.15 and 0.3 M NaCl were shown to bear heparan sulfate chains with K_d's less than 50 nM apart (162 and 114 nM, respectively; see figure 2.5, chapter 2). Whether heparin-binding to PN-1 is more sensitive to ionic changes, causing greater shifts in K_d values, is not known. In any event, the K_d values marked on figure 3.6 provide reasonable estimates of where half-maximal GAG binding occurs for the proteases and for PN-1, while use of a lower ionic strength buffer in the kinetic assays might have shifted the Q-versus-GAG curves toward lower GAG concentrations.

Short-term kinetic assays of heparin acceleration of thrombin inhibition by PN-1 reveal that the magnitude of PN-1 acceleration is much higher with heparin than other GAGs. A recently published study by Olson and colleagues (Streusand et al., 1995) showed that for antithrombin inhibition of thrombin, two heparin populations with 1000-fold difference in affinity for antithrombin accelerate the serpin reaction by identical mechanisms: Like high affinity heparin, the low affinity form bridges thrombin to antithrombin, but with a reverse order of ternary complex formation; also, both heparins induce a conformational change in antithrombin, although the change induced by the low affinity heparin was not the full activating conformational change induced by the high affinity pentasaccharide sequence found in strong-binding heparin. These authors suggest that the magnitude of antithrombin acceleration relies most on the strength of binding to heparin. However, further derivation of the equation for Q, the apparent rate constant, reveals that in the ternary complex model, the

maximum-fold stimulation of Q† depends not so much on strength of binding *per se* as on (K_{d1}/K_{d3}), the *ratio* of protease-GAG K_d to inhibitor-GAG K_d, as well as the rate constants for GAG-bound protease binding to free inhibitor (k_1) and for GAG-bound inhibitor binding to free protease (k_2). For example, for a particular serpin-protease combination that has the same (K_{d1}/K_{d3}) for binding to two *different* GAGs, even if, for both proteins, binding to GAG_1 is much weaker than binding to GAG_2, it is possible for the maximal increase in Q to be the same, but only if k_1 and k_2 remain the same for both GAG-containing reactions. More importantly, if (K_{d1}/K_{d3}) is the same with two different GAGs, but the increase in Q is not similar, then it is clear that k_1 and/or k_2 are changed when the different GAGs are present. Both k_1 and k_2 are essentially "on" rates, as the reverse reaction is negligible in each case. Thus, for antithrombin that is saturated with heparin, k_2 should be nearly the same as the "on" rate for thrombin binding to heparin alone. Indeed, the antithrombin-thrombin reaction in the presence of high affinity heparin reaches a maximum at near diffusion controlled rates. Because PN-1 also binds heparin with a K_d similar to that of antithrombin, Q in PN-1-thrombin reactions might be expected to be similarly increased.

PN-1 inhibition of thrombin by the tissue-derived heparan and chondroitin sulfates gave similar patterns of acceleration as heparin, but significantly lower magnitudes of effect than did heparin. The (K_{d1}/K_{d3}) for thrombin/PN-1 binding to heparin was 6.2, while (K_{d1}/K_{d3}) values for binding to the other GAGs ranged from 10 to 27 (mean = 17.3). Thus, if k1 and k2 were the same for both heparin- and the other GAG-containing reactions, then the maximal rates for the non-heparin GAGs are predicted to be at least as high as the highest heparin Q value. In fact, even though the maximal Q was plainly not reached for heparin (figure 3.6 A), the highest rate

---

† Theoretical maximal acceleration of Q is:

$$\left.\frac{Q}{k_o}\right|_{max} = \frac{s^2\sqrt{a(s-1)(s-a)}}{(s-a+\sqrt{a(s-1)(s-a)})(as-a+\sqrt{a(s-1)(s-a)})}$$

where $a = (K_{d1}/K_{d3})$ and $s = [(k_1/k_0) + a(k_2/k_0)]$ (Arthur Lander, personal communication).

obtained was more than 90-fold higher than the maximal Q induced by any of the other GAGs. Therefore, the ternary complex model applied here predicts that the association rate constants for the heparin-mediated reaction are significantly higher than those of the other GAGs. It is possible that heparin has an additional effect on PN-1 activation, similar to the conformational activation of antithrombin. It is also possible that for the non-heparin GAGs, differences in GAG structure, such as the domain structure of HeS, may result in different "on" and "off" rates along a given GAG chain, differences that may not be apparent in measurements of equilibrium binding.

The changes in the apparent rate constant for uPA inhibition by PN-1 are nearly opposite those seen with thrombin inhibition. For uPA, protease inhibition is slowed at GAG concentrations near the K_d of PN-1 binding to GAG (figure 3.6; Table 3.4). As GAG concentrations increase, this effect appears to plateau. For heparin, the falling phase of the curve is followed by a rising phase, a pattern that might have also been seen with the other GAGs had high enough concentrations been attainable. These changes are not predicted by the model in equation 4 or in the simulations of Q in figure 3.4. While decreases in PN-1 inhibition may occur if the rate constants for GAG-bound protease binding to inhibitor (k_1) or GAG-bound inhibitor binding to protease (k_2) are smaller than the rate constant for free protease binding to free inhibitor (k_0), the model predicts that such decreases in PN-1 inhibition should become steadily greater as GAG concentration increases. In contrast, the slowing of PN-1 inhibition induced by GAGs was observed to plateau or to reverse as GAG concentration increased (Figure 3.6 B).

It is unlikely that the decrease in the apparent rate constant is caused by increased uPA activity: Although uPA protease activity is known to be activated by heparin (Andrade-Gordon and Strickland, 1986), the heparin-mediated decrease in PN-1 inhibition of uPA begins occurring at concentrations roughly five orders of magnitude below the K_d for uPA-heparin binding. Also, uPA protease assays in the presence of heparin at the concentrations used in the inhibition assays (up to 10 μg/ml) showed no activation of uPA activity toward the peptide substrate (data not shown).

Heparin-mediated deceleration of serpin inhibition has been documented for other serpin-protease combinations. For instance, protein C inhibitor (PCI) inhibition of factor Xa demonstrates reduced apparent rate constants at heparin concentrations from 0.1 to 3.0 μg/ml; above these concentrations, inhibition is increased (Pratt and Church, 1992). Factor Xa, unlike uPA, does not bind heparin; thus, the low-concentration heparin-mediated deceleration of factor Xa inhibition by PCI is likely due to serpin rather than protease binding to GAG (Pratt and Church, 1992). Two other proteases, elastase and cathepsin G, also demonstrate heparin-mediated deceleration of inhibition by the serpins α_1-proteinase inhibitor (α_1-PI) and heparin cofactor II (HCII) (Pratt et al., 1990; Ermolieff et al., 1994). Elastase and cathepsin G both bind heparin strongly (Kd ~ 90 ng/ml) (Ermolieff et al., 1994), about 100-fold more strongly than does uPA. For α_1-PI, which does not bind heparin, the mechanism of deceleration is not known, but in the case of HCII, a heparin-binding serpin, deceleration of inhibition of elastase and cathepsin G has been shown to be heparin-mediated, and caused by protease cleavage and subsequent destruction of serpin activity (Pratt et al., 1990). With these proteases, the HCII-protease complex is not a long-lived intermediate complex when heparin is present, as the active protease is released from the cleaved serpin. While cleavage of PN-1 by uPA at the lower GAG concentrations is a possibility, all GAGS demonstrated deceleration effects at GAG concentrations below the K_d's for GAG binding to PN-1 and more than 50 fold below the K_d for uPA-GAG binding. These observations suggest that the GAG-mediated deceleration of PN-1 inhibition is more likely to be an effect of GAG binding to PN-1 than to uPA, and that the inhibition mechanism for uPA is different than those used by cathepsin G or elastase.

As heparin concentrations increase, uPA inhibition by PN-1 changes from a reduction in the apparent rate constant, Q, to a mode where Q is increasing (figure 3.6 B). Heparin also affects uPA inhibition by another heparin-binding serpin, protein C inhibitor (PCI), in a reaction that accelerates with the heparin-dependent bell-shaped curve that is typical of ternary complex formation (Pratt and Church, 1992). Unlike PN-1 and uPA, no decelerative phase was seen

at low heparin concentrations in the PCI-uPA reaction. However, acceleration of the apparent rate constant for PCI and uPA began at a heparin concentration of 1 μg/ml, similar to the concentration where rate acceleration starts in the PN-1-uPA reaction, and peaked at 100 μg/ml heparin, ~10-fold the K_d for uPA-heparin binding measured in this study. Therefore, the rising part of the curve for heparin's effect on uPA inhibition by PN-1 resembles the curve for heparin's effect on uPA inhibition by PCI, suggesting that the accelerative phase of the PN-1 uPA curve is more a feature of heparin binding to uPA than to PN-1, and reflects ternary complex formation.

A paradox is presented by the data here: how does the same event, that is GAG-binding to PN-1, have the effect of inhibiting PN-1's ability to inactivate one substrate, uPA, while promoting the inactivation of a related substrate, thrombin? One explanation for these opposing effects is that thrombin and uPA may have different binding sites *on PN-1*, and perhaps the site for uPA binding is partially blocked when GAG is bound. This scenario allows room for explanation of the switch to promotion of PN-1 inhibition of uPA at higher concentrations: Perhaps, GAG binding to uPA changes its conformation sufficiently to allow it to bind PN-1 productively.

Thrombin, uPA and PN-1 are all highly abundant molecules in the brain and each appears to exert significant effects on neural behaviors. Thus control of these molecules is likely to be crucial for proper development. For both thrombin and uPA, GAG effects on inhibition by PN-1 were both conspicuous and opposite and were not specific to particular GAG species. Thus, the feature of a GAG that may most affect PN-1 in vivo may be GAG concentration rather than GAG type.

Some rough calculations of GAG concentrations in the brain using measurements of μmoles of hexosamine/gram lipid-free dry weight for newborn and adult rat brain (Margolis et al., 1975a) and a mean GAG disaccharide M_r of 480 daltons [as is the case for HeS; (Gallagher et al., 1992), provide overall GAG concentrations of 461 μg/ml and 238 μg/ml of heparan sulfate and 1.2 mg/ml and 1.3 mg/ml chondroitin sulfate in newborn and adult brain, respectively. If most of these GAGs are assumed to be confined to extracellular spaces, then

these concentrations may increase as much as ten fold. Although these values are high, they are probably reasonable estimates: comparison of these GAG concentrations with measurements of brain PG protein concentration (chapter 1) reveal that brain GAG concentration by weight is only 3.6-fold the concentration of PG protein by weight in newborn brain.

Localized concentrations of GAGs probably vary considerably from these estimates, depending on the brain regions and developmental age. For example, chondroitin and keratan sulfate "barriers" containing GAG concentrations that are significantly higher than in other brain regions are found at various times during brain development, and appear to act as selective barriers to axons (Cole and McCabe, 1991; Snow et al., 1991; Brittis et al., 1992; Geisert and Bidanset, 1993; Silver, 1993). Also, the amounts of particular GAGs are found to vary both temporally and regionally during brain development (Burkart and Weismann, 1987; David et al., 1992; Fuxe et al., 1994).

The results presented here showed that both major types of GAGs from the brain, HeS and ChS, act equally well with respect to PN-1 inhibition of uPA or of thrombin. The thrombin results showed that the maximal rate acceleration and the effective concentration range for the brain GAGs are similar to those reported for thrombin-PN-1 reactions using other tissue-derived GAGs (Farrell and Cunningham, 1987). Together with our results, these data suggest that GAGs from most tissues may behave similarly with respect to PN-1 inhibition of thrombin.

More importantly, PN-1 specificity is preferentially shifted away from uPA and toward thrombin, at brain GAG concentrations that exist in vivo. Previous investigations of uPA and thrombin inactivation by PN-1 have hinted at this GAG-mediated shift in PN-1 specificity: PN-1 bound to neuroblastoma or glioblastoma cells will form complexes with thrombin, but not uPA. However, uPA-PN1 complexes are recoverable from the culture medium, suggesting that a cell surface component inhibits uPA complex formation at the cell surface (Wagner et al., 1991). Treatment of fibroblast cell surfaces with either heparitinase or chondroitinase reduces acceleration of PN-1 inhibition of thrombin,

while treatment with both lyases abolishes acceleration, suggesting that GAGs can mediate the acceleration of thrombin inhibition (Farrell and Cunningham, 1987).

Finally, several extracellular matrix proteins have been found alter protease inhibition: Although collagen IV is not found in the brain, in vitro, collagen IV inhibits PN-1 complex formation with plasmin and uPA, but not with thrombin (Donovan et al., 1994). Vitronectin, a molecule that has been localized in embryonic chick neuroretina, decreases the heparin-mediated acceleration of uPA inhibition by protein C inhibitor (Neugebauer et al., 1991; Seiffert et al., 1992). Other extracellular matrix molecules that are found in the brain have been shown to interact with serpins and serine proteases in other tissues. Laminin and fibronectin produced by kidney epithelial cells immunoprecipitate with uPA, while purified laminin preparations from the murine EHS sarcoma tumor contain tissue plasminogen activator (McGuire and Seeds, 1989). Thrombospondin-1 (TSP-1), in particular, is a potent candidate for serpin and serine protease regulation in the brain. TSP-1 binds and protects uPA from type 1 plasminogen activator inhibitor (Silverstein et al., 1990). And the serine proteases cathepsin G, elastase, and plasmin are each bound and inhibited by TSP-1 (Hogg et al., 1992; Hogg et al., 1993a; Hogg et al., 1993b). Thus, these large extracellular matrix proteins are good prospects as regulators of serpin-protease reactions in the brain. Since each of these matrix molecules also binds to glycosaminoglycans, the number of potential mechanisms for cellular control of serpin-protease interactions and their effects in vivo rises considerably. However, only two molecules, collagen IV (Donovan et al., 1994) and brain GAGs have been shown to shift the specificity of PN-1 toward thrombin and away from uPA. Of these two, only GAGs have relevance in normal brain development.

Acknowledgements

The soluble brain proteoglycans used for glycosaminoglycan isolation were heroically purified by John Slover. Arthur Lander is especially thanked not only for his contribution of the mathematical analyses that made this work possible, but for his patient explanations

of that math during many long, fruitful discussions. My appreciation to Chris Stipp for thoughtful suggestions and assistance in figure preparation.

REFERENCES

Andrade-Gordon, P. and S. Strickland. 1986. Interaction of heparin with plasminogen activators and plasminogen: Effects on the activation of plasminogen. Biochemistry 25:4033-4040.

Bjork, I. and U. Lindahl. 1982. Mechanism of the anticoagulant action of heparin. Molec. Cell. Biochem. 48:161-182.

Brittis, P.A., D.R. Canning, and J. Silver. 1992. Chondroitin sulfate as a regulator of neuronal patterning in the retina. Science 255:733-736.

Burkart, T. and U.N. Weismann. 1987. Sulfated glycosaminoglycans (GAG) in the devloping mouse brain: Quantitative aspects on the metabolism of total and individual sulfated GAG in vivo. Dev. Biol. 120:447-456.

Cavanaugh, K.P., D. Gurwitz, D.D. Cunningham, and R.A. Bradshaw. 1990. Reciprocal modulation of astrocyte stellation by thrombin and protease nexin-1. J. Neurochem. 54:1735-1743.

Cheng, F., D. Heinegard, A. Malmstrom, A. Schmidtchen, K. Yoshida, and L.A. Fransson. 1994. Patterns of uronosyl epimerization and 4-/6-O-sulphation in chondroitin/dermatan sulphate from decorin and biglycan of various bovine tissues. Glycobiology 4:685-696.

Cole, G.J. and C.F. McCabe. 1991. Identification of a developmentally regulated keratan sulfate proteoglycan that inhibits cell adhesion and neurite outgrowth. Neuron 7:1007-1018.

Cunningham, D.D. 1992. Regulation of neuronal cells and astrocytes by protease nexin-1 and thrombin. Ann. N. Y. Acad. Sci. 674:228-236.

David, G., X.M. Bai, B.V.D. Schueren, J.J. Cassiman, and H.V.D. Berghe. 1992. Developmental changes in heparan sulfate expression: In situ detection with mAbs. J. Cell Biol. 119:961-975.

Dent, M.A.R., Y. Sumi, R.J. Morris, and P.J. Seeley. 1993. Urokinase-type plasminogen activator expression by neurons and oligodendrocytes during process outgrowth in developing rat brain. Eur. J. Neurosci. 5:633-647.

Deutsch, A.J., R.J. Midura, and A.H. Plaas. 1995. Structure of chondroitin sulfate on aggrecan isolated from bovine tibial and costochondral growth plates. J. Orhop. Res. 13:230-239.

Dihanich, M., M. Kaser, E. Reinhard, D. Cunningham, and D. Monard. 1991. Prothrombin mRNA is expressed by cells of the nervous system. Neuron 6:575-581.

Donovan, F.M., P.J. Vaughan, and D.D. Cunningham. 1994. Regulation of protease nexin-1 target protease specificity by collagen type IV. J. Biol. Chem. 269:17199-17205.

Ermolieff, J., C. Boudier, A. Laine, B. Meyer, and J.G. Bieth. 1994. Heparin protects cathepsin G against inhibition by protein proteinase inhibitors. J. Biol. Chem. 269:29502-29508.

Evans, D.L., M. McGrogan, R.W. Scott, and R.W. Carrell. 1991. Protease specificity and heparin binding and activation of recombinant protease nexin I. J. Biol. Chem. 266:22307-22312.

Farrell, D.H. and D.D. Cunningham. 1987. Glycosaminoglycans on fibroblasts accelerate thrombin inhibition by protease nexin-1. Biochem. J. 245:543-550.

Filisetti-Cozzi, T.M.C.C. and N.C. Carpita. 1991. Measurement of uronic acids without interference from neutral sugars. Anal. Biochem. 197:157-162.

Fuxe, K., G. Chadi, B. Tinner, L.F. Agnati, R. Pettersson, and G. David. 1994. On the regional distribution of heparan sulfate proteoglycan immunoreactivity in the rat brain. Brain Res. 636:131-138.

Gallagher, J.T., M. Lyon, and W.P. Steward. 1986. Structure and function of heparan sulphate proteoglycans. Biochem. J. 236:313-325.

Gallagher, J.T., J.E. Turnbull, and M. Lyon. 1992. Patterns of sulphation in heparan sulfate: polymorphism based on a common structural theme. Int. J. Biochem. 24:553-560.

Gebbink, R.K., C.H. Reynolds, D.M. tollefsen, K. Mertens, and H. Pannekoek. 1993. Specific glycosaminoglycans support the inhibition of thrombin by plasminogen activator inhibitor 1. Biochemistry 32:1675-1680.

Geisert, E.E. and D.J. Bidanset. 1993. A central nervous system keratan sulfate proteoglycan: localization to baoundaries in the neonatal rat brain. Dev. Brain Res. 75:163-173.

Hogg, P.J., D.A. Owensby, and C.N. Chesterman. 1993a. Thrombospondin 1 is a tight-binding competitive inhibitor of neutrophil cathepsin G. Determination of the kinetic mechanism of inhibition and localization of cathepsin G binding to the thrombospondin 1 type 3 repeats. J. Biol. Chem. 268:21811-21818.

Hogg, P.J., D.A. Owensby, D.F. Mosher, T.M. Misenheimer, and C.N. Chesterman. 1993b. Thrombospondin is a tight-binding competitive inhibitor of neutrophil elastase. J. Biol. Chem. 268:7139-7146.

Hogg, P.J., J. Stenflo, and D.F. Mosher. 1992. Thrombospondin is a slow tight-binding inhibitor of plasmin. Biochemistry 31:265-269.

Hoylaerts, M., W.G. Owen, and D. Collen. 1984. Involvement of heparin chain length in the heparin-catalyzed inhibition of thrombin by antithrombin III. J. Biol. Chem. 259:5670-5677.

Jordan, R.E., G.M. Oosta, W.T. Gardner, and R.D. Rosenberg. 1980a. The binding of low molecular weight heparin to hemostatic enzymes. J. Biol. Chem. 255:10073-10080.

Jordan, R.E., G.M. Oosta, W.T. Gardner, and R.D. Rosenberg. 1980b. The kinetics of hemostatic enzyme-antithrombin interactions in the presence of low molecular weight heparin. J. Biol. Chem. 255:10081-10090.

Karamanos, N.K. 1992. Two squid proteoglycans each containing chondroitin sulfates with different sulfation patterns. Biochem. Cell Biol 70:629-635.

Lander, A.D. and A.L. Calof. (1993). Extracellular matrix in the developing nervous system. In Molecular Genetics of Nervous System Tumors, A. J. L. a. H. H. Schmidek, editors. (New York: Wiley), pp. 341-355.

Lee, M.K. and A.D. Lander. 1991. Analysis of affinity and structural selectivity in the binding of proteins to glycosaminoglycans: Development of a sensitive electrophoretic approach. P.N.A.S. 88:2768-2772.

Lim, W.A., R.T. Sauer, and A.D. Lander. 1991. Analysis of DNA-protein interactions by affinity coelectrophoresis. Meth. Enzymol. 208:196-210.

Lindner, J., J. Guenther, H. Nick, G. Zinser, H. Antonicek, M. Schachner, and D. Mondar. 1986. Modulation of granule cell migration by a glia-derived protein. Proc. Natl. Acad. Sci. (USA) 83:4568-4571.

Linker, A. and P. Hovingh. 1973. The heparitin sulfates (heparan sulfates). Carbohydrate Res. 29:41-62.

Mansuy, I.M., H.v.d. Putten, P. Schmid, M. Meins, F.M. Botteri, and D. Mondar. 1993. Variable and multiple expression of protease nexin-1 during mouse organogenesis and nervous system development. Development 119:1119-1134.

Margolis, R.K., R.U. Margolis, C. Preti, and D. Lai. 1975a. Distribution and metabolism of glycoproteins and glycosaminoglycans in subcellular fractions of brain. Biochem. 14:4797-4804.

McGuire, P.G. and N.W. Seeds. 1989. The interaction of plasminogen activator with a reconstituted basement membrane matrix and extracellular macromolecules produced by cultured epithelial cells. J. Cell. Biochem. 40:215-227.

Monard, D., E. Niday, A. Limat, and F. Solomon. 1983. Inhibition of protease activity can lead to neurite extension in neuroblastoma cells. Prog. Brain Res. 58:359-.

Moonen, G., M.-P. Grau-Wagemans, and I. Selak. 1992. Plasminogen activator-plasmin system and neuronal migration. Nature 298:753-755.

Neugebauer, K.M., C.J. Emmett, K.A. Venstrom, and L.F. Reichardt. 1991. Vitronectin and thrombospondin promote retinal neurite outgrowth: developmental regulation and role of integrins. Neuron 6:345-358.

Olson, S.T. 1985. Heparin and ionic strength-dependent conversion of antithrombin III from an inhibitor to a substrate of α-thrombin. J. Biol. Chem. 260:10153-10160.

Olson, S.T., H.R. Halvorson, and I. Bjork. 1991. Quantitative characterization of the thrombin-heparin interaction. J.C.B. 266:6342-6352.

Pittmann, R.N., J.K. Ivins, and H.M. Buettner. 1989. Neuronal plasminogen activators: Cell surface binding sites and involvement in neurite outgrowth. J. Neurosci. 9:4269-4286.

Potempa, J., E. Korzus, and J. Travis. 1994. The serpin superfamily of proteinase inhibitors: Structure, function and regulation. J. Biol. Chem. 269:15957-15960.

Pratt, C.W. and F.C. Church. 1992. Heparin binding to protein C inhibitor. J. Biol. Chem. 267:8789-8794.

Pratt, C.W., R.B. Tobin, and F.C. Church. 1990. Interaction of heparin cofactor II with neutrophil elastase and cathepsin G. J. Biol. Chem. 265:6092-6097.

Pratt, C.W., H.C. Whinna, and F.C. Church. 1992. A comparison of three heparin-binding serine proteinase inhibitors. J. Biol. Chem. 267:8795-8801.

Rovelli, G., S.R. Stone, A. Guidolin, J. Sommer, and D. Monard. 1992. Characterization of the heparin-binding site of glia-derived nexin/protease nexin-1. Biochemistry 31:3542-3549.

Ruoslahti, E. 1988. Structure and biology of proteoglycans. Ann. Rev. Cell Biol. 4:229-255.

Seiffert, D., M. Geiger, S. Ecke, and B.R. Binder. 1992. Vitronectin modulates glycosaminoglycan dependent reactions of protein C inhibitor. Thromb. Haem. 68:657-661.

Sheehan, J.P. and J.E. Sadler. 1994. Molecular mapping of the heparin-binding exosite of thrombin. Proc. Natl. Acad. Sci. (USA) 91:5518-5522.

Sheehan, J.P., D.M. Tollefsen, and J.E. Sadler. 1994. Heparin cofactor II is regulated allosterically and not primarily by template effects. J. Biol. Chem. 269:32747-32751.

Sheehan, J.P., Q. Wu, D.M. Tollefsen, and J.E. Sadler. 1993. Mutagenesis of thrombin selectively modulates inhibition by serpins heparin cofactor II and antithrombin III. Interaction with the anion-binding exosite determines heparin cofactor II specificity. J. Biol. Chem. 268:3639-3645.

Silver, J. (1993). Glial-neuron interactions at the midline of the developing mammalian brain and spinal cord. In Perspecitves on Developmental Neurobiology, C. A. Mason, editors. (Gordon and Breach, Science Publishers S. A.), pp. 227-236.

Silverstein, R.L., R.L. Nachman, R. Pannell, V. Gurewich, and P.C. Harpel. 1990. Thrombospondin forms complexes with single-chain and two chain forms of urokinase. J. Biol. Chem. 265:11289-11294.

Snow, D.M., M. Watanabe, P.C. Letourneau, and J. Silver. 1991. A chondroitin sulfate proteoglycan may influence the direction of retinal ganglion cell outgrowth. Development 113:1473-1485.

Stone, S.R., M.L. Brown-Luedi, G. Rovelli, A. Guidolin, E. McGlynn, and D. Mondard. 1994. Localization of the heparin-binding site of glia-derived nexin/protease nexin-1 by site-directed mutagenesis. Biochemistry 33:7731-7735.

Stone, S.R. and J.M. Hermans. 1995. Inhibitory mechanism of serpins. Interaction of thrombin with antithrombin and protease nexin 1. Biochemistry 34:5164-5172.

Streusand, V.J., I. Bjork, P.G.W. Gettins, M. Petitou, and S.T. Olson. 1995. Mechanism of acceleration of antithrombin-proteinase reactions by low affinity heparin. J. Biol. Chem. 270:9043-9051.

Sumi, Y., M.A.R. Dent, D.E. Owen, P.J. Seeley, and a.R.J. Morris. 1992. The expression of tissue and urokinase-type plasminogen activators in neural development suggests different modes of proteolytic involvement in neuronal growth. Development 116:625-637.

Turnbull, J.E. and J.R. Gallagher. 1990. Molecular organization of heparan sulphate from human skin fibroblasts. Biochem. J. 265:715-724.

Wagner, S.L., A.L. Lau, A. Nguyen, J. Mimuro, D.J. Loskutoff, P.J. Isackson, and D.D. Cunningham. 1991. Inhibitors of urokinase and thrombin in cultured neural cells. J. Neurochem. 56:234-242.

Weinstein, J.R., S.J. Gold, D.D. Cunningham, and C.M. Gall. 1995. Cellular localization of thrombin receptor mRNA in rat brain: Expression by mesencephalic dopaminergic neurons and codistribution with prothrombin mRNA. J. Neurosci. 15:2906-2919.

Wight, T.N., M.G. Kinsella, and E.E. Qwarnstrom. 1992. The role of proteoglycans in cell adhesion, migration and proliferation. Curr. Opin. Cell Biol. 4:793-801.

Figure 3.1. Reverse Affinity Coelectrophoresis (Reverse ACE). The experimental setup for reverse ACE is shown schematically. In reverse ACE, a labeled protein ligand is embedded into a thin sample well in a horizontal agarose gel, and unlabeled glycosaminoglycans at various concentrations are electrophoresed through the protein zone. If the protein binds to the glycosaminoglycan it is shifted to an extent that depends upon the K_d for the interaction. The resulting affinity pattern can be converted to a binding isotherm and a value for K_d can be calculated as described in Materials and Methods.

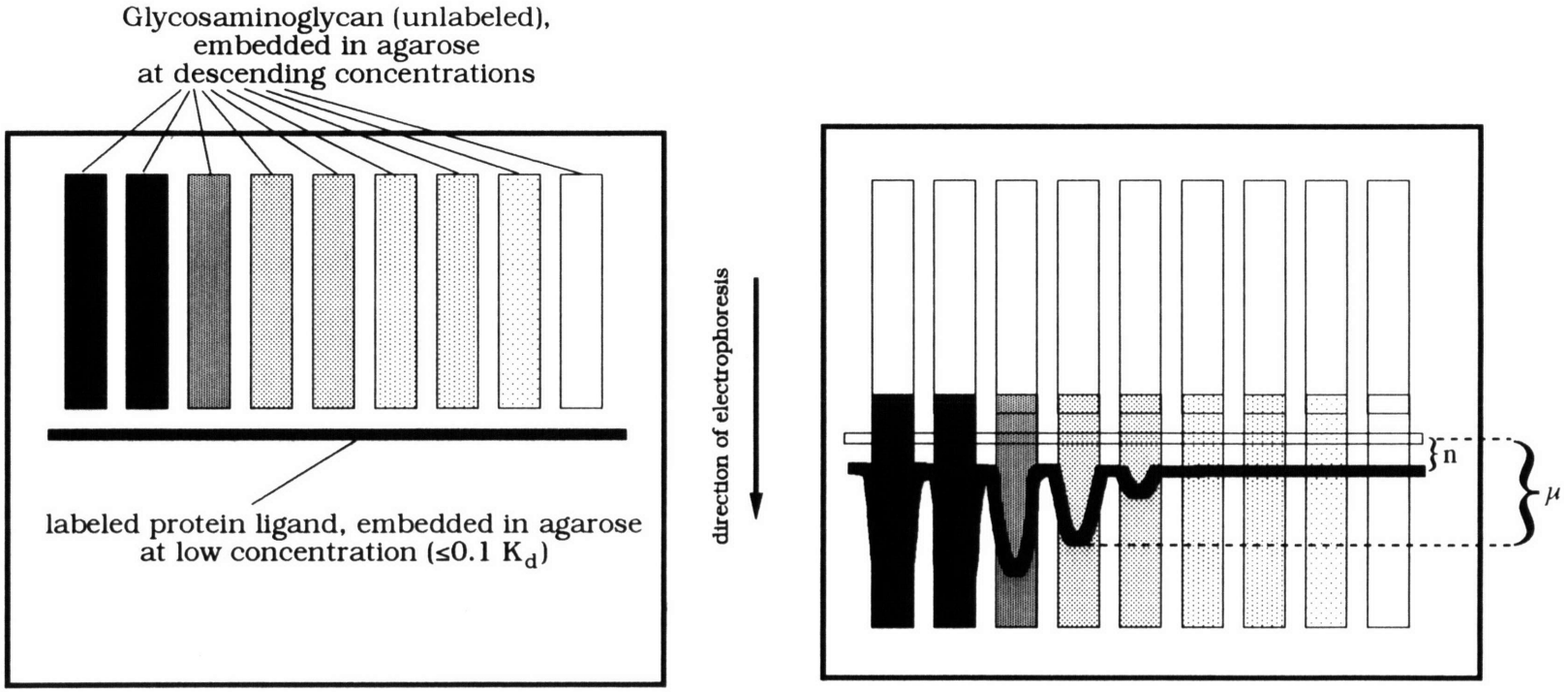

Before Electrophoresis

After Electrophoresis

Figure 3.2. Affinity Coelectrophoresis of Antithrombin III and Protease Nexin-1. ^{125}I-labeled low molecular weight (lM_r) heparin was tested for binding to antithrombin III (ATIII) and protease nexin-1 (PN-1) by affinity coelectrophoresis (see Chapter 2). (A) Autoradiograph of the ATIII gel: ATIII fractionates low molecular weight heparin into high and low affinity subpopulations. The high affinity subpopulation has a K_d of around 16 nM (Lee and Lander, 1991). (B) Autoradiograph of the PN-1 gel: unlike ATIII, PN-1 does not selectively bind a subpopulation of the heparin. Estimated K_d for PN-1 binding to heparin is 20 nM.

Antithrombin gel is courtesy of Matt Lee and Arthur Lander

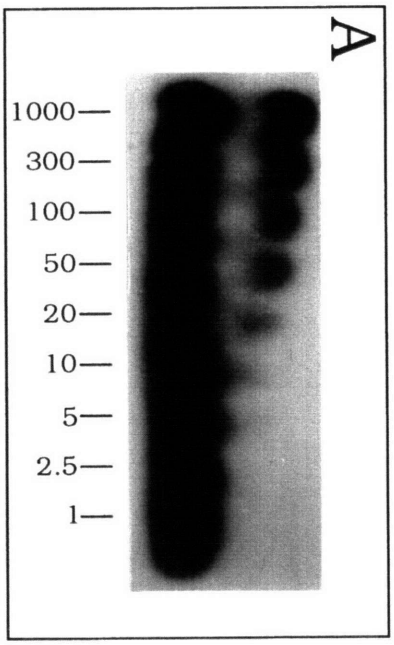
A
1000
300
100
50
20
10
5
2.5
1

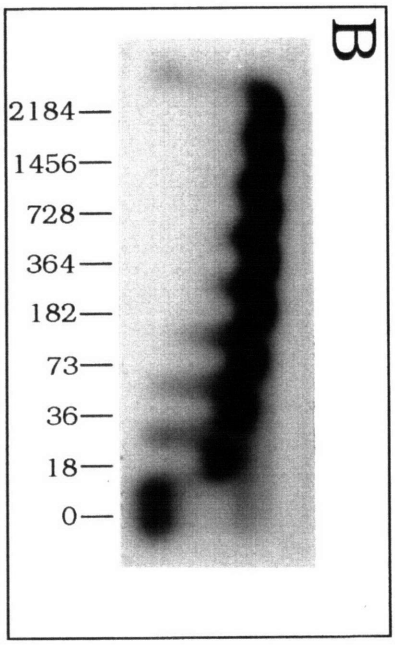
B
2184
1456
728
364
182
73
36
18
0

Table 3.1. Forward ACE Equilibrium Dissociation Constants for GAG binding to Protease Nexin-1, uPA, and Thrombin.

GAG:	Protease Nexin-1	uPA	Thrombin
$1M_r$-Heparin, porcine intestinal	20 nM[e]	312 nM[b]	123 nM[c]
HeS, P0 rat brain soluble fraction	101 nM[a]	2310 nM[a]	1025 nM[a]
HeS, bovine kidney	62 nM[a]	n.d.	1710 nM[a]
ChS, P0 rat brain soluble fraction	239 nM[a]	21.9 μM[a]	2500 nM[a]
ChS, bovine tracheal	478 nM[d]	17.1 μM[a]	10.3 μM[a]
ChS, shark cartilage	425 nM[a]	n.d.	n.d.

Equilibrium dissociation constants were derived from ACE analysis as described in text. All values listed are based on the assumption of first order binding mechanism; a = K_d value is from a single determination; b, c, d, e = K_d value is mean of two, three, four, or five determinations, respectively; f = soluble fraction refers to initial homogenization of brain tissue with buffered isotonic sucrose (see Chapter 1); g = no measurable binding in ACE. $K_{d,min}$ is determined as outlined in text. C_{max} = maximal concentration of ligand tested in ACE; h = K_d value reported in Lee & Lander (1991); n.d. = no determination was made.

Figure 3.3 Reverse ACE of Protease Nexin-1. Protease nexin-1 binding to porcine intestinal heparin (that was not size fractionated), panel **(A)** , and binding to bovine tracheal chondroitin-4-sulfate (Ch4S), panel **(B)**, was measured by reverse affinity co-electrophoresis (see Methods sections for description). K_d values are estimated at 77 ng/ml for heparin binding to PN-1, and 27 μg/ml for Ch4S binding to PN-1

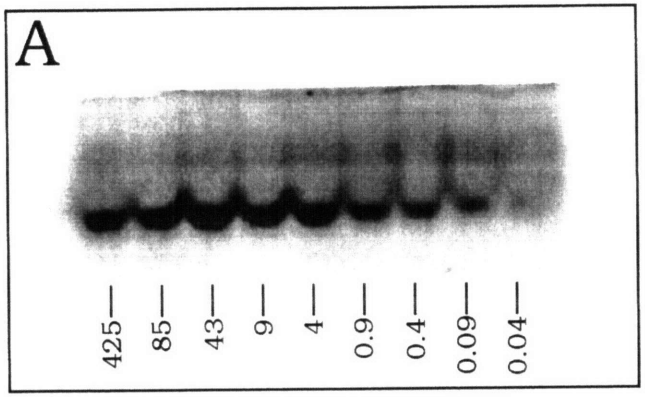

K_d = 77 ng/ml

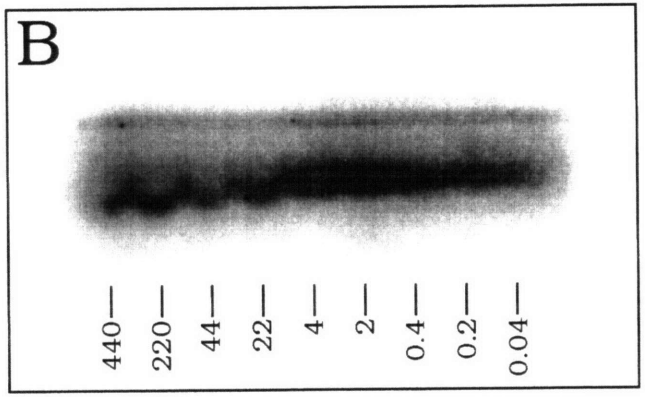

K_d = 27 μg/ml

Table 3.2. Reverse ACE Equilibrium Dissociation Constants for GAG binding to Protease Nexin-1, uPA, and Thrombin.

GAG:	Protease Nexin-1	uPA	Thrombin
1M_r-Heparin, porcine intestinal	0.077 μg/ml (7.7 nM)[a]	9.4 μg/ml (940 nM)[a]	3.0 μg/ml (300 nM)[a]
ChS, bovine tracheal	27 μg/ml (1929 nM)[b]	528 μg/ml (37,715 nM)[b]	264 μg/ml (18,858 nM)[b]

Equilibrium dissociation constants were derived from reverse ACE analysis as described in Materials and Methods. All values listed are based on the assumption of first order binding mechanism; a = K_d value in (nM) is based on a heprin mean M_r of 10 kDa, as reported by the manufacturer; b = K_d value in (nM) is based on a ChS mean M_r of 14 kDa as reported by the manufacturer.

Figure 3.4. Simulation of Q, the Apparent Rate Constant as a Function of Glycosaminoglycan Concentration. Based on the model depicted in equation 4 in the text, measured K_d values for uPA and PN-1 binding to Ch4S were substituted into the equation for Q, the apparent rate constant of inhibition (equation 5, text), to simulate the effects of a range of GAG concentrations and using various values for the internal rate constants in the model. k_0 = inhibition rate constant in the absence of GAG; k_1 = rate constant for binding between GAG-bound protease and free inhibitor; k_2 = rate constant for binding between GAG-bound inhibitor and free protease. Panel **(A)**: Change in Q when k_1 alone is varied. Panel **(B)**: Change in Q when k_2 alone is varied. Panel **(C)**: Change in Q when k_1 and k_2 both are varied similarly.

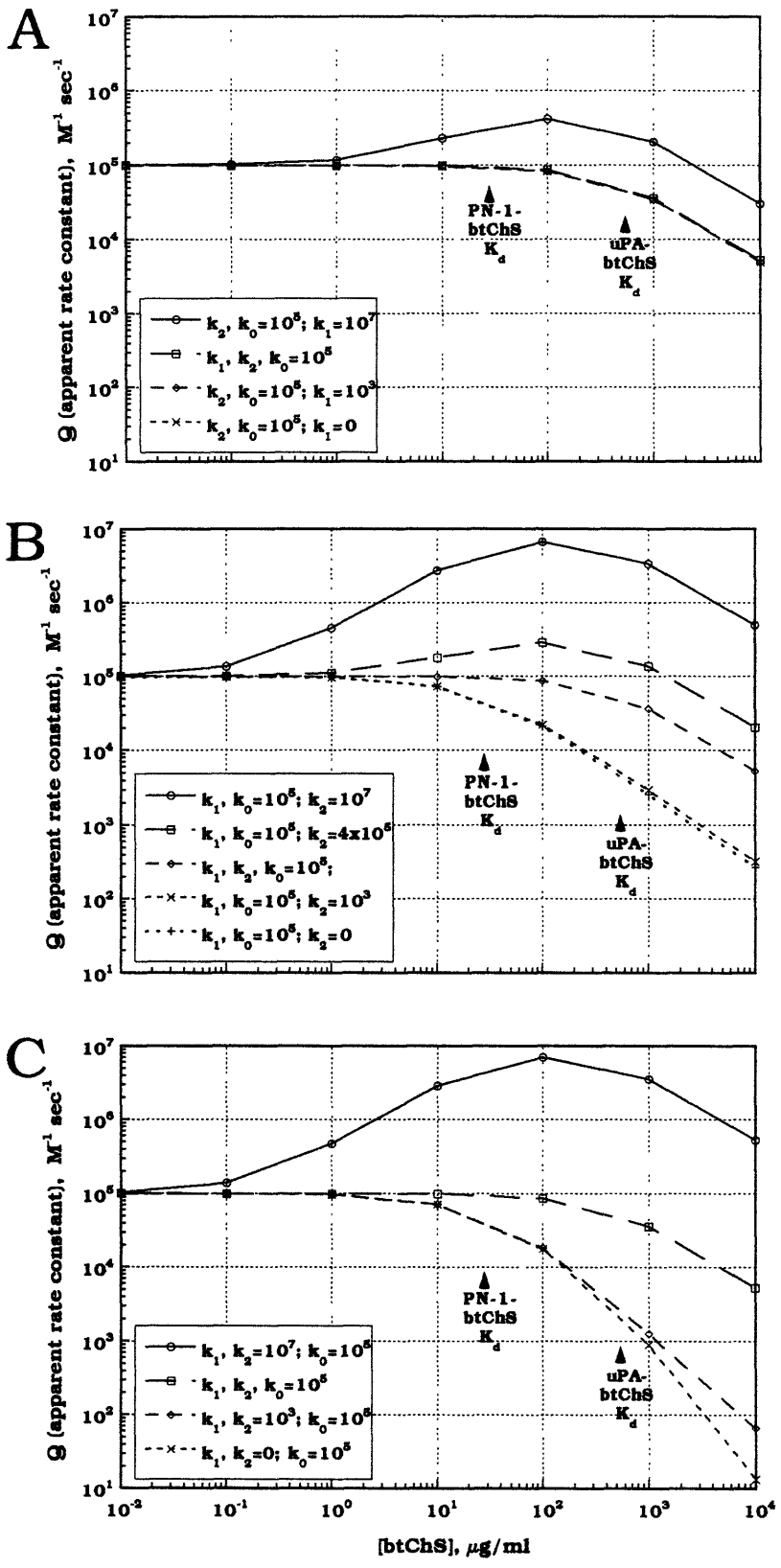
A
B
C
Q (apparent rate constant), M⁻¹ sec⁻¹
PN-1-btChS K_d
uPA-btChS K_d
k_2, k_0=10^5; k_1=10^7
k_1, k_2, k_0=10^5
k_2, k_0=10^5; k_1=10^3
k_2, k_0=10^5; k_1=0
k_1, k_0=10^5; k_2=10^7
k_1, k_0=10^5; k_2=4x10^5
k_1, k_2, k_0=10^5;
k_1, k_0=10^5; k_2=10^3
k_1, k_0=10^5; k_2=0
k_1, k_2=10^7; k_0=10^5
k_1, k_2, k_0=10^5
k_1, k_2=10^3; k_0=10^5
k_1, k_2=0; k_0=10^5
[btChS], μg/ml

Figure 3.5. Kinetic Assay of Protease Nexin-1 Inhibition of Thrombin. Data from three short term assays of PN-1 inhibition of thrombin, without GAG, and with 10 or 100 μg/ml of brain HeS, were taken from spectrographs and fit to equation 3 (see Methods). The curves that fall below the control (no GAG) curve indicate that the inhibition reaction has been accelerated by the addition of the HeS.

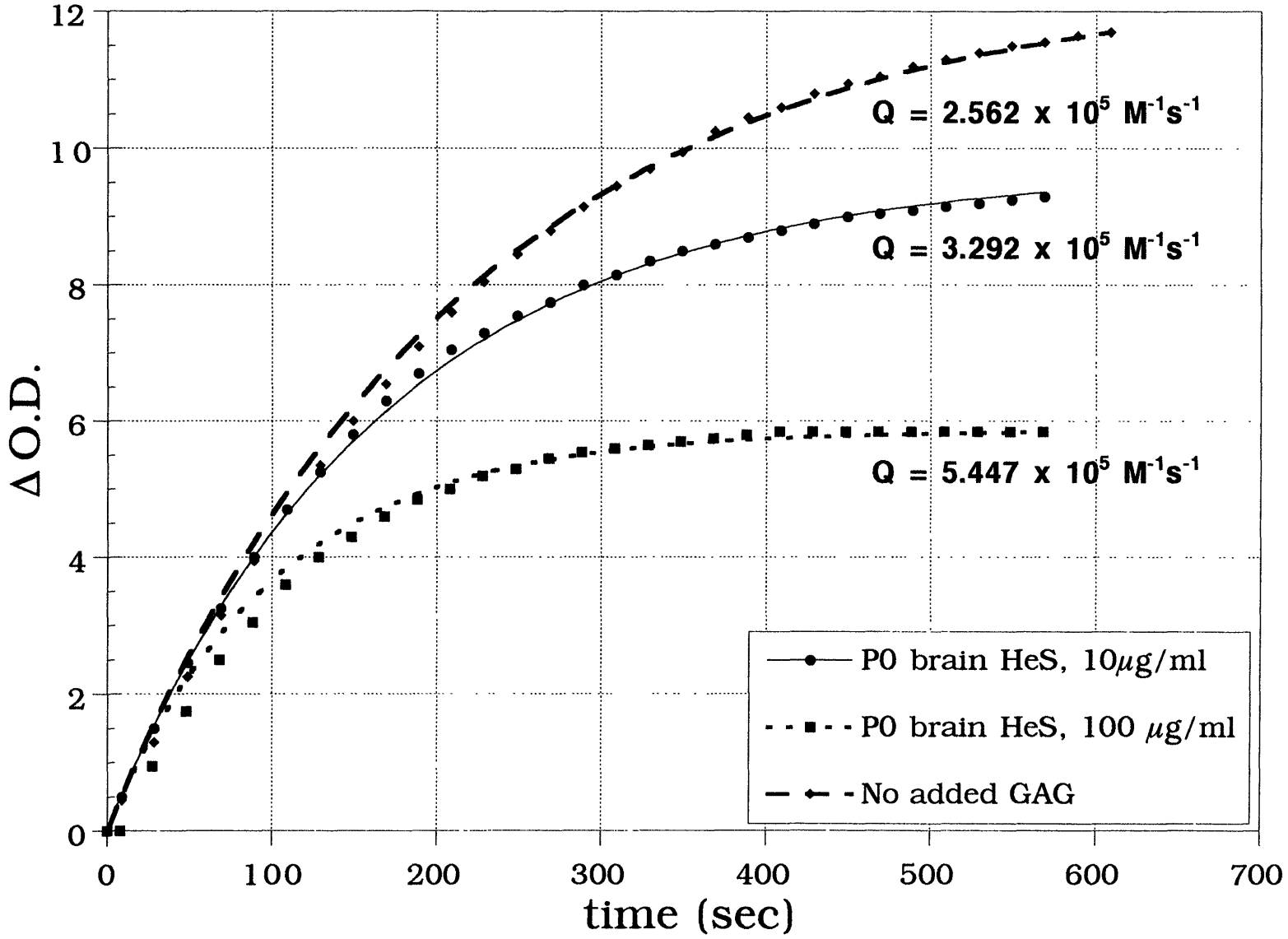
12
10
8
6
4
2
0
ΔO.D.
0
100
200
300
400
500
600
700
time (sec)
Q = 2.562 x 10^5 M^-1s^-1
Q = 3.292 x 10^5 M^-1s^-1
Q = 5.447 x 10^5 M^-1s^-1
P0 brain HeS, 10μg/ml
P0 brain HeS, 100 μg/ml
No added GAG

Figure 3.6. The influence of Glycosaminoglycans on the Inhibition of uPA and Thrombin by Protease Nexin-1. Values for Q were obtained from kinetic assays of inhibition in the presence of various glycosaminoglycans. Panel **(A)** shows the effects of heparin addition on PN-1 inhibition of thrombin; arrowheads show the K_d concentrations for heparin binding to PN-1 and thrombin. Panel **(B)** shows the effects of various tissue-derived GAGs on PN-1 inhibition of thrombin; arrowheads show the K_d concentrations for cartilage Ch4S binding to PN-1 and thrombin. Panel **(C)** shows the effects of heparin and brain HeS and ChS on PN-1 inhibition of uPA; closed arrowheads show the K_d concentrations for heparin binding to PN-1 and uPA, while open arrowheads mark the K_d concentrations for cartilage Ch4S binding to PN-1 and uPA. See text for details.

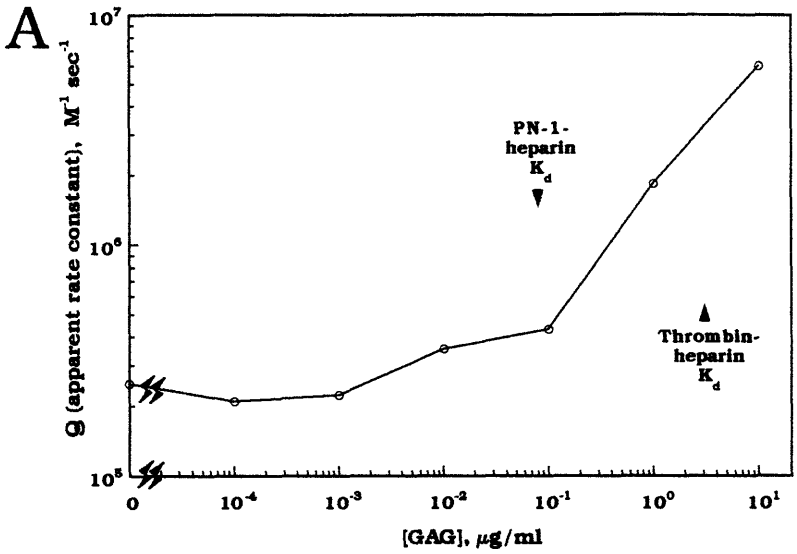
A
Q (apparent rate constant), M⁻¹ sec⁻¹
PN-1-heparin K_d
Thrombin-heparin K_d
[GAG], μg/ml

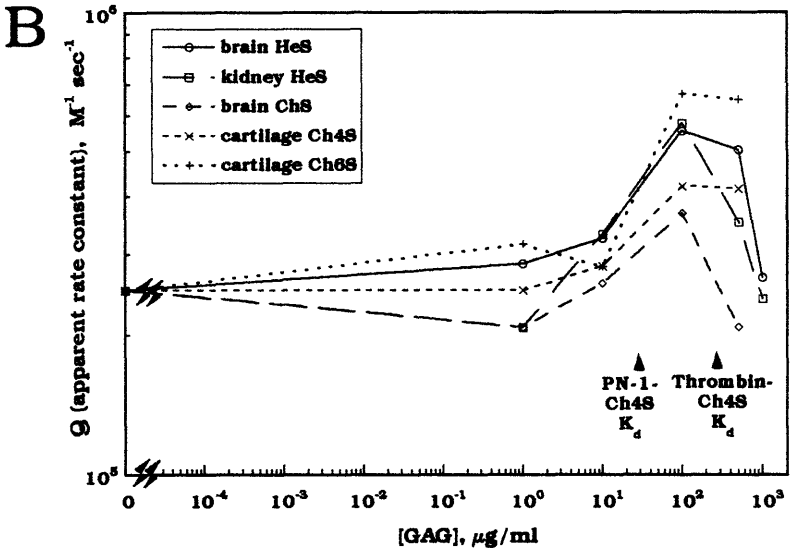
B
Q (apparent rate constant), M⁻¹ sec⁻¹
brain HeS
kidney HeS
brain ChS
cartilage Ch4S
cartilage Ch6S
PN-1-Ch4S K_d
Thrombin-Ch4S K_d
[GAG], μg/ml

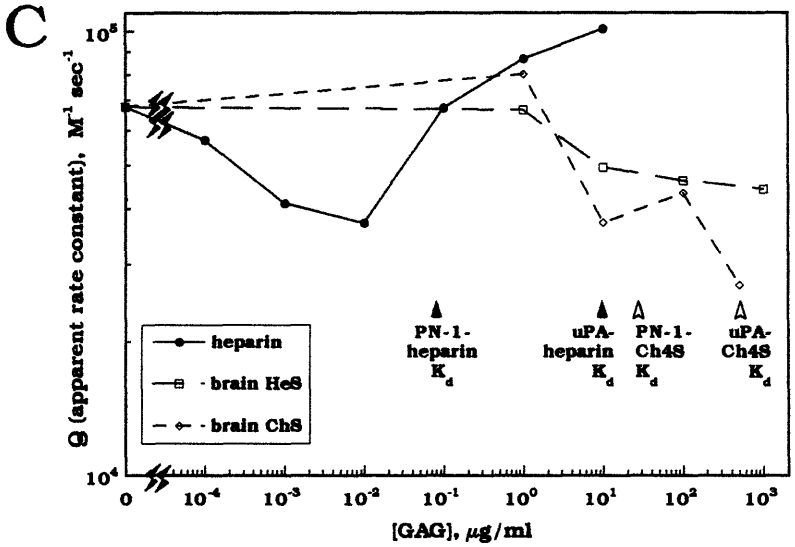
C
Q (apparent rate constant), M⁻¹ sec⁻¹
heparin
brain HeS
brain ChS
PN-1-heparin K_d
uPA-heparin K_d
PN-1-Ch4S K_d
uPA-Ch4S K_d
[GAG], μg/ml

Table 3.3. Properties of Protease Nexin-1--Thrombin reactions in the presence of Glycosaminoglycans.

GAG:	GAG conc.	$\mathcal{Q}$ ($M^{-1}s^{-1}$)	Protease nexin-1		Thrombin		$\frac{K_{d,[thrombin]}}{K_{d,[PN\text{-}1]}}$	GAG-mediated change in $\mathcal{Q}$
			$K_{d,[GAG]}$ [c]	$K_{d,[PN\text{-}1]}$ [d]	$K_{d,[GAG]}$ [c]	$K_{d,[thrombin]}$ [d]		
Heparin, ($1M_r$) porcine intestinal	10 μg/ml [a]	6.01×10^6	77 ng/ml	20 nM	3.0 μg/ml	123 nM	6.2	26-fold increase
Ch6S, shark cartilage	100 μg/ml [b]	6.67×10^5	n.d.	425 nM	n.d.	n.d.	–	2.9-fold increase
HeS, bovine kidney	100 μg/ml [b]	5.75×10^5	n.d.	62 nM	n.d.	1.7 μM	27	2.5-fold increase
HeS, P0 rat brain soluble fraction	100 μg/ml [b]	5.54×10^5	n.d.	101 nM	n.d.	1.0 μM	10	2.4-fold increase
ChS, bovine tracheal	100 μg/ml [b]	4.2×10^5	27 μg/ml	478 nM	264 μg/ml	10.3 μM	22	1.8-fold increase
ChS, P0 rat brain soluble fraction	100 μg/ml [b]	3.68×10^5	n.d.	239 nM	n.d.	2.5 μM	10	1.6-fold increase

$\mathcal{Q}$ (apparent rate constant of inhibition) were obtained from analysis of short term kinetic assays of thrombin inhibition by PN-1. K_d values are from affinity coelectrophoresis. a = highest concentration of glycosaminoglycan tested in kinetic assays (optimum may be higher); b = optimal glycosaminoglycan concentration in kinetic assays (gave greatest change in $\mathcal{Q}$); c = K_d based on reverse affinity co-electrophoresis; d = K_d based on "forward" affinity co-electrophoresis.

Table 3.4. Properties of Protease Nexin-1--Urokinase Plasminogen Activator (uPA) reactions in the presence of Glycosaminoglycans.

GAG:	GAG conc.	Q ($M^{-1}s^{-1}$)	Protease nexin-1		uPA		$\frac{K_{d,[uPA]}}{K_{d,[PN\text{-}1]}}$	GAG-mediated change in Q
			$K_{d,[GAG]}$ [c]	$K_{d,[PN\text{-}1]}$ [d]	$K_{d,[GAG]}$ [c]	$K_{d,[uPA]}$ [d]		
ChS, P0 rat brain soluble fraction	500 μg/ml [a]	2.69×10^4	(27 μg/ml)[e]	239 nM	(528 μg/ml)[e]	22 μM	92	2.5-fold decrease
Heparin [f], ($1M_r$) porcine intestinal	0.01 μg/ml [b] ------- 10 μg/ml [a]	3.71×10^4 ------- 1.01×10^5	77 ng/ml	20 nM	9.4 μg/ml	312 nM	16	1.8-fold decrease ------- 1.5-fold increase
HeS, P0 rat brain soluble fraction	1000 μg/ml [a]	4.42×10^4	n.d.	101 nM	n.d.	2.3 μM	23	1.5-fold decrease

Q (apparent rate constant of inhibition) values were obtained from analysis of short term kinetic assays of uPA inhibition by PN-1. K_d values are from affinity coelectrophoresis. a = highest concentration of glycosaminoglycan tested in kinetic assays (optimum may be higher); b = optimal glycosaminoglycan concentration in kinetic assays (gave greatest change in Q); c = K_d based on reverse affinity co-electrophoresis; d = K_d based on "forward" affinity co-electrophoresis.; e = reverse ACE K_d for bovine tracheal Ch4S is provided for comparison; f = heparin demonstrated both GAG-mediated decrease and increase in the apparent rate constant, Q.

DISCUSSION

The last two chapters of this work focused on the binding and a functional effects of brain glycosaminoglycan (GAGs). One conclusion that can be drawn, is that while heparan and chondroitin sulfates (HeS and ChS) derived from brain exhibit distinct affinities for many ligands, the HeS and ChS populations behave rather uniformly with respect to binding. Also, HeS and ChS from brain behaved similarly in their GAG-mediated effects on protease nectin-1 activation: while both GAGs accelerated thrombin inhibition, both also decelerated uPA inhibition by PN-1, suggesting that despite their different types, they have similar effects. If GAGs mediate PG behavior, then one might suppose that the 25 different developmentally regulated core proteins also have effects similar to each other. This scenario is unlikely: Not only have we seen that the presence of a PG core protein may strengthen binding by ~250-fold (fibronectin binding to the strong-binding PG vs. to brain HeS; chapter II), but also that a particular core, cerebroglycan, increases PG binding to laminin ~1800-fold over HeS chain binding (Stipp, 1996), while for thrombospondin, the increase with intact PG over HeS alone is only ~5.5-fold. Thus, even if the GAG chains on these cores were the same, binding to relevant ligands is variably and significantly increased. It would seem, therefore, that the next step for understanding the roles of proteoglycans in cellular events will come from learning more about intact PGs and their core protein molecules.

Proteoglycan identification

The work presented in chapter I of this thesis showed that, in the developing brain, proteoglycans represent a class of biochemically diverse molecules that have distinct patterns of temporal regulation. Subsequent to this work, two of the PGs have been cloned and characterized further: David Litwack cloned and identified M12 as the rat version of glypican, a cell-surface glycosylphosphatidylinositol-(GPI)-linked HSPG (Litwack, 1995; Litwack et al., 1994). Molecular cloning and characterization of M13, accomplished by Chris Stipp (Stipp, 1996; Stipp et al., 1994), showed that M13 is a glypican-related GPI-linked HSPG; the nervous system limited expression of M13 led to its new designation, cerebroglycan.

The identities of the other PGs characterized in chapter I have not been affirmed, but several of them, like glypican, may be PGs that have been characterized elsewhere. For example, the observed molecular weight and PG type of M7 suggests this highly expressed and developmentally regulated HSPG may be sydecan-4 (N-syndecan). Cat-301, a CSPG with a remarkably restricted distribution in the nervous system (Hockfield et al., 1990) might represent a subset of the abundant S1 CSPG, while the core size of S2 is suggestive of neurocan. The recently identified member of the glypican family, k-glypican (Watanabe et al., 1995), may be a subset of M12: Indeed, fractionation of M12/M13 preparations by fibronectin ACE revealed a previously unidentified high affinity PG with a core protein size that was at the lower end of the usual broad M12/glypican smear in SDS-PAGE (chapter II). Even if each of these possible assignments turned out to true, there remain a large number of unidentified PG molecules shown in chapter I, many that present interesting expression patterns.

Proteoglycan-ligand binding

Most of the binding studies presented here had to do with binding between protein ligand and glycosaminoglycans. As antibodies directed at specific PG core proteins become available, more studies of intact PG binding to protein ligands would be welcome. Of particular interest would be comparisons of PG binding to particular ligands, using identical PGs (i.e., having the same core) purified from different tissues, cell types, or developmental stages. A difference in PG affinity for a given ligand might then be dissected apart with respect to the relative contributions of GAG and core binding to the ligand.

While GAG measurements of binding are straightforward using affinity coelectrophoresis (ACE), direct measurements of core binding to ligand are not possible in ACE if the core and the ligand have similar electrophoretic mobilities. In such cases, solid-phase binding of the labelled core to plated ligand could be tried -- provided the intact PG will also bind the ligand in solid phase as it does in ACE. If the protein ligand is abundant enough, labeled core protein binding to ligand could be measured by equilibrium gel-filtration chromatography

(aka Hummel-Dreyer analysis), again with the proviso that in the same system, intact PG should bind the ligand as well as it does in ACE. Another way to get at the core would be to produce it in an expression system where large amounts of core could be isolated, such as baculovirus; however, any tissue-specific core modifications would be lost by this method. An expression system, however, could provide sufficient amounts of core protein for its use as an ACE ligand or in equilibrium gel filtration analysis.

Another feature of PG binding that would be interesting to discover is how number and type of GAG chains attached to the core protein affect ligand binding. Various core protein-encoding cDNAs, with substitutions at the putative GAG attachment sites, could be expressed in the chinese hamster ovary (CHO) GAG cell lines, including those that express only (or mostly) either heparan or chondroitin sulfate. Purification and analysis of the PGs produced in such cell lines could provide information about which GAG attachment sites are used, which are permissive for the attachment of different GAG types, and which forms of the PG retain ligand binding. Additionally, how multiple GAG chains versus a single GAG chain on a core affect ligand binding, especially the binding of proteins with multiple and/or distant heparin binding domains, could be examined. Such experiments might provide insight into which features of PGs control their binding to, and thus their interactions with pericellular proteins.

Proteoglycan effects on cell behaviors

Proteoglycan binding is, presumably, only the first step to understanding the functions of proteoglycans in the nervous system; however, it is a step that may point one in the right direction. As an example, the binding of immunopurified cerebroglycan to laminin is very strong [~500 pM; (Stipp, 1996)] while thrombospondin binding is weaker (33 nM; chapter II). One might expect, therefore, that cerebroglycan would affect a laminin-mediated cell response more strongly than a thrombospondin-mediated response. One way to test this would be to quantify changes in cell adhesion due to expression of cerebroglycan in a cell line that normally adheres to both laminin and

thrombospondin (e.g., PC12 cells), or to see if cerebrogycan expression will transform a non-adherent cell type to an adherent one.

In addition, the relationship between PG binding and cell behavior may be investigated using PGs as reagents in assays of cell behaviors. For example, a tissue or cell culture source of cerebroglycan that binds strongly to laminin could be used to isolate the purified PG, which could then be used in neurite outgrowth assays on laminin. Based on PG recoveries shown in chapter I and unpublished data on immunopurification of cerebroglycan [C. Stipp, personal communication], a conservative estimate for recovery of immunopurified cerebroglycan from newborn rat brain is ~50 ng/g wet brain weight. Preparation of testing medium containing cerebroglycan at 10-fold the K_d for laminin binding would require 300 ng cerebroglycan (protein weight) per ml of testing medium. This translates to only 17 grams of brain tissue for 3 ml of medium -- enough for more than 25 neurite outgrowth assays. Thus proteoglycans purified from tissues may provide a viable means of acquiring biologically relevant reagents for in vitro analysis of cell behaviors. A caveat of this approach is that the binding of proteoglycan to the ligand molecule needs to be strong, or the PG needs to be extremely abundant in the tissue source: for example, if the affinity of cerebroglycan for laminin were 10-fold weaker, then ten times as many dissections, etc., would be required to obtain enough sufficient proteoglycan for relevant concentrations of the PG in the testing medium. Experiments such a these might shed some light on how proteoglycans exert their effects in vivo.

Proteoglycans are a large, diverse, and significant group of molecules. Further, their dual nature, being both protein and GAG, provides interesting challenges to the researcher, both technically and intellectually. The path from proteoglycan structure to proteoglycan function promises to be a fascinating one.

REFERENCES

Hockfield, S., Kalb, R. G., Zaremba, S., and Fryer, H. J. L. (1990). Expression of neural proteoglycans correlates with the acquisition of mature neruonal properties in the mammalian brain. Cold Spring Harbor Symp. Quant. Biol. *55*, 505-514.

Litwack, E. D. (1995). Expression and function of proteoglycans in the nervous system: Massachusetts Institute of Technology).

Litwack, E. D., Stipp, C. S., Kumbasar, A., and Lander, A. D. (1994). Neuronal expression of glypican, a cell-surface glycosylphosphatidylinositol-anchored heparan sulfate proteoglycan, in the adult rat nervous system. J. Neurosci. *14*, 3713-3724.

Stipp, C. S. (1996). Identification, Molecular Cloning, and Characterization of Cerebroglycan, A Cell Surface Heparan Sulfate Proteoglycan of the Developing Rat Brain: Massachusetts Institute of Technology).

Stipp, C. S., Litwack, E. D., and Lander, A. D. (1994). Cerebroglycan: an integral membrane heparan sulfate proteoglycan that is unique to the developing nervous system and expressed specifically during neuronal differentiation. J. Cell Biol. *124*, 149-160.

Watanabe, K., Yamada, H., and Yamaguchi, Y. (1995). K-glypican: a novel gpi-anchored heparan sulfate proteoglycan that is highly expressed in developing brain and kidney. J. Cell Biol. *130*, 1207-1218.